CZECH TECHNICAL UNIVERSITY IN PRAGUE

FACULTY OF MECHANICAL ENGINEERING

12105 DEPARTMENT OF MECHANICS, BIOMECHANICS AND MECHATRONICS

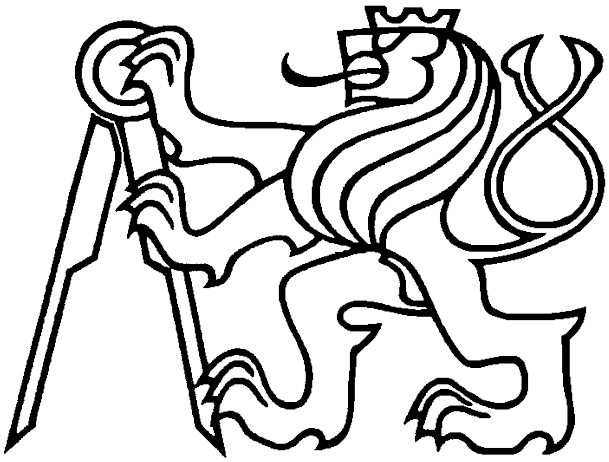

MASTER'S THESIS

Fatigue Analysis of a Combustion Engine Block

Bc. Kirill LOSHKAREV 2018/2019

CTU CZECH TECHNICAL UNIVERSITY IN PRAGUE

MASTER'S THESIS ASSIGNMENT

I. Personal and study details

Student's name: **Loshkarev Kirill** Personal ID number: **424669**

Faculty / Institute: **Faculty of Mechanical Engineering**

Department / Institute: **Department of Mechanics, Biomechanics and Mechatronics**

Study program: **Mechanical Engineering**

Branch of study: **Applied Mechanics**

II. Master's thesis details

Master's thesis title in English:

Fatigue analysis of a combustion engine block

Master's thesis title in Czech:

Únavová analýza bloku spalovacího motoru

Guidelines:

1. Make a literature review on uniaxial and multiaxial approaches in fatigue analysis also with regard to FEMFAT and FE-safe software.
2. Take over FEM model of the engine block and make any edits suitable for effective fatigue assessment.
3. Perform fatigue analysis in FEMFAT and FE-safe using selected approaches.
4. Collect and process the results of the FEM and fatigue calculations appropriately.
5. Compare the results obtained and draw conclusions.

Bibliography / sources:

Manuály Abaqus, FEMFAT, FE-safe
Růžička, M., Hanke, M., Rost, M.: Dynamická pevnost a životnost. ČVUT, 1987.

Name and workplace of master's thesis supervisor:

Ing. Martin Nesládek, Ph.D., Department of Mechanics, Biomechanics and Mechatronics, FME

Name and workplace of second master's thesis supervisor or consultant:

Date of master's thesis assignment: **22.10.2018** Deadline for master's thesis submission: **18.01.2019**

Assignment valid until: _____

Ing. Martin Nesládek, Ph.D.	prof. Ing. Milan Růžička, CSc.	prof. Ing. Michael Valášek, DrSc.
Supervisor's signature	Head of department's signature	Dean's signature

III. Assignment receipt

The student acknowledges that the master's thesis is an individual work. The student must produce his thesis without the assistance of others, with the exception of provided consultations. Within the master's thesis, the author must state the names of consultants and include a list of references.

31.10.2018
Date of assignment receipt

Student's signature

Annotation

Author's name:	Bc. Kirill Loshkarev
Title of master's thesis:	Fatigue Analysis of a Combustion Engine Block
Title of master's thesis (in Czech):	Únavová analýza bloku spalovacího motoru
Year:	2018/2019
Field of study:	Applied Mechanics
Department:	Department of Mechanics, Biomechanics and Mechatronics
Master's thesis supervisor:	Ing. Martin Nesládek, Ph.D., FME, CTU in Prague
Consultant:	Ing. Václav Uzlík, ŠKODA AUTO

Bibliographical data:	number of pages	69
	number of figures	77
	number of tables	16
	number of appendices	1

Keywords:

multiaxial fatigue, finite element method , fatigue post-processor, Abaqus, FE-safe, FEMFAT

Keywords (in Czech):

multiaxiální únava, metoda konečných prvků, únavový post-procesor, Abaqus, FE-safe, FEMFAT

Abstract:

The work deals with fatigue analysis of a combustion engine block. First of all, a short research of material fatigue with focus on lifetime prediction (especially using multiaxial approaches) is provided. Then a brief overview of fatigue post-processors FE-safe and FEMFAT follows where its functionality is described on an easy sample problem. Afterwards, Finite Element Analysis of an engine block is conducted in Abaqus software and its critical places are identified with respect to fatigue. The next step is creation of a submodel which contains these critical places. Finally, fatigue analysis of the submodel is carried out in FEMFAT and FE-safe and the conclusions are drawn.

Abstract (in Czech):

Práce se zabývá únavovou analýzou bloku spalovacího motoru. Nejprve je provedena krátká rešerše únavy materiálu se zaměřením na predikci životnosti, hlavně pak na multiaxiální přístupy. Pak bude čtenář seznámen s únavovými post-procesory FE-safe a FEMFAT během řešení jednoduchého ukázkového příkladu. Následně je proveden výpočet modelu spalovacího motoru pomocí metody konečných prvků v programu Abaqus a jeho rozbor s identifikací kritických míst z hlediska únavy. Dalším krokem je tvorba submodelu, který tato kritická místa obsahuje. Nakonec je provedena únavová analýza submodelu v FEMFAT a FE-safe a diskuse jejích výsledků.

Declaration

This thesis is a presentation of my original research work. Wherever contributions of others are involved, every effort is made to indicate this clearly, with due reference to the literature, and acknowledgement of collaborative research and discussions.
The work was done under the guidance of Ing. Martin Nesládek Ph.D. (Czech Technical University in Prague) and Ing. Václav Uzlík (ŠKODA AUTO).

Date:……. Signature:……

Acknowledgement

I would like to thank my supervisor Ing. Martin Nesládek Ph.D. for leadership and consultation of topics covered in the thesis. Next I would like to thank my consultant and chief of my internship in ŠKODA AUTO Ing. Václav Uzlík for making up the topic of this thesis, allowing me to work on it in EPO/5 department (Calculations and simulations of aggregates) and leading me through the whole work to its end. Also I would like to thank the colleagues from EPO/5 (especially Ing. Jan Sýkora and Ing. Jiří Bárta) for little but essential help during the work on this thesis.

Content

1 Introduction

The main target of this work is to perform fatigue analysis of the engine block using two different fatigue solvers (FEMFAT and FE-safe), to compare results and make conclusions.

The engine block will be analyzed by the method which is commonly used in practice, specifically in ŠKODA AUTO. It is based on:

1) Finite Element model creation including its meshing, assignment of boundary conditions, contacts and loads;
2) Finite Element Analysis (FEA) of the model in Abaqus program (other FEM software can be surely used, e.g. Ansys);
3) Reduction of global model to obtain a submodel and its FEA (optional);
4) Fatigue analysis of global model or its submodel in particular post-processor.

The process of fatigue analysis of an engine block or other aggregate is a comprehensive issue: at the beginning it is necessary to have CAD (Computer Aided Design) model of an analyzed part and its operating conditions. CAD construction is the work of a design engineer; then follow the simulations – e.g. EHD (Elastohydrodynamic) analyses of sliding bearings, MBS (Multibody Simulations) of crankshaft dynamics considering combustion pressures. The simulations are usually validated by experiments or, in the case of virtual assessment of a non-existing engine, predictively derived from previous experience.
Then the obtained CAD model is needed to prepare for FEA (Finite Element Analysis): the geometry has to be cleaned and then correctly meshed, the analysis parameters have to be assigned – material properties, boundary conditions, conditions of contact couplings and loading etc. After that, the FEA is carried out; it is also necessary to check if its result is plausible, e.g. if all contacts correctly worked.
Afterwards, the FEA result is taken to fatigue post-processors. Then the adjusting of fatigue analysis parameters is carried out – they have a significant influence on the final result. The user can choose a fatigue criterion as well as a way of safety factor evaluation, use of various corrections (relative stress gradient, elasto-plastic corrections, statistical influence, surface roughness etc.) – it depends on operating conditions of the aggregate and facilities of the used fatigue solver.
Generally speaking, the multiaxial fatigue approaches are the most used and reliable in practice – they can relatively correctly evaluate even complicated stress states. The way of damage parameter definition is also important – the critical plane method is often used for it, however exist alternative ones.
The last stage is the fatigue results evaluation – are calculated values of safety factors greater than minimum acceptable value (typically 1.2)?
For correct assessment of the fatigue results, it is necessary to have experience from previous projects and model validations with strain-gauge measures and pulse tests. A lot of factors play an important role: the used fatigue criterion, software, correctness of inputs for FEA and fatigue post-processor and also a comparison with results of previous analyses of similar aggregates.

Why is fatigue analysis of an engine block necessary?

The department of ŠKODA AUTO where I was attending my internship and working on this thesis is responsible for development, tests and release to series production of great amount of engines within Volkswagen concern. Virtual assessment of lifetime of engine parts is standard process in engine development to avoid material strength problems. An overload as well as a periodic loading of particular components is considered.

2 Overview of material fatigue

One of the most important limit state in mechanical engineering is material fatigue – up to 90% operation failures are caused by this damaging effect in the case that it was not properly considered during the design.

Limit fatigue state is the state when as the result of an effect of time-variable loading the construction will lose its functional eligibility, while maximum level of the oscillating stress is usually lower than ultimate tensile stress of the part. [1]

For describing cyclic material response some parameters need to be introduced, they are apparent in Fig. 2.1.

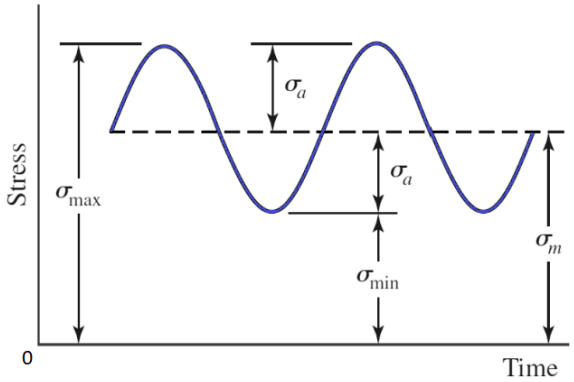

Fig. 2.1 Description of the cycle quantities.

One of the basic parameters that are used for description of cyclic material response is stress amplitude σ_a

$$\sigma_a = \frac{\sigma_{max} - \sigma_{min}}{2}, \tag{2.1}$$

mean stress σ_m

$$\sigma_m = \frac{\sigma_{max} + \sigma_{min}}{2} \tag{2.2}$$

and R factor

$$R = \frac{\sigma_{min}}{\sigma_{max}} \tag{2.3}$$

Dependence of R on type of loading cycle is illustrated in Fig. 2.2.

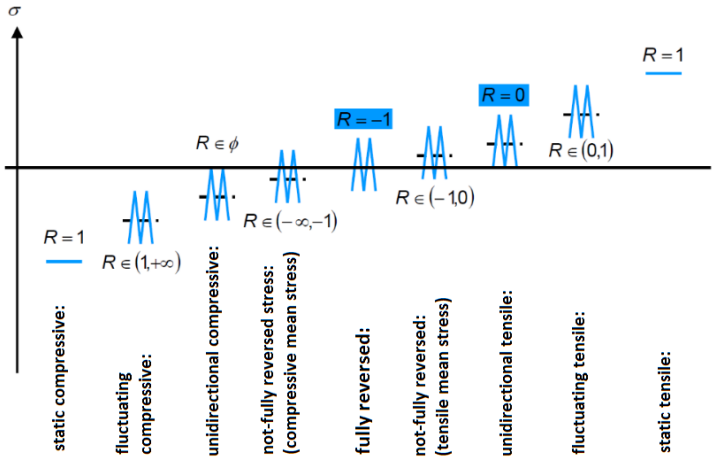

Fig. 2.2 Types of cycles depending on R [2].

One of the first experimental researcher of the material fatigue was railway engineer August Wöhler, who formulated empirical conclusions that are generally valid nowadays. Statistically evaluated experimental fatigue stress curve with stress amplitude σ_a and failure number of cycles N is called S-N curve or Wöhler curve. It is convenient to illustrate this curve in semilogaritmic (Fig. 2.3) or log-log coordinates (Fig. 2.4). These basic fatigue life curves are the result of experiments with constant mean stress σ_m or with constant R factor. [1]

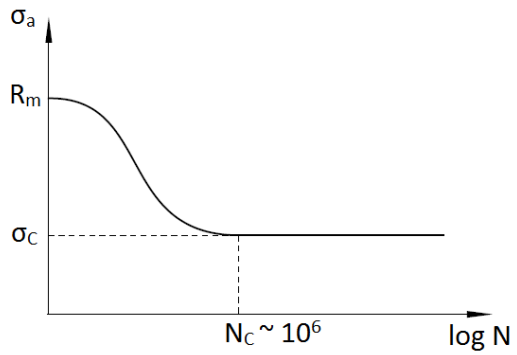

Fig. 2.3 S-N curve in semilog. coordinates.

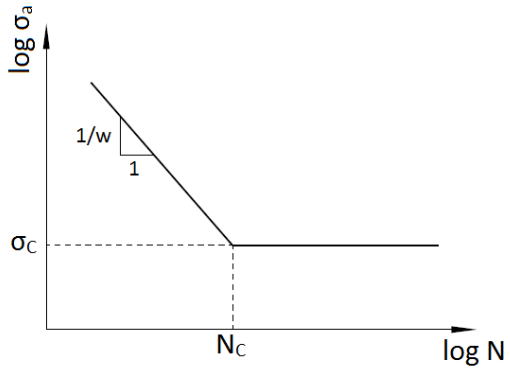

Fig. 2.4 S-N curve in log-log coordinates.

There are a lot of forms of the S-N curve description in technical literature. The simplest and often completely efficient is linear description of inclined part of S-N curve in log-log co-ordinates that is applicable in the range between yield and fatigue limit

$$\sigma_a^w \cdot N = C \,, \tag{2.4}$$

where constant C and exponent w will be defined by the statistic evaluation of the experimental results.

It is also possible to use Basquin approach of inclined part of the S-N curve

$$\sigma_a = \sigma_f'(2N)^b \,, \tag{2.5}$$

where σ_f' is fatigue strength coefficient and b is fatigue strength exponent. [1]

According to size of the stress amplitude the area of the S-N curve is split up to permanent and limited fatigue strength. The boarder of those two areas is the fatigue limit σ_C. The fatigue limit is oscillating limit stress that can be repeatedly excited in the part without failure at any number of cycles. Sometimes it has only conventional meaning, because some materials do not have constant fatigue limit, e.g. aluminum or magnesium alloys.

The basic fatigue limit is defined on smooth polished specimens ($\emptyset d = 7.5…10\ mm$) in fully reversed push-pull, bending or torsion loading. For other type of loading that is not fully reversed the mean stress value or R factor should be given.

Other criterion that divides the fatigue into 4 areas is number of cycles to failure:

a) **Quasi-static fracture area** – failure will occur after one or maximally after tens of cycles of loading. There is not a fatigue process, because the growth of fracture surface is very fast and the surface has signs of ductile fracture as well as at static fracture.
b) **Low-cycle fatigue area** – belongs to lifetime from 10^2 to 10^5 cycles maximally. The stresses in the part are so high that cyclic plastic deformations of the material are arising. The upper boarder of this area (10^4…10^5 cycles) is characterized by discontinuities in the S-N curve in the area of yield limit that show differences on fracture mechanism. Low-cycle fatigue fracture has usually observable rougher

structure with intercrystalline progress of fracture and cracked surface with pronounced plastic deformation.

c) **High-cycle fatigue** – covers lifetimes greater than $5 \cdot 10^4$ cycles. If the fatigue fracture occurs, it's characterized with smooth appearance with transcrystalline structure without apparent signs of plastic deformation. It's easy to differ it from the other part of fracture surface, which is made by a single pull resulting to severe plastic deformations. [1]
d) **Giga-cycle fatigue** – it's a quite new concept, refers to number of cycles about 10^9. Due to existence of giga-cycle fatigue it's possible to declare that materials don't have fatigue limit generally speaking; the term of fatigue limit mentioned above is only conventional value in high-cycle fatigue area and it's assumed that during operation that enormous number of cycles will not be applied to the part. This phenomenon is connected with material non-homogeneities when crack starts to grow under the surface of the part.

However exact determination of single fatigue areas is not clearly defined and is rather related to behavior of individual materials.

2.1 Fatigue lifetime prediction

There are several ways to classify the fatigue calculation methods. The decisive point can be e.g.:

- **Load effect localization**

- *Nominal methods* – the local state of loading is estimated from nominal stress and notch factor; the method is unsuitable for automated computation, because the notch factor is very hard to be correctly set from the FE-data. An interaction with the user's own computations is required.

- *Local methods* – local state of loading is assessed directly from FE-calculation results.

- **Physical meaning of the damage parameter**

- *Stress-based methods*;
- *Strain-based methods*;
- *Energy-based methods*.

- **Constitution of damage parameter**

- *Uniaxial analysis* – the damage parameter is constituted from some equivalent value of only load amplitude or range;

- *Multiaxial analysis* – the damage parameter consists of more than one load components (e.g. it is a composition of normal and shear stresses acting on an examined plane).

- **Expectation, if the load states on different planes can interact**

- *Critical plane methods* – final damage in the point examined is related to the damage found on some specific plane. Among all the planes examined, the maximum of the damage parameter is decisive.

- *Integral methods* – final damage is related to an integral of the damage parameter. Among all the planes examined, the average value of the damage parameter is decisive.

- **Question, how the critical plane is set**

- *MSSR method* (Maximum Shear Stress / Strain Range) – the maximum of the shear stress or strain range is looked for;

- *MD method* (Maximum Damage) – planes are scanned so that the maximum of the damage parameter was found. [3]

2.2 Uniaxial analysis

The specific property of uniaxial computation methods is that they convert the complex local stress or strain state in some examined point to one scalar value, which is the only input into the damage parameter of any uniaxial criteria for fatigue damage computation. The reduced equivalent value is achieved via: [3]

- von Mises equivalent stress

$$\sigma_{eqv} = \frac{1}{\sqrt{2}}\sqrt{\left(\sigma_{xx}-\sigma_{yy}\right)^2+\left(\sigma_{yy}-\sigma_{zz}\right)^2+(\sigma_{zz}-\sigma_{xx})^2+6\left(\sigma_{xy}^2+\sigma_{yz}^2+\sigma_{xz}^2\right)} \quad (2.6)$$

- Tresca's maximum shear stress theory, where the diameter of the maximum Mohr's circle (the difference between maximum σ_1 and minimum σ_3 principal stress) is looked for

$$\sigma_{eqv} = \sigma_1 - \sigma_3 \quad (2.7)$$

- Signed von Mises equivalent stress with a sign based on the sign of the first stress invariant

$$\sigma_{eqv} = \frac{sgn\left(\sigma_{xx}+\sigma_{yy}+\sigma_{zz}\right)}{\sqrt{2}}\sqrt{\left(\sigma_{xx}-\sigma_{yy}\right)^2+\left(\sigma_{yy}-\sigma_{zz}\right)^2+(\sigma_{zz}-\sigma_{xx})^2+6\left(\sigma_{xy}^2+\sigma_{yz}^2+\sigma_{xz}^2\right)} \quad (2.8)$$

- Modified equivalent stress on a plane (this option is based on the proposal introduced in FEMFAT v.4.6):

$$\sigma_{eqv} = sgn(N)\cdot\sqrt{N^2+\left(\frac{f_{-1}}{t_{-1}}\cdot C\right)^2}, \quad (2.9)$$

where *N* and *C* are the normal and shear stress on some examined plane and the symbols f_{-1} and t_{-1} stand for fatigue limits in fully reversed push-pull and fully reversed torsion.

The uniaxial methods are efficient for solution of cases where only one load channel is, or where more load channels act proportionally (see Fig. 2.5). If there is a non-proportional loading (see Fig. 2.6), the arising rotation of principal directions cannot be correctly reproduced in uniaxial methods – here the solution obtained from multiaxial methods should be preferred.

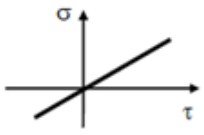

Fig. 2.5 An example of proportional loading [2].

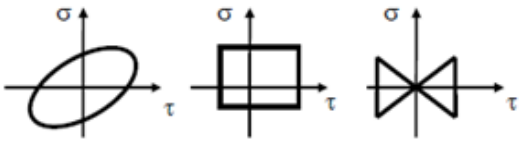

Fig. 2.6 Examples of non-proportional loadings [2].

2.2.1 The nominal stress approach

Thanks to its simplicity, this solution remains to be the most commonly used approach to fatigue calculation. It operates over S-N (Wöhler) curve, which relates level of loading (stress *S*) with number of cycles to final damage (*N*) – see Fig. 2.3 and Fig. 2.4.

The method often does not require knowledge of exact values of local loads in the critical place. Instead, a categorization of the notch and loading leads to a specified value of a notch factor. The level of loading is related to a nominal stress σ_{nom} found in a near cross-section. Then local maximum stress can be calculated with the shape factor K_t

$$K_t = \frac{\sigma_{max}}{\sigma_{nom}} \tag{2.10}$$

Basic fatigue limit σ_C to fatigue limit on notched geometry ratio is defined by the notch factor K_f

$$K_f = \frac{\sigma_C}{\sigma_C^x} \tag{2.11}$$

So the fatigue factor *n* is set as follows

$$n = \frac{K_t}{K_f} \tag{2.12}$$

The oldest method of calculation of K_f was invented by Thum who introduced the notch sensitivity of material *q*

$$q = \frac{K_f - 1}{K_t - 1} \tag{2.13}$$

In conjunction with knowledge of technological effects in the surface layer, effect of size of the component and other influences, a fatigue factor is set. The fatigue factor changes position of fatigue limit or slope of S-N curve so that it corresponds to the special loading conditions achieved in the critical place.

To set a notch factor for complicated structures can be a very speculative task. If there are more places examined, the notch factor has to be specified separately in each of them. The accessibility of FE-methods made possible to evaluate exact local values of loads in the critical places. It is very inconvenient for any user to compute the notch factor for each examined place and then relate it to that place. The local elastic stress analysis goes more straightforward. [3]

2.2.2 The local stress or strain approach

Local methods for fatigue calculation operate directly with more or less exact values of local loading in the critical place.

Two ways can be found among them:

a) Local elastic stress analysis – only elastic stresses are evaluated even in low-cycle fatigue, where pronounced plasticity effects can be expected.

b) Local elastic-plastic strain analysis – real elastic-plastic strain (or stress) state is processed. [3]

ad a) Local elastic stress analysis

This type of analysis initiated in nominal stress analysis. When the FEM started to be more widely used, the engineers got a better insight into precise description of local load states. A solution of nominal S-N curves looking for nominal cross-section, so that the nominal stress could be enumerated, became to be too cumbersome. There are other ways, how to describe the effect of shape and load changes. The most often method nowadays is to analyze the stress gradient around the node examined – see Fig. 2.7. [3]

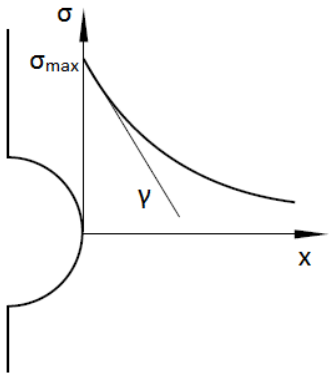

Fig. 2.7 Relative stress gradient method.

$$\gamma = \frac{1}{\sigma}\left(\frac{\partial \sigma_y}{\partial x}\right)_{x=0} \tag{2.14}$$

The fatigue factor *n* could be given as

$$n = f(\gamma, R_m) \equiv n_\gamma \,, \tag{2.15}$$

where R_m is ultimate strength of material.

Another method of description of the effect of shape is the critical distance method: stress σ_r which is used for further computations is read in some defined distance r_c which is a material parameter – see Fig. 2.8.

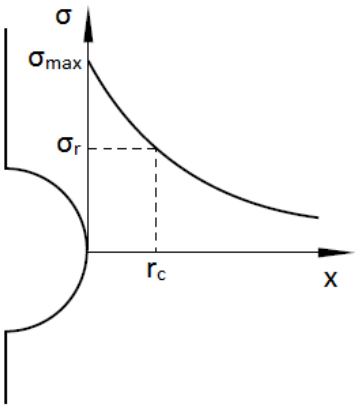

Fig. 2.8 Critical distance method.

The local elastic stress analysis can be used in mid-cycle as well as high-cycle region, but its use below 50.000 cycles should be very cautious. It requires an elastic FE-calculation only.

The advantage of such solution lies in the ability to post-process the elastic FE-solution, which is much more handy, than the elastic-plastic solution and in the possibility to superpose loads from individual load channels. [3]

ad b) Local elastic-plastic strain and stress analysis

Except for a local elastic stress analysis, this is the other common way how to examine low-cycle fatigue. There is an expectation hidden behind, that the local plastified volume of material on some examined industrial component can be very well replaced by a specimen with a cross-section size related to this volume. Such an expectation allows that the material parameters of Basquin-Manson-Coffin (BMC) curve (relating the number of cycles to initiation of some crack and amplitude of strain – see Fig. 2.9) obtained from common fatigue specimens to be used even in this finite volume. [3]

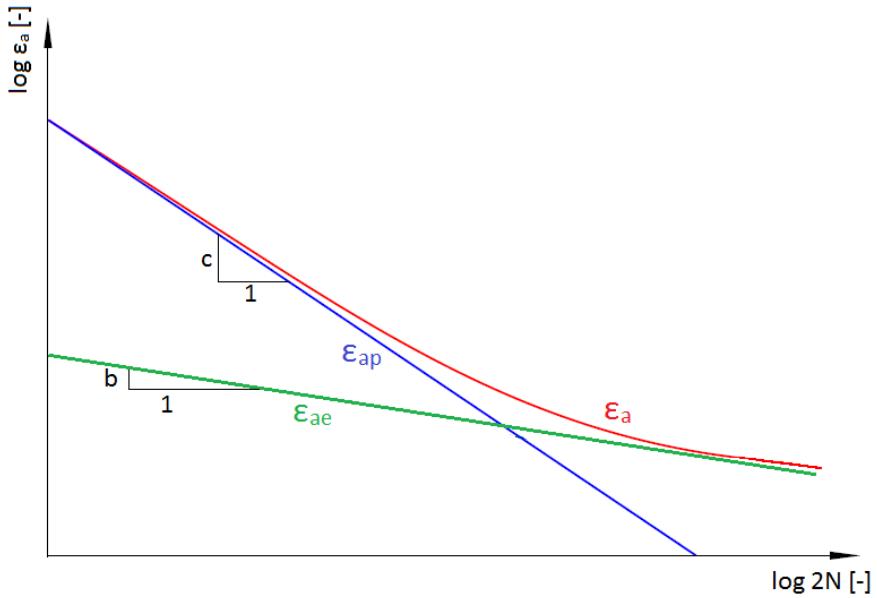

Fig. 2.9 Manson-Coffin curve.

The total amplitude of strain ε_a is

$$\varepsilon_a = \varepsilon_{ae} + \varepsilon_{ap} = \frac{\sigma_f'}{E}(2N)^b + \varepsilon_f'(2N)^c\,, \tag{2.16}$$

where σ_f' and b are coefficient and exponent of fatigue strength, ε_f' and c are coefficient and exponent of fatigue ductility.

The damage parameter is set from cyclic elastic-plastic local response. There is a lot of definitions of the damage parameter, however the most commonly used is the so-called SWT parameter (Smith, Watson & Topper)

$$P_{SWT} = \sqrt{(\sigma_a + \sigma_m)\varepsilon_a E} \tag{2.17}$$

The Manson-Coffin curve corresponds to the plastic part of strain. The local load data, which are confronted with the BMC curve, should thus conform to real elastic-plastic strains (or stresses). Their computation can be prepared in the FE-solver (non-linear transient analysis), or they can be prepared by post-processing of results of a linear FE-analysis (here Neuber and Glinka methods applicable to uniaxial computation only). [3]

Necessity to involve plasticity effects in the FE-computation or in the fatigue calculation sets relatively unpleasant obstacle to any simple engineering use of these methods.

2.3 Multiaxial analysis

A frequently used concept in multiaxial analysis is an examination of local load state on a plane. The normal and shear components on a plane are evaluated usually. An external sign of the criterion's multiaxiality is the composition of the damage parameter from at least two local load components. This is in contrast to uniaxial methods, which process one scalar equivalent load only.

The interaction of the two or more load quantities should better describe the problematic cases of non-proportional loading. It is expected usually, that the shear component has a primary effect on the lifetime, whereas the normal component has a secondary although significant effect. [3]

The commonly used formula in this group of criteria can be rewritten as a combination of shear τ and normal stress σ on some plane or planes

$$a \cdot f(\sigma) + b \cdot g(\tau) \leq f_{-1}\,, \tag{2.18}$$

or with wholly general left hand side (*LHS*)

$$LHS(load) \leq f_{-1}, \tag{2.19}$$

where the f_{-1} corresponds to fatigue limit in fully reversed tension-compression.
The fatigue index is then defined as

$$FI = \frac{LHS(load)}{f_{-1}} \tag{2.20}$$

If it is lower than one, the local loading is lower than fatigue limit. If the fatigue limit separates the region of infinite life (which is not wholly true), than the local place should withstand infinite loading of the range given. Higher values correspond to the other case – the component would break. [3]

There are several ways, in which the multiaxial criteria are build:

- *Critical plane criteria* – the damage in the point examined is related to one specific plane;
- *Integral criteria* – either whole damage parameter or some its components are integrated over all planes in the point examined - the introduction of the integration into the final damage corresponds to averaging of the plane specific damage parameter;
- *Criteria using Ilyushin deviatoric space* – one load parameter is retrieved from a load path transformed to a 5-dimensional Ilyushin space, the other parameter is related to some other unique scalar quantity. [3]

2.3.1 Critical plane method

This group of criteria expects that there is some unique critical plane to which the total damage in some point examined can be related. A position of the critical plane is influenced by an external loading or material parameters. There are different assumptions concerning its orientation: MSSR, MD and others, more detailed description will follow.

A very important target in the work with multiaxial fatigue criteria is to get to the goal as fast as possible. Thus the way of thorough mapping of fatigue damage parameter on a dense predefined system of planes by integral methods is not desirable here. If a more sparse

scanning is used, the important plane directions can be missed. This could be very unpleasant by critical plane methods, since only the plane with a maximum load or damage defines the exact damage of the whole construction.

There is one important aspect concerning this type of solution. Although there can be more planes with very high level of loading, no interaction among these different potential break systems is expected. [3]

a) MSSR method

Criteria utilising the MSSR concept expect, that damage in the point examined is directly related to the plane, where Maximum Shear Stress/Strain Range (MSSR) is found during whole load history. This assumption is in a close relation to the "axiom" that the shear stress has a primary influence on the crack initiation, but it wholly misses any secondary effect of the normal stress.

There are following methods that utilize the MSSR concept:
- McDiarmid method – it could be used as MD method;
- Wang & Brown method – it could be used as MD method;
- Matake method – this is the same damage parameter as in Findley method, which nevertheless utilizes the MD concept. [3]

b) MD method

The MD concept searches for maximum of the whole damage parameter. The method is much more straightforward in contrast to MSSR concept, where the maximization has two levels. The only target here is the maximum damage.

There are some methods that belong to this group of criteria (Findley, Socie, McDiarmid and other methods). As an example could serve *Papuga PCr*: [4]

The formulation of this model amplifies influence of the shear stress in contrast with the normal stress component. This is expressed by the square of the shear stress in combination with the linear term of the normal stress

$$\sqrt{a_{PC} \cdot \tau_a^2 + b_{PC} \cdot \left(\sigma_a + \frac{t_{-1}}{f_0}\sigma_m\right)} \leq f_{-1}\,, \tag{2.21}$$

where t_{-1} is fatigue limit in fully reversed torsion and f_0 is fatigue limit in repeated axial loading ($R = 0$).

Coefficients a_{PC} and b_{PC} are set in dependence on ratio $\kappa = \frac{f_{-1}}{t_{-1}}$

$$a_{PC} = \frac{\kappa^2}{2} + \frac{1}{2}\sqrt{\kappa^4 - \kappa^2}\,, b_{PC} = f_{-1} \;\; for \;\; \kappa < \sqrt{\frac{4}{3}}\,, \tag{2.22), (2.23}$$

$$a_{PC} = \left(\frac{4\kappa^2}{4 + \kappa^2}\right)^2\,, b_{PC} = \frac{8 f_{-1} \kappa^2 (4 - \kappa^2)}{(4 + \kappa^2)^2} \;\; for \;\; \kappa \geq \sqrt{\frac{4}{3}} \tag{2.24), (2.25}$$

The most comprehensive overview of the Papuga PCr criterion quality can be achieved by comparison of results in the FatLim Database [5]. This method gives the best results from all the methods there. [3]

c) Dang Van method

This approach is often applied in fatigue post-processors.

The following text is taken over from [4]:

The method defines the so-called mesoscopic stress deviator ***s(t)*** as

$$\boldsymbol{s}(t) = \boldsymbol{S}(t) - \boldsymbol{C}\,, \tag{2.26}$$

where ***S(t)*** is the deviatoric stress tensor in a time instant *t* and ***C*** is the so-called stabilized deviatoric residual stress tensor, which is computed as the center of the minimum circumscribed hypersphere enclosing the deviatoric stress path.

Then the fatigue criterion is a simple formula combining the instantaneous shear stress $\tau(t)$ and the hydrostatic stress $\sigma_H(t)$, the linear combination of which is about to be maximized over the time period

$$\max_t [a_{DV} \cdot \tau(t) + b_{DV} \cdot \sigma_H(t)] \leq f_{-1}\,, \tag{2.27}$$

where $\tau(t)$ can be computed as one half of the difference between the maximum and minimum eigenvalues of ***s(t)*** (i.e. one half of the Tresca stress of ***s(t)***)

$$\tau(t) = \frac{1}{2}\left[s_{1p}(t) - s_{3p}(t)\right] \tag{2.28}$$

The material parameters a_{DV} and b_{DV} are defined as

$$a_{DV} = \frac{f_{-1}}{t_{-1}}\,, \tag{2.29}$$

$$b_{DV} = 3 - \frac{3f_{-1}}{2t_{-1}}\,, \tag{2.30}$$

where f_{-1} and t_{-1} are fatigue limits in fully reversed axial loading and torsion.

2.3.2 Integral approach

The basic assumption of critical plane criteria that a load state on only one specific plane is responsible for total damage induced in the point examined does not seem to be wholly legitimate in the case where changes of principal directions during load history is very frequent (as e.g. is the case of a random multiaxial loading). On the other hand, the integral criteria expect an integration of the damage parameter related to individual planes over all of them. This in turn means that an average equivalent load over all planes is the resulting value of integral methods. The criteria are thus much closer to Ilyushin deviatoric space methods that also process complete load effect in the point than to critical plane criteria that are related to some plane found in this point. [3]

A relatively significant drawback of integral methods is their time consuming computation. In contrast to critical plane criteria, where some optimization routines were programmed, the integration process expects relatively small step in rotation of examined planes so that the final damage was computed acceptably accurately. This seems to be the main reason, why the integral criteria are not implemented in any commercial fatigue solver today and also why the methods of this type are designed only for use in the solution setting the exceedance of the local fatigue limit (where the assumption of a constant amplitude loading is hidden). [3]

2.4 Damage evaluation

Loading history could not mostly be characterized by constant amplitude and constant mean stress – see Fig. 2.10.

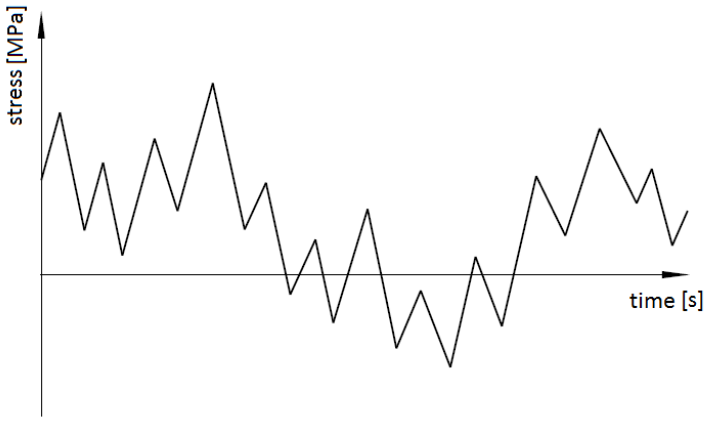

Fig. 2.10 Example of loading history with variable amplitude and mean stress.

A lot of methods can be used to evaluate influence of loading history on lifetime of the construction: methods of consequent, maximum or paired amplitudes, Wang-Brown method etc. The most frequently used is the Rain Flow method.

2.4.1 Rain Flow method

This method is derived from the study of cyclic strain properties and hysteresis between stress σ and strain ε of real metal materials. It tries to simulate its behavior in plastic stress-strain region. It is drew on the fact that plastic strain is decisive factor for fatigue damage accumulation which can be added up only by closed hysteresis loops. Half-cycles which do not close the hysteresis loop are also taken into consideration (see Fig. 2.11).

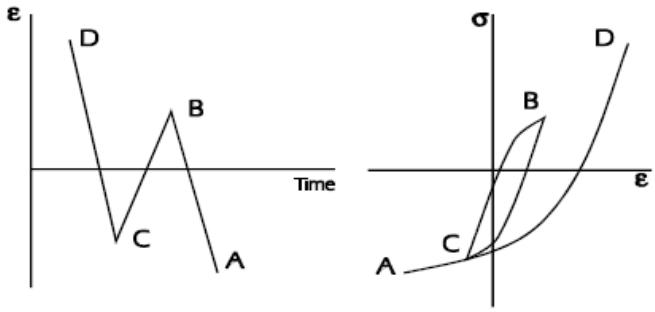

Fig. 2.11 Association between loading history and hysteresis loop. [6]

An example of use of Rain Flow method is in Fig. 2.12.

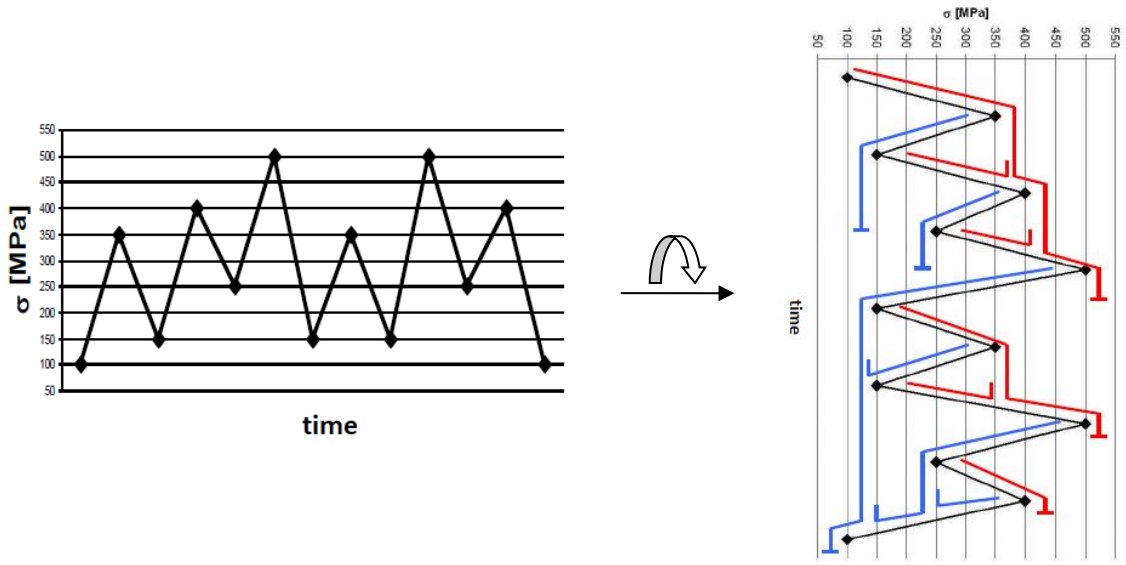

Fig. 2.12 Example of use of Rain Flow method. [2]

The result of this analysis is the Tab. 2.1, where n_i is frequency of occurrence of particular cycle in loading history and $\sigma_{a,eqv}$ is an equivalent amplitude of fully reversed cycle with the same fatigue effect, e.g. according to Goodman

$$\sigma_{a,eqv} = \frac{\sigma_a}{\left(1 - \frac{\sigma_m}{R_m}\right)} \tag{2.31}$$

Tab. 2.1 Example of use of Rain Flow method. [2]

σ_{min} [MPa]	σ_{max} [MPa]	n_i [-]	R [-]	σ_a [MPa]	σ_m [MPa]	$\sigma_{a,eqv}$ [MPa]
100	500	1	0,20	200	300	280
150	350	2	0,43	100	250	131
150	500	1	0,30	175	325	253
250	400	2	0,63	75	325	109

Note: there are other relations for equivalent amplitude cycle computation, e.g. according to Gerber

$$\sigma_{a,eqv} = \frac{\sigma_a}{1 - \left(\frac{\sigma_m}{R_m}\right)^2} \tag{2.32}$$

2.4.2 Damage accumulation

The process of damage of material is influenced by a lot of factors. Not only number and amplitude of damaging cycles should be counted, but also prestresses, time sequences, frequency and stress/strain rate, temperature, structure of the material and shape of the part. If a degree of fatigue damage D_n after n cycles of constant amplitude σ_a is taken as a set of partial damages caused by particular cycles, it can be written as

$$D_n = \sum_{i=1}^{n} \Delta D_i \tag{2.33}$$

The specimen which has initially damage $D_0 = 0$ is expected to break at N cycles when the degree of damage is reached the limit value

$$D_N = \sum_{i=1}^{N} \Delta D_i = 1 \tag{2.34}$$

The relation between damage and applied cycles n with amplitude $\sigma_a = const.$ can be defined as

$$D_n = \left(\frac{n}{N}\right)^m \tag{2.35}$$

where the number of cycles N is read for particular amplitude σ_a from the corresponding basic S-N curve.

If the exponent $m = 1$, it is about linear damage accumulation – *Palmgren-Miner hypothesis*. This is the oldest and simplest method of damage accumulation which is based on the assumption of uniform linear damage growth with every cycle

$$D_Z = \frac{n_1}{N_1} + \frac{n_2}{N_2} + \cdots + \frac{n_p}{N_p} = \sum_{i=1}^{p} \frac{n_i}{N_i} = \sum_{i=1}^{p} D_i \tag{2.36}$$

Expected number of repeatings of considered loading history up to fracture can be defined as

$$Z = \frac{1}{D_Z} \tag{2.37}$$

When considering materials with constant fatigue limit σ_C, could be made the conclusion that fatigue damage can be caused only by amplitudes higher than fatigue limit ($\sigma_a > \sigma_C$). It was proven that level of loading under fatigue limit in combination with episodic overloads above fatigue limit influences fatigue lifetime. Corten and Dolan offered a relatively easy modification of liner hypothesis: it is based on multiplication of S-N curve exponent by a coefficient – $k \cdot w$ (see Fig. 2.13). Damage effect is assumed on all levels of loading $\sigma_{ai} > 0$. N_p is the number of cycles up to fracture for prestress $\sigma_m = const.$ corresponding to maximum amplitude of the spectrum σ_{ap}. Constant k is a reduction of exponent w of basic S-N curve. It increases from value 0.7 for normal carbon steels up to 1.2 for high-strength steels and light alloys.

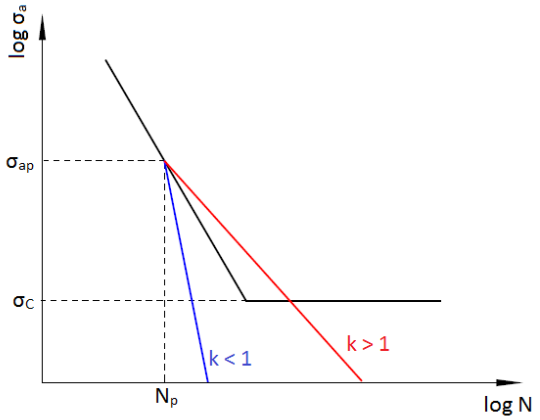

Fig. 2.13 Correction according to Corten & Dolan.

This method is simple and effective – it respects damage caused by level of loading lower than fatigue limit, so calculated values of fatigue lifetime are mostly safer than values got by Palmgren-Miner method. [1]

2.4.3 Safe fatigue life

Mostly the fatigue limit is given for so-called mean fatigue life, i.e. for probability of failure $P_f = 50\%$ (normal distribution is assumed) – see Fig. 2.14.

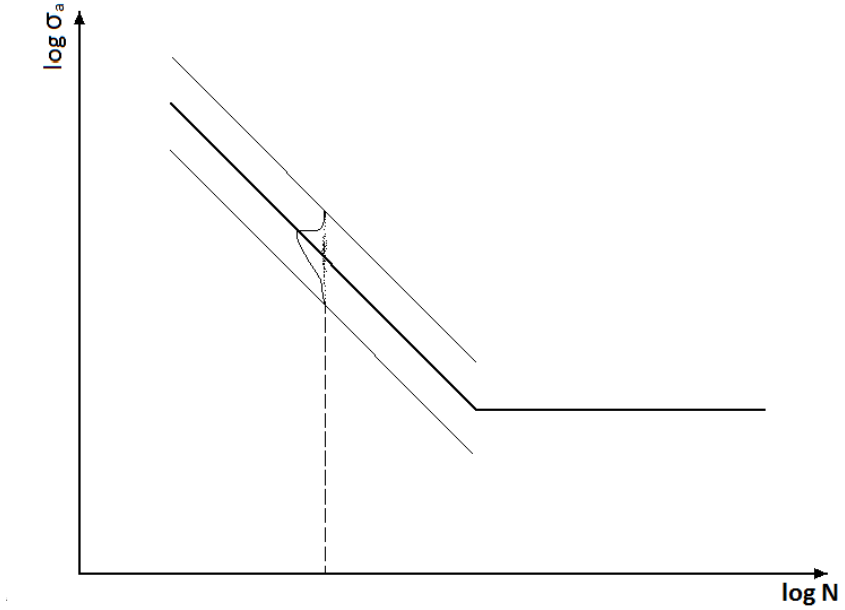

Fig. 2.14 S-N curve with normal distribution.

However for technical computations the failure probability is needed much lower – e.g. 0.001 up to 0.00001%.

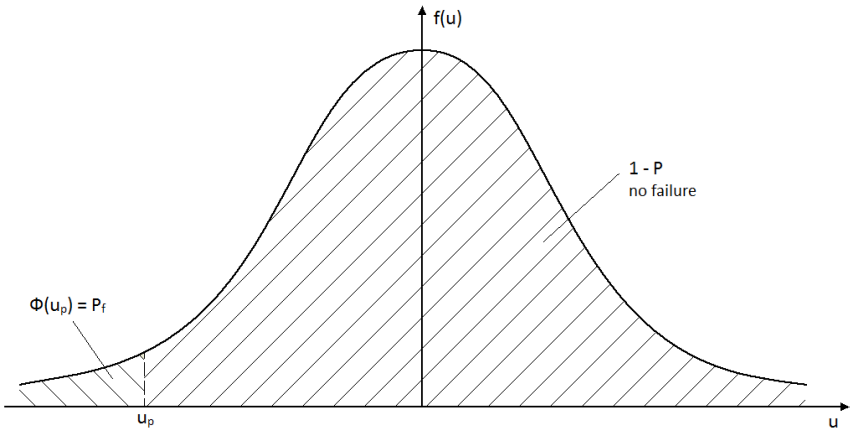

Fig. 2.15 Probability density function of normal distribution.

The quantile of failure probability u_p needs to be introduced – see also Fig. 2.15

$$u_p = \frac{\log L_B - \log L_{50\%}}{\sqrt{s^2_{\log N} + s^2_{\log n}}}, \tag{2.38}$$

where L_B is safe life of the part (desired failure probability), $L_{50\%}$ is mean fatigue life (failure probability is 50%), s_{logN} is life standard deviation of S-N curve, s_{logn} is life standard deviation of loading history.

Then the failure probability is defined as area to the left from the quantile u_p. To determine it the tables of normal distribution or a computational algorithm for calculating an integral of probability density function of normal distribution are needed.

3 Brief overview of FE-safe and FEMFAT functions

Basic functions and options of FE-safe and FEMFAT will be demonstrated on a simple instance. Besides, some theoretical backgrounds of these fatigue post-processors will be also discussed.

3.1 Assignment and analytical solution of a simple instance

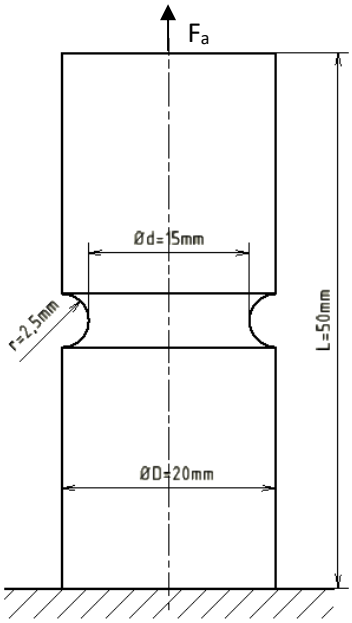

Fig. 3.1 The diagram of the problem.

Input

The notched part (see Fig. 3.1) is loaded by a fully-reversed axial force F_a = *12560 N*. The goal is to compute the maximum stress in the notch and to define the safety factor for infinite life.

The material is steel S235JR [7]:

$$R_m = 414\ MPa$$
$$E = 207000\ MPa$$
$$\sigma_C = 146\ MPa\ \ for\ \ N_C = 10^6$$
$$\tau_C = \frac{\sigma_C}{\sqrt{3}} = 84\ MPa$$

Analytical solution

The nominal stress amplitude $\sigma_{a,nom}$ in a section where the notch is placed is calculated by

$$\sigma_{a,nom} = \frac{4F_a}{\pi d^2} = 71.1\ MPa \qquad (3.1)$$

Then the stress concentration factor K_t is defined – see Fig. 3.2, Fig. 3.3 and Fig. 3.4.

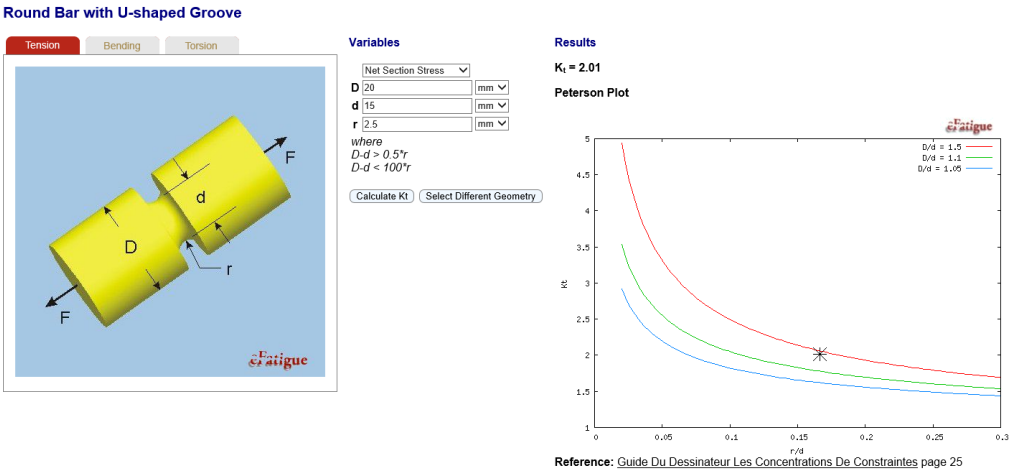

Reference: Guide Du Dessinateur Les Concentrations De Constraintes page 25

Fig. 3.2 The determination of the stress concentration factor K_t on efatigue.com [7].

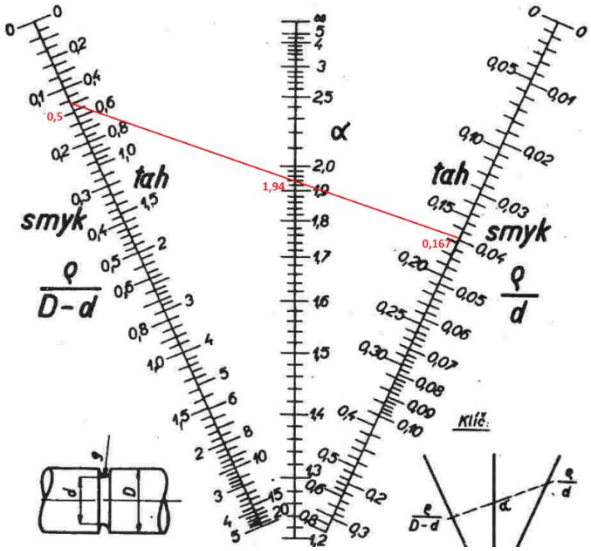

Fig. 3.3 The determination of α with nomograms. [1]

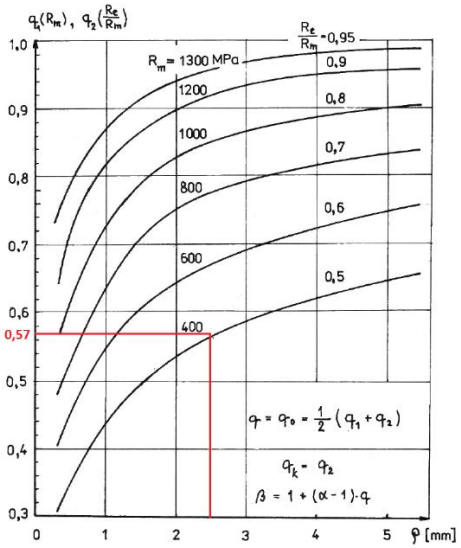

Fig. 3.4 The reading of q. [1]

The results are slightly different: $\alpha_{efat} = 2.01$ and $\alpha_{norm} = 1.94$. So the maximum stress in the notch σ_{max} is equal

$$\sigma_{max}^{anal} = \alpha\sigma_{nom} = (137.9 \div 142.9)MPa \tag{3.2}$$

The shape factor $\alpha = 1{,}98$ will be further considered.

Note: symbols K_t and α have the same meaning (stress concentration factor).

Then the notch sensitivity of the material is read from the Fig. 3. (*q = 0.57*) and the notch factor K_f is defined by using the Thum's relation as

$$K_f = 1 + q(K_t - 1) = 1.5586 \tag{3.3}$$

Then the reduced fatigue strength is determined σ_C^x

$$\sigma_C^x = \frac{\sigma_C}{K_f} = 93.67\ MPa \tag{3.4}$$

and finally the safety factor k_{anal} is calculated

$$\boldsymbol{k_{anal}} = \frac{\sigma_C^x}{\sigma_{nom}} = \mathbf{1.317} \tag{3.5}$$

Numerical solution

The model was created and meshed in ANSA software. Boundary conditions, kinematic coupling of nodes on the frontal surface and axial loading was also assigned – see Fig. 3.5.

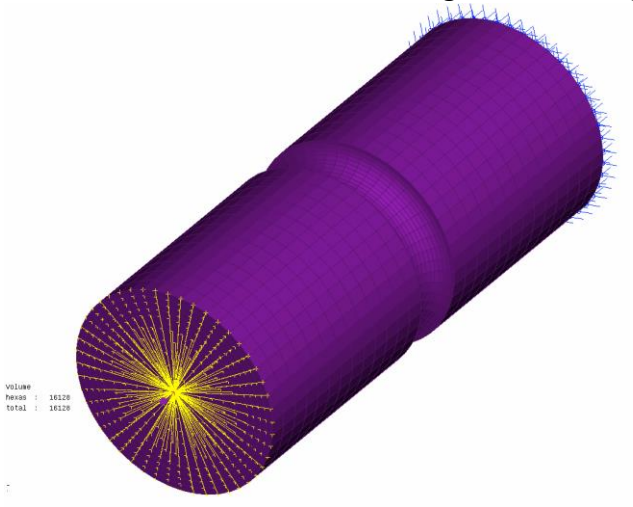

Fig. 3.5 Model creation and meshing in ANSA.

Afterwards the computation was carried out and the results were written into ODB-file which will serve as an input for fatigue post-processors (see Fig. 3.).

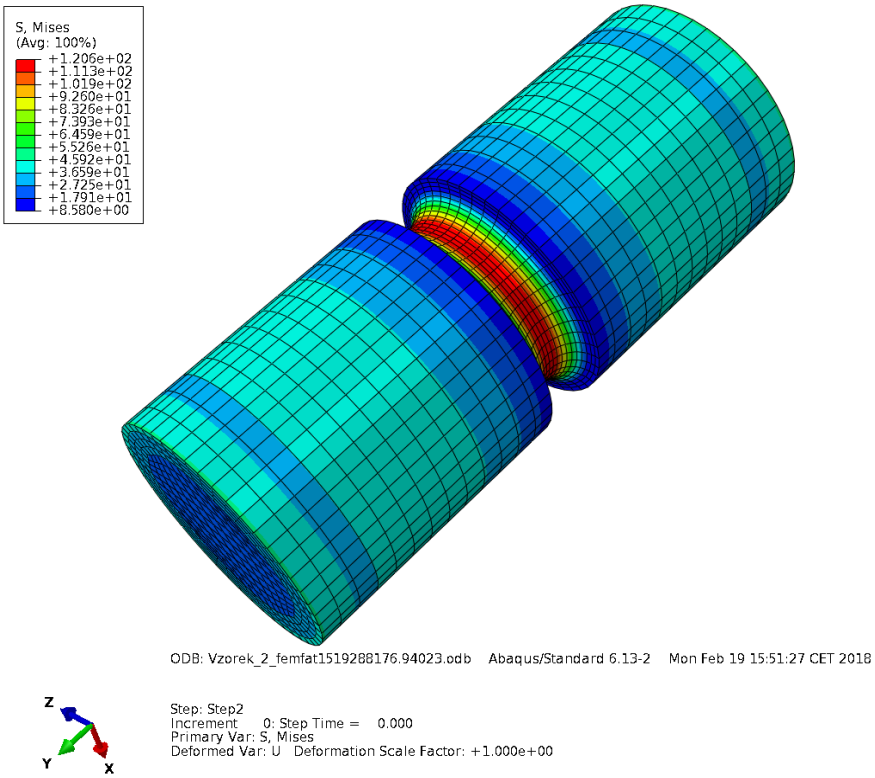

Fig. 3.6 The result of numerical computation.

As may be seen in Fig. 3.6, the maximum von Mises stress in the notch from FE-solution is $\boldsymbol{\sigma_{max}^{FEM} = 120.6\,MPa}$. This value does not belong to σ_{max}^{anal} interval, but it is situated acceptably close to desired value. However, the value computed by the FEA may be considered as more representative since it takes the biaxial stress state in the notch root into account.

3.2 FE-safe

The program FE-safe was developed by the company Safe Technology Ltd. in Sheffield (England, UK). This software is distributed by The 3DEXPERIENCE Company either with Abaqus software or as a stand-alone product. [8]

FE-safe is used by leading companies in automotive, heavy truck, off-highway, marine, defense, offshore, power generation, wind energy, medical engineering and many other industries.

Fig. 3.7 SIMULIA fe-safe.

FE-safe has been developed continuously since the early 1990's in collaboration with industry to ensure that it continues to set the benchmark for fatigue analysis software. FE-safe was the first commercially available fatigue analysis software to focus on modern multiaxial strain based fatigue methods. FE-safe provides unique capabilities for thermomechanical fatigue and creep-fatigue, the fatigue analysis of composite materials, the fatigue analysis of elastomers and the Verity Structural Stress Method for welded joints.

This software does not have an own internal interface for result visualization; however user has a lot of facilities for its import: Abaqus, Ansys, Nastran, Beasy, Hypermesh etc.

3.2.1 Key features of FE-safe

FE-safe includes a wide range of analysis methods, all of which are included in the standard package:
- Strain-based multiaxial fatigue algorithms—axial strain, shear strain, Brown-Miller with a multiaxial Neuber's rule and cyclic plasticity model;
- S-N curve analysis including multiaxial fatigue using axial stress or a new Brown-Miller analysis formulated for use with S-N curves;
- Dang Van multiaxial fatigue for high-cycle design;
- Plots of material data including the effect of temperature, strain rate etc.;
- Advanced analysis methods for fatigue of cast irons;
- Analysis of welded joints;
- High temperature fatigue;
- Analysis from elastic and elastic-plastic FEA stresses, linear and non-linear analysis;
- Automatic detection of surfaces;
- Automatic detection of fatigue hot-spots;
- Critical distance algorithms;
etc. [9]

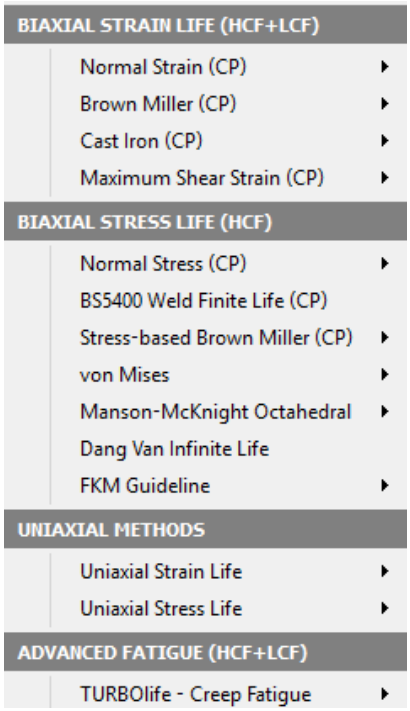

Fig. 3.8 Calculation methods offer in FE-safe.

3.2.2 Dang Van method (FE-safe)

This criterion is implemented in FE-safe as a multiaxial method of prediction of part lifetime. However this method in FE-safe slightly differs from the Dang Van criterion presented in Par. 2.3.1(c) of this thesis, so it is worth discussing it in detail.

This is the way, how the Dang Van method is explained in [6]:

On a microscopic scale, fatigue damage initiates in plastically deformed grains, and the stress state in individual grains will deform plastically even if the engineering stress is elastic. The restraining effect of adjacent grains will be to produce residual stresses in the plastically deformed grain. The Dang Van theory relates fatigue damage to the stress state in these grains.

The microscopic stress is related to the engineering stress by

$$\sigma_{ij}(P,t) = \Sigma_{ij}(P,t) + S_{ij}(P,t)\,, \tag{3.6}$$

where σ_{ij} is microscopic stress tensor, Σ_{ij} is macroscopic stress tensor, S_{ij} is residual stress tensor, P and t are position and time coordinates.

At long lives, applied stresses are low and cyclic loading causes the microscopic stresses to converge to a specific state and the residual stresses to stabilize (and become time-independent).

The Dang Van criterion for a specific level of loading (e.g. for an endurance limit) can be expressed as

$$\tau = \alpha S \leq \tau_0\,, \tag{3.7}$$

where τ is local shear stress, S is hydrostatic stress and α and τ_0 are material-specific constants.

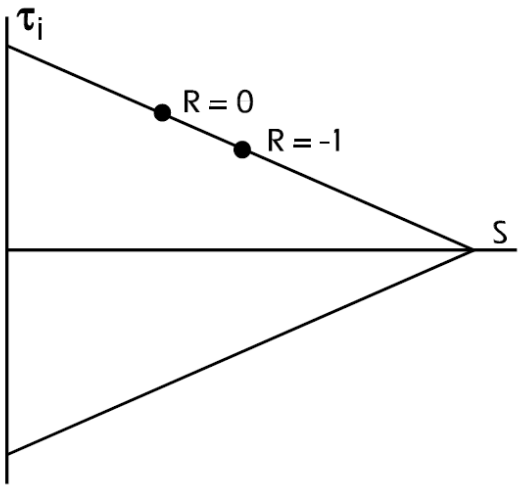

Fig. 3.9 Dang Van plot for the endurance limit. [6]

This equation is similar to a Haigh mean stress correction, i.e.

$$cyclic\ stress + mean\ stress = constant\ given\ at\ any\ endurance$$

and the equation can be plotted – see Fig. 3.9.

Two commonly available test cases are constant amplitude cyclic loading at zero mean stress (*R = -1*), and at zero minimum stress (*R = 0*). For these cases

$$S = \frac{\Sigma_{max}}{3} \; a \; \tau = \frac{\Sigma - \sigma_m}{2} \qquad (3.8), (3.9)$$

These cases give two points on the Dang Van diagram which allow the strain line to be constructed. A second line is a mirror image of the first one.

For complex biaxial stresses, the stabilizing residual stress is calculated by using one repeat of the signal, using kinematic and isotropic hardening. The microscopic stress tensor is then the difference between the macroscopic and residual stress tensors. Its time history can be plotted on the Dang Van diagram (see Fig. 3.10), and if its locus is within the two straight lines, the component will have infinite life. [6]

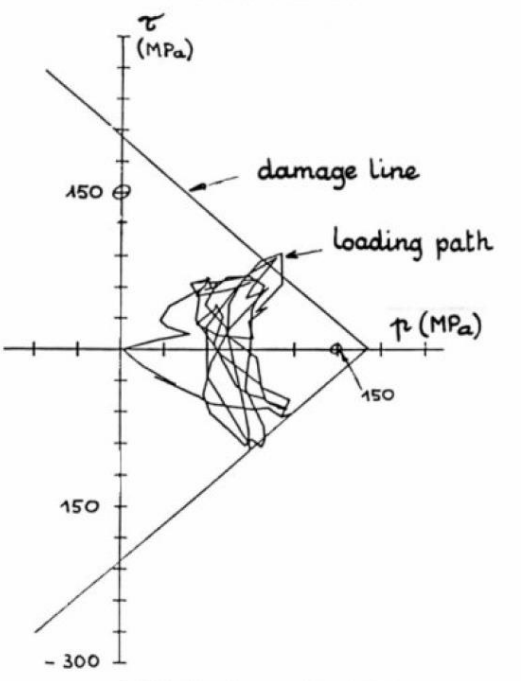

Fig. 3.10 Result from a Dang Van analysis. [5]

The distance between the loading path and the Dang Van line can be interpreted as a stress-based factor of strength. In Fig. 3.11, the ration *b/a* is the factor of safety. Alternatively, this ratio may be calculated using a vertical line.

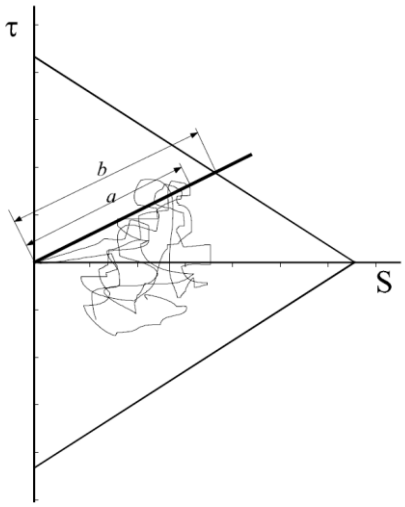

Fig. 3.11 Factor of safety from the Dang Van analysis. [6]

3.2.3 Analysis process

The analysis process in the way presented in [8] is valid for Brown-Miller algorithm (combined strain criterion). Partly it is valid for Normal Stresses algorithm (step 6 is skipped and steps 3 and 4 are skipped either when the plasticity correction (Neuber's rule) is turned off).

The fatigue life for each node is calculated as follows (*the following text is overtaken from [8]*):

1) The stress tensors are multiplied by the time history of the applied loading, to produce a time history of each of the 6 components of the stress tensor;
2) The time histories of the in-plane principal stresses are calculated;
3) The time histories of the three principal strains are calculated from the stresses;
4) A multiaxial cyclic plasticity model is used to convert the elastic stress-strain histories into elastic plastic stress-strain histories;
5) A 'critical plane' method is used to identify the most damaging plane by calculating the damage on planes at 10° intervals between 0° and 180° in the surface of the component;
6) For each of the critical planes, strains are resolved onto the three shear planes (1-2, 2-3 and 1-3);
7) The time history of the damage parameter (which in this case, using the Brown-Miller algorithm, is the shear and normal strain) is cycle counted;
8) Individual fatigue cycles are identified using a 'Rain Flow' cycle algorithm, the fatigue damage for each cycle is calculated and the total damage is summed;
9) The plane with the shortest life defines the plane of crack initiation, and this life is written to the output file.

Dang Van criterion in the form applied in FE-safe does not belong to the group of critical plane methods. At first, the principal stresses σ_{1P}, σ_{2P} and σ_{3P} are calculated from the stress tensor in the node; than the hydrostatic stress S is defined for this node

$$S = \frac{\sigma_{1P} + \sigma_{2P} + \sigma_{3P}}{3} \tag{3.10}$$

The shear stress τ can be assumed as maximum shear stress τ_{max}

$$\tau = \tau_{max} = \frac{\sigma_{1P} - \sigma_{3P}}{2} \tag{3.11}$$

Note: the relation 3.11 is not explicitly presented in [6].

3.2.4 Solution of the sample problem

At first the ODB-file is read and all needed data are derived from this file (for this case – stress values). Then the material with desired properties is assigned. After that for every dataset the loading history is created by multiplying by values imported from txt-file or entered directly in software (i.e. it is a possibility to carry out FE-solution considering loading history per unit).

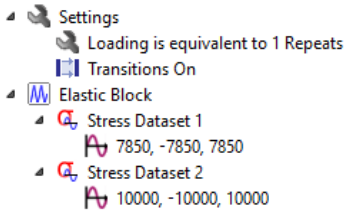

Fig. 3.12 An example of loading history.

Next in the window shown in Fig. 3.13 calculation for surface layer only, surface finish, material, calculation algorithm (multiaxial analysis with Dang Van criterion) is set; other parameters are left as default. As an option, location and name of the output file are offered to change. Since the safety factor for infinite life is to be defined, it is necessary to set ´Factor of Strength …´ – ´Infinite design life´.

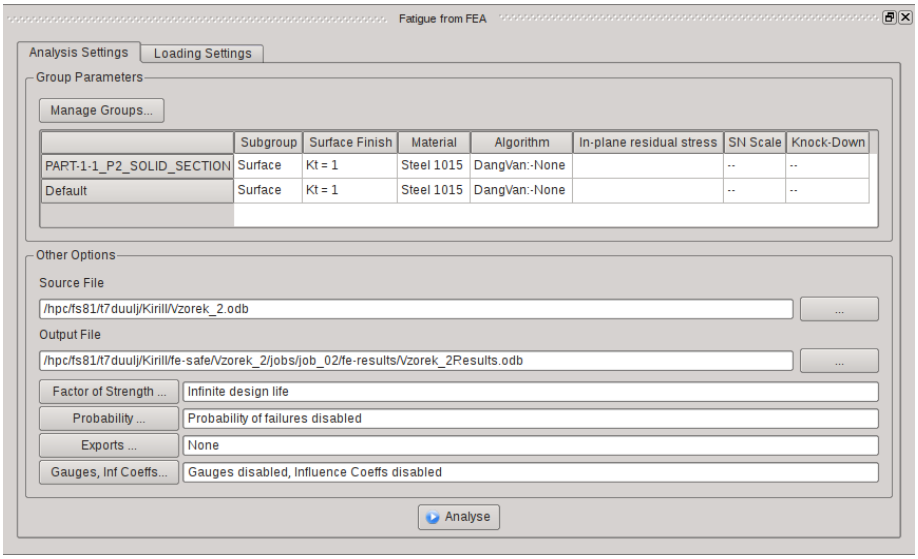

Fig. 3.13 Analysis settings.

An endurance limit in unidirectional loading f_0 is required for Dang Van analysis. It can be estimated by the relation

$$f_0 = \frac{2\sigma_f' f_{-1}}{\sigma_f' + f_{-1}}, \tag{3.12}$$

where f_{-1} is endurance limit in fully reversed loading and σ_f' is material parameter called curve intercept.

The calculation is carried out and result is shown in Fig. 3.14 (Abaqus Viewer was used for visualization of the ODB-file).

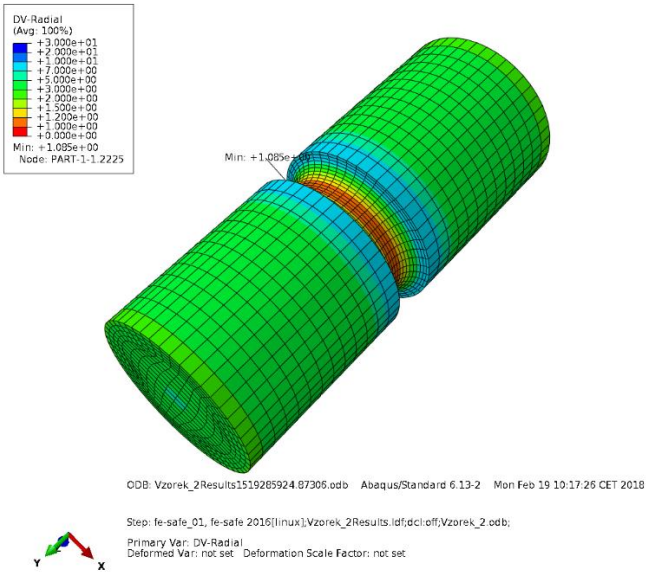

Fig. 3.14 Analysis result (Fe-safe – Dang Van method).

As shown in Fig. 3.14, the minimum value of safety factor is $\boldsymbol{k_{fe-safe} = 1.085}$.

3.3 FEMFAT

FEMFAT (Finite Element Method FATigue) was developed by ECS (Engineering Center Steyr GmbH & Co KG) which is a daughter company of Magna Steyr based in St Valentine (Austria).

Fig. 3.15 FEMFAT.

FEMFAT is a universally applicable software program for the fatigue analysis of statically and/or dynamically loaded components and complete systems. Based on stresses from finite element analysis, FEMFAT delivers analysis results such as fatigue life or damage as well as safety factors. This enables the identification of lightweight design potentials as well as potential weak spots already at an early product development phase.

The methods used are a combination of classical nominal-stress or stress-strain concepts and calculation standards such as TGL (germ. *Technische Gute und Lieferbedingungen*) and FKM (germ. *Forschungskuratorium Maschinenbau*) as well as methods that have been developed at ECS. These include the support effect concept by means of relative stress gradients and mean stress influence in combination with the critical cutting plane method as well as new methods for the determination of equivalent stresses. [10]

FEMFAT offers wide range of modules:

- **FEMFAT basic** – for strength analyses on components with proportional loading for which an FEM entity and calculated structural stresses exist;
- **FEMFAT max** – for strength analyses on components with multiple axis loading on the basis of load-time curves from multi-body simulation or recorded measurement data;
- **FEMFAT plast** – can be used to take stress redistribution for local plastification into consideration;
- **FEMFAT weld** – a module enabling very precise and reliable analysis of the fatigue behavior of complex welded structures

etc. [11]

The interface FEMFAT LAB is also offered which is the binding link between test track, laboratory and CAE (*Computer Aided Engineering*). It's a powerful software solution to visualize and analyze large amounts of data. FEMFAT LAB analyzes time histories with millions of data points and hundreds of channels within seconds. [10]

3.3.1 Analysis criterion

When adjusting analysis settings in FEMFAT, ´Stress Selection´ is usually left as Automatic – see Fig. 3.16.

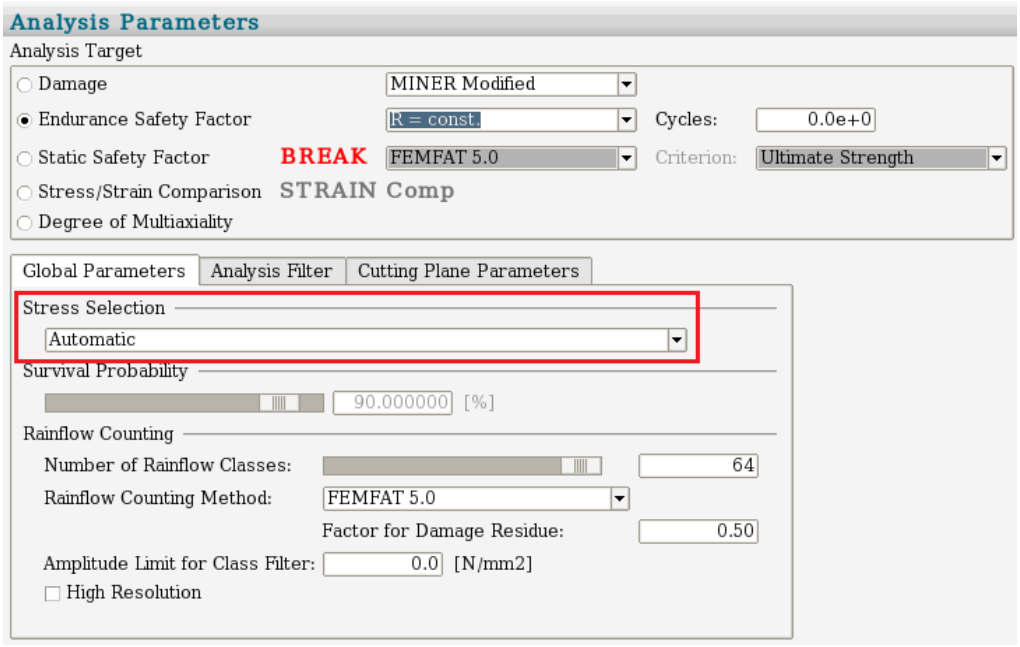

Fig. 3.16 Analysis parameters (FEMFAT).

It means that the program branches automatically based on the material assigned to the current node to be analyzed:

- Gray cast iron – assessment using Normal Stress in Critical Plane;
- All other materials – assessment using Scaled Normal Stress in Critical Plane. [11]

Gray cast irons will not be considered in this thesis, so the **Scaled Normal Stress in Critical Plane** method needs to be discussed (*the following text was taken over from [11]*):

Procedure is as follows:

1) Calculation of principal normal stresses $\sigma_1 > \sigma_2 > \sigma_3$ at every point in time. In *ChannelMAX* the existing superimposed stress states are used.

2) Calculation of the ratio of minimum/maximum principal normal stress at all times:

$$V = \frac{\sigma_3}{\sigma_1} \quad for \ |\sigma_1| > |\sigma_3| \tag{3.13}$$

$$V = \frac{\sigma_1}{\sigma_3} \quad for \ |\sigma_3| > |\sigma_1| \tag{3.14}$$

V is a value between -1 and +1 has the following meanings:

- *V = -1*: dominant shear load
- *V = 0*: dominant tensile/compressive load
- *V = +1*: hydrostatic stress state

3) The stress tensor at all times is now scaled as a function of *V*. The scaling factor is

$$f = 1 + (1 - k) \cdot V, \qquad where\ k = \frac{\sigma_W}{\tau_W} \tag{3.15}$$

Note: σ_W and τ_W are endurance limits in tensile and shear loading.

So the stress remains unaltered for tension/compression. For shear it is scaled up by the factor *k*, in order to model the damaging effect of shear. For the hydrostatic stress state, *f* is linearly extrapolated. This really makes sense because the reduction of the stress state associated with it is compliant with the maximum shear strain energy criterion.

4) The critical cutting plane method is subsequently employed. The Rain Flow classification of the normal stress with subsequent damage analysis using the influence parameter concept is performed in the cutting plane.

Note: using this option can solve the problem of signs for some equivalent stresses.

3.3.2 Solution of the sample problem

The sample problem will be solved using multiaxial approaches of lifetime prediction, so ***FEMFAT TransMAX*** module will be used.

Firstly, geometry of the part is read, e.g. from ODB-file – see Fig. 3.17.

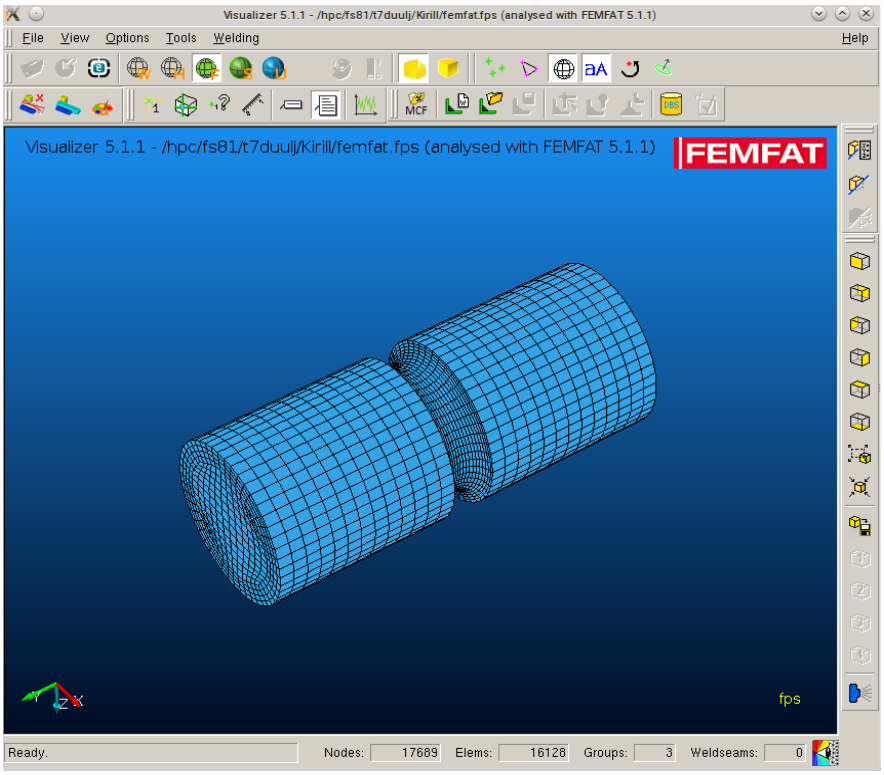

Fig. 3.17 Reading the geometry from ODB-file.

Then the loading is read separately, e.g. from the same file like in the previous step – see Fig. 3.18.

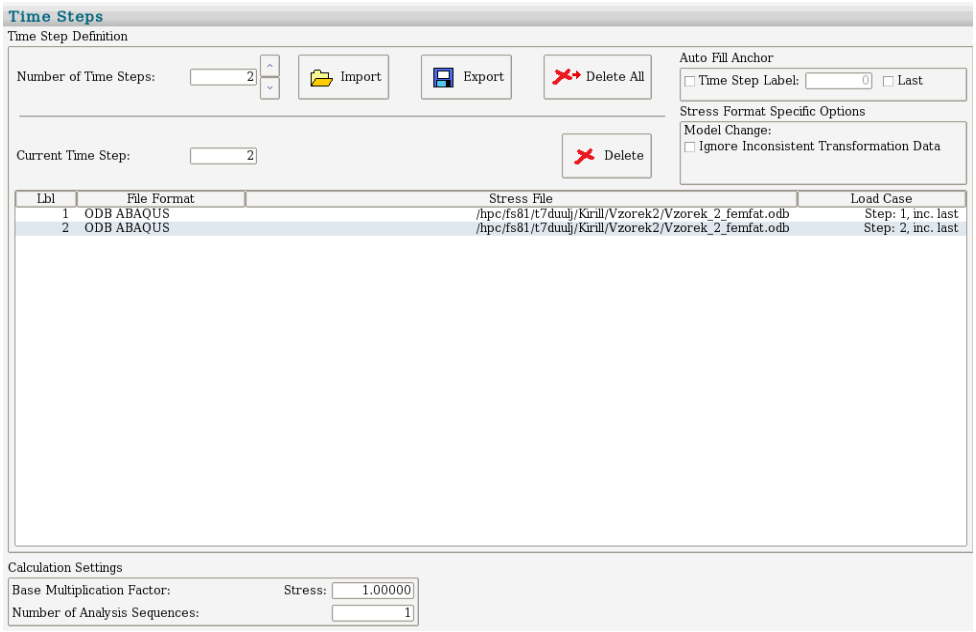

Fig. 3.18 Reading the loading.

Next the material is assigned or it is made out of entered properties by Material Generator (see Fig. 3.19).

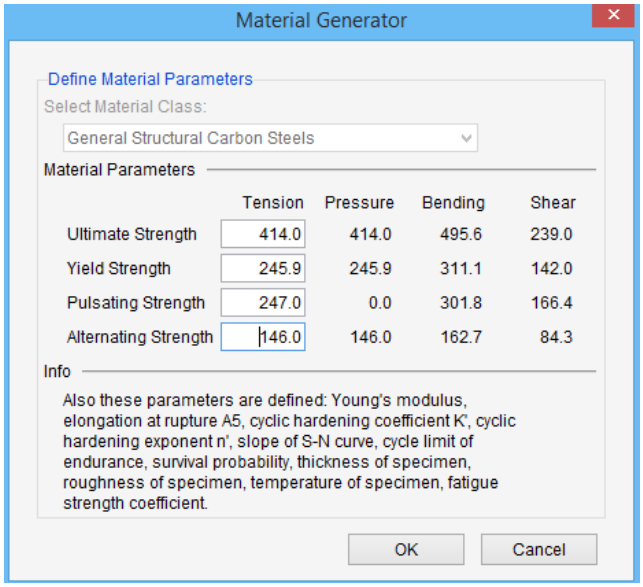

Fig. 3.19 Material Generator.

After that other options that influence the calculation are set: use of relative stress gradient, consideration of mean stress effect, surface finish etc. – see Fig. 3.20.

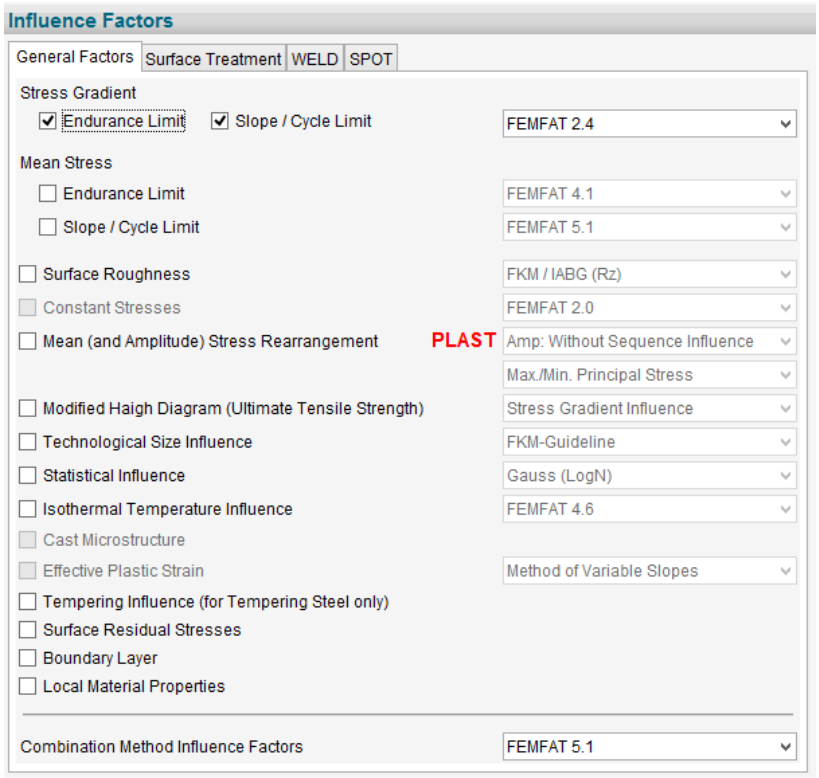

Fig. 3.20 Influence Factors.

Then the analysis parameters are defined: analysis target (the safety factor for infinite life at constant *R* ratio), damage accumulation method etc. – see Fig. 3.21.

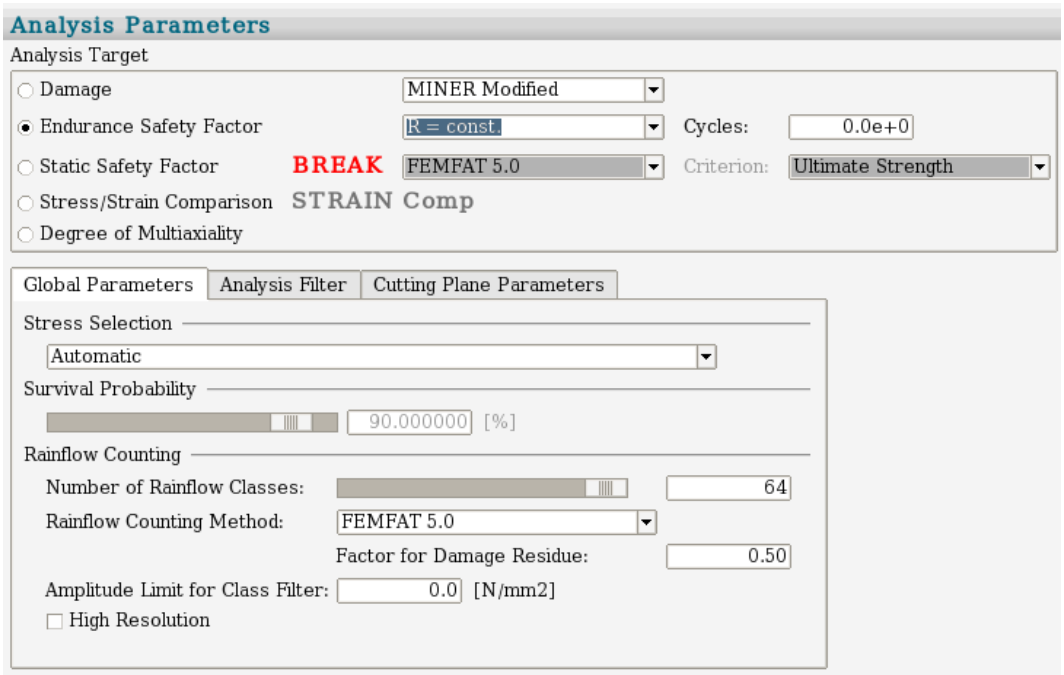

Fig. 3.21 Analysis parameters.

Moreover the type of the result file is set (ODB Abaqus), the scratch data are created (the file that contains all stresses from the model), input data are controlled and finally the fatigue calculation is carried out (the results are shown in Fig. 3.22).

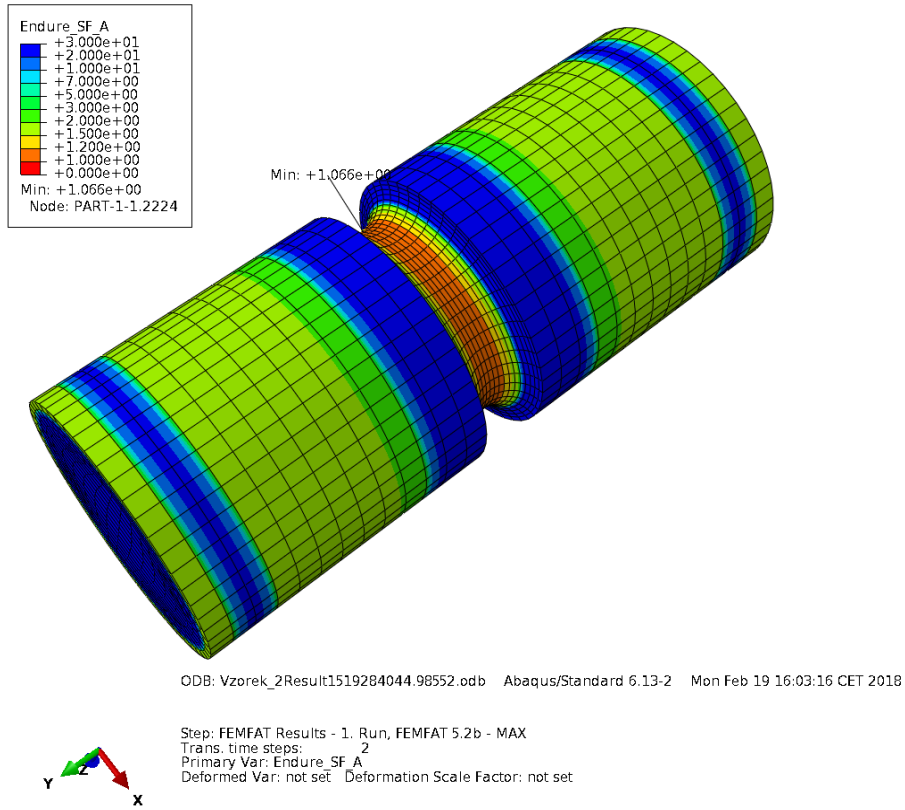

Fig. 3.22 The results of calculation in FEMFAT.

As shown in Fig. 3.22, the minimum value of safety factor is $\boldsymbol{k_{FEMFAT} = 1.066}$.

3.4 Discussion of the results

All results of the sample problem solution are presented in Tab. 3..

Tab. 3.1 The results of the fatigue calculations.

	Analytically	FE-safe	FEMFAT
Safety factor *k* [-]	**1.317**	**1.085**	**1.066**

The data in Tab. 3.1 show that the safety factor calculated analytically is significantly higher than the safety factor calculated by the fatigue post-processors. The results obtained by FE-safe and FEMFAT are almost equal – it implies that there is probably no mistake here; the issue might be an inaccuracy of the notch factor and the notch sensitivity determination by tables and nomograms as well as the type of stress used for analysis (nominal axial stress vs. full stress tensors).

4 Model and analysis of the engine block

The concept of the analysis is:

1) Creation and calculation of the global model;
2) Definition of the critical place/places;
3) Reduction of the global model to make a submodel that contains defined critical places from step 2;
4) Submodel calculation and its comparison with global model calculation;
5) Fatigue analysis of the submodel.

The whole procedure of making a submodel is necessary (in this case) to reduce difficulty and computational time of fatigue analyses in fatigue post-processors.

The Finite Element Analysis (FEA) will be linear elastic. Essential corrections due to elasto-plastic material behavior will be applied during fatigue analyses.

4.1 Conditions of the FE-solution

The calculation and its analysis will be conducted with an engine R4 1.5 l which is now produced in China. The engine block is made from the aluminum alloy AlSi9Cu3, the engine head – from AlSi6Cu4 material. The block and the head are sealed and fastened by 10 bolts M9 12.9 which are tightened up to yield strength. The bearing caps are made from the ductile iron GJS500 and mounted by 10 bolts M10 8.8 which are also tightened up to yield strength.

The engine block is loaded by mounting and operational forces: dynamic forces from the crankshaft, pressure in the cylinders and thermal effects. However, the calculation will be conducted at room temperature (20 °C): work temperature of the engine oil is considered about 140 °C – there is no significant degradation of mechanical properties of the aluminum alloy at this temperature (thermomechanical behavior of this material type is considered to start at 250 °C). Besides other things, there is lack of information about fatigue behavior of AlSi9Cu3 alloy at elevated temperatures; however, this omission will be taken into account when analyzing the obtained safety factors.

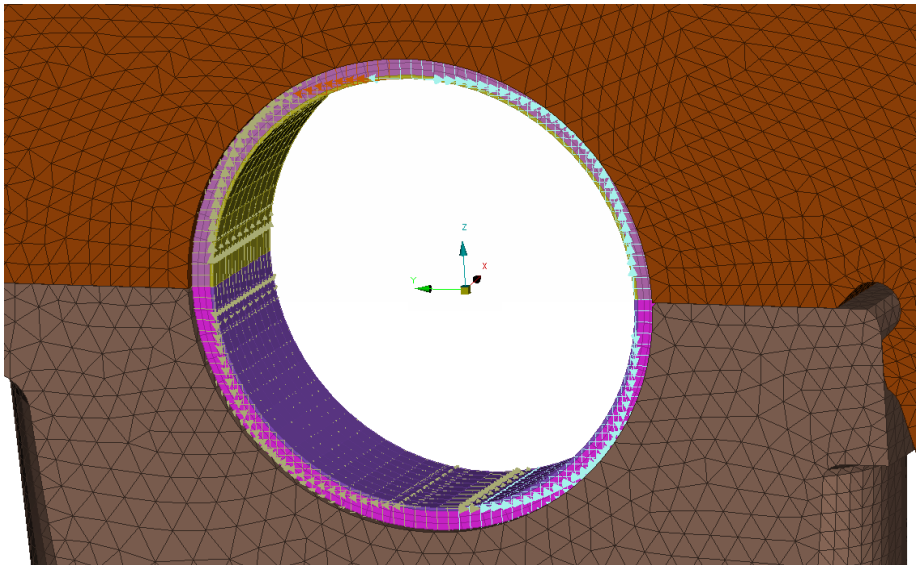

Fig. 4.1 Application of the dynamic load from the crankshaft.

Then the pressure effects in the cylinders will be neglected – they play an important role in the upper part of the engine block and in its head. Taking into account long-standing experience of ŠKODA AUTO employees, comparing with the dynamic load from the crankshaft, these pressure effects in the cylinders can be omitted in fatigue calculations – the bottom part of the engine block is more cracking-prone, especially in a groove where the bearing cap leans against the engine block (see the discussion further in the thesis work).

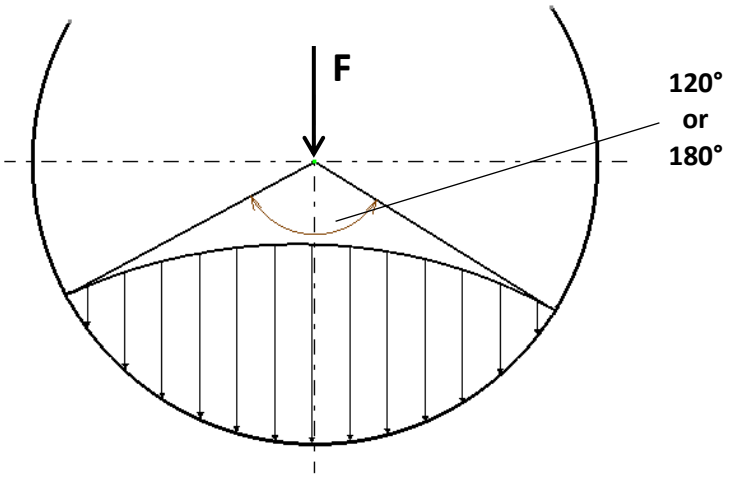

Fig. 4.2 Cosine distribution of force.

Force values in individual nodes at every load step (see Fig. 4.1) are taken over from Multibody Dynamics using cosine distribution of force (see Fig. 4.2) – for the particular bearing at the particular load step (in other words, at the particular rotation angle of the crankshaft) a diagram like the one in Fig. 4.3 is created. One colour of the particular line in Fig. 4.3 represents load at the particular engine speed – the result load at the specific load step is defined like an envelope of those lines.

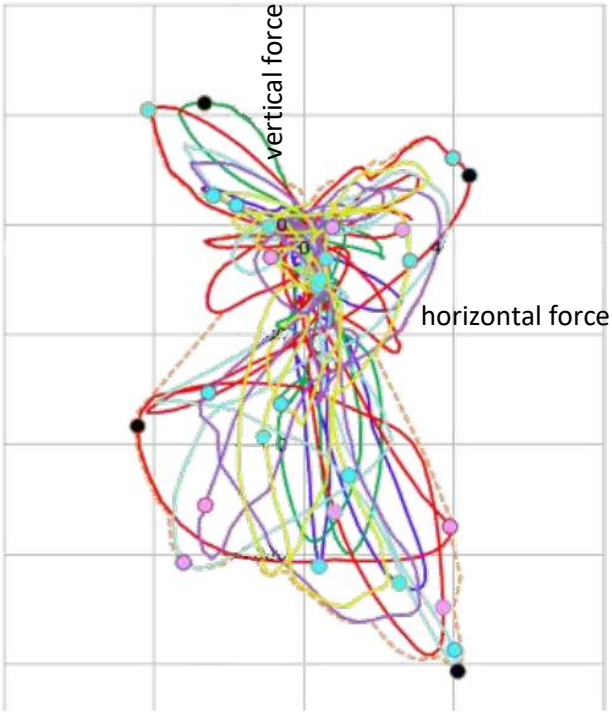

Fig. 4.3 Diagram of dynamic load at the particular loading step.

The points in Fig. 4.3 stand for maximum load at the specific engine speed.

4.2 The model of engine block

The global isometric view of the analyzed engine block is in Fig. 4.4.

The mesh was mostly made of tetrahedral quadratic elements.

The same angle of isometric view of engine block without the head (and the sealing) is provided in Fig. 4.5.

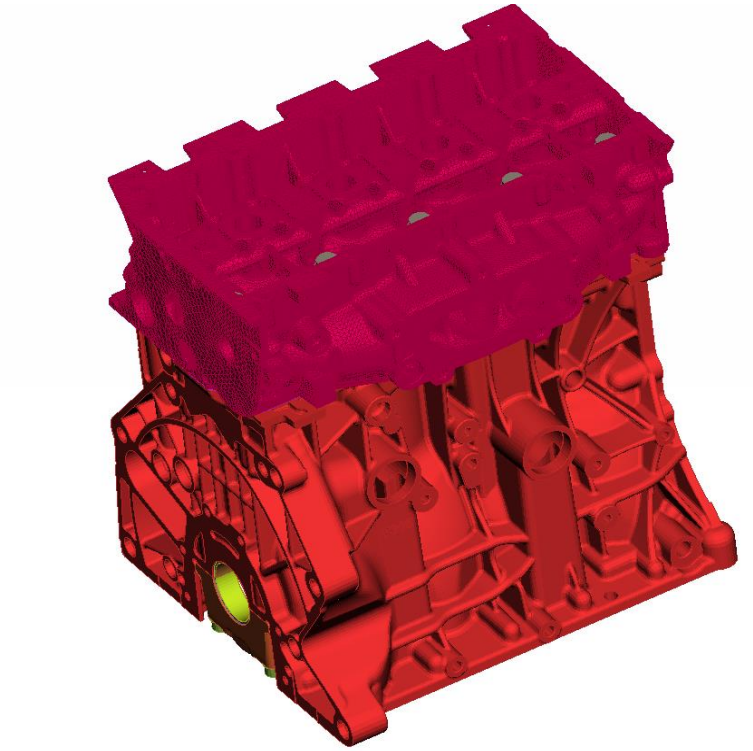

Fig. 4.4 Isometric view of the engine block including the engine head.

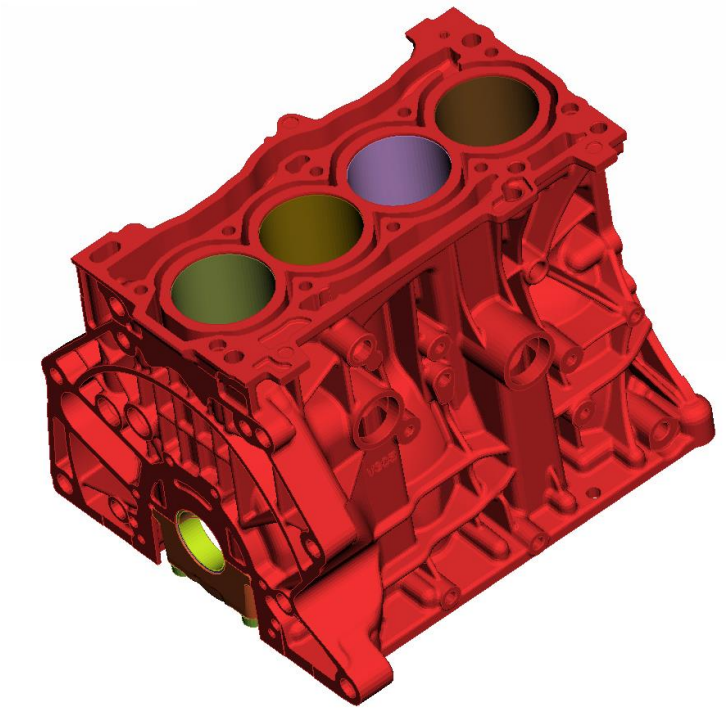

Fig. 4.5 Isometric view of the engine block without the head.

The side view of the engine block is in Fig. 4.6.

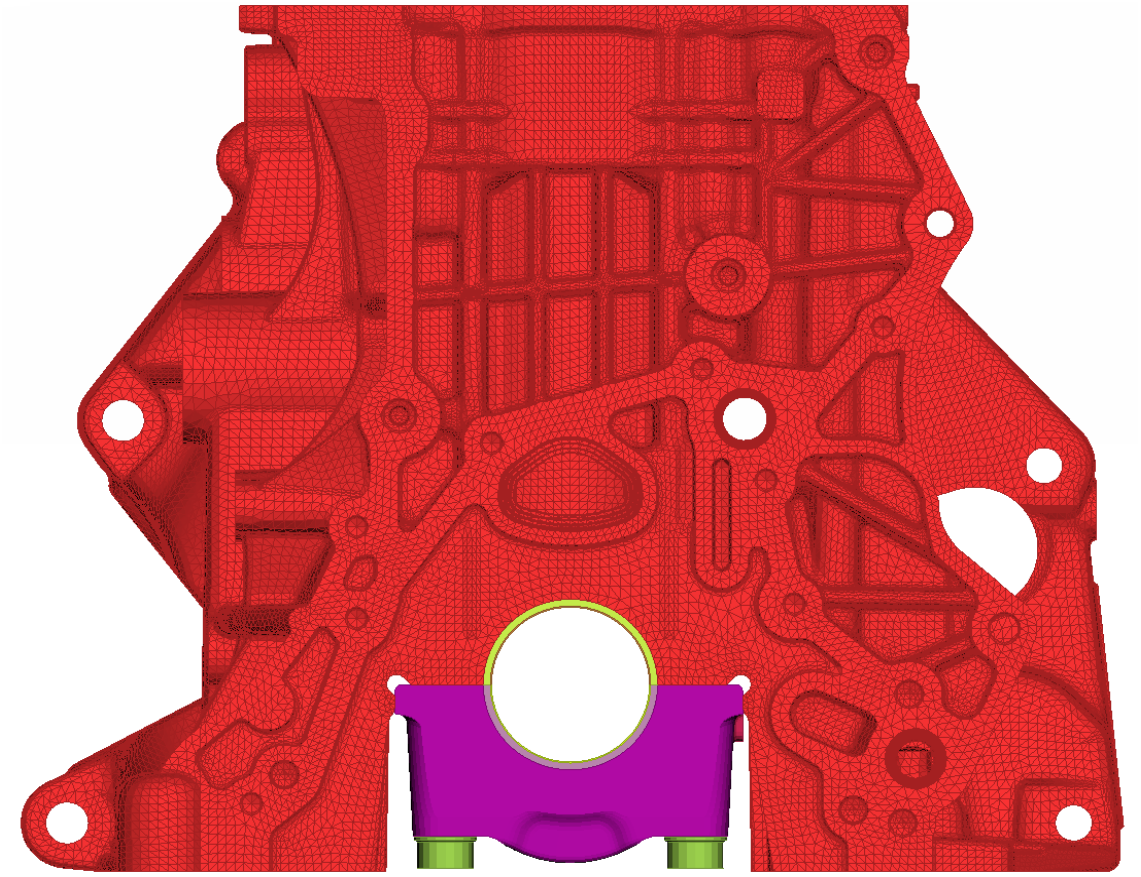

Fig. 4.6 Side view of the engine block.

Crankshaft bearing assembly is shown in Fig. 4.7Fig. 4..

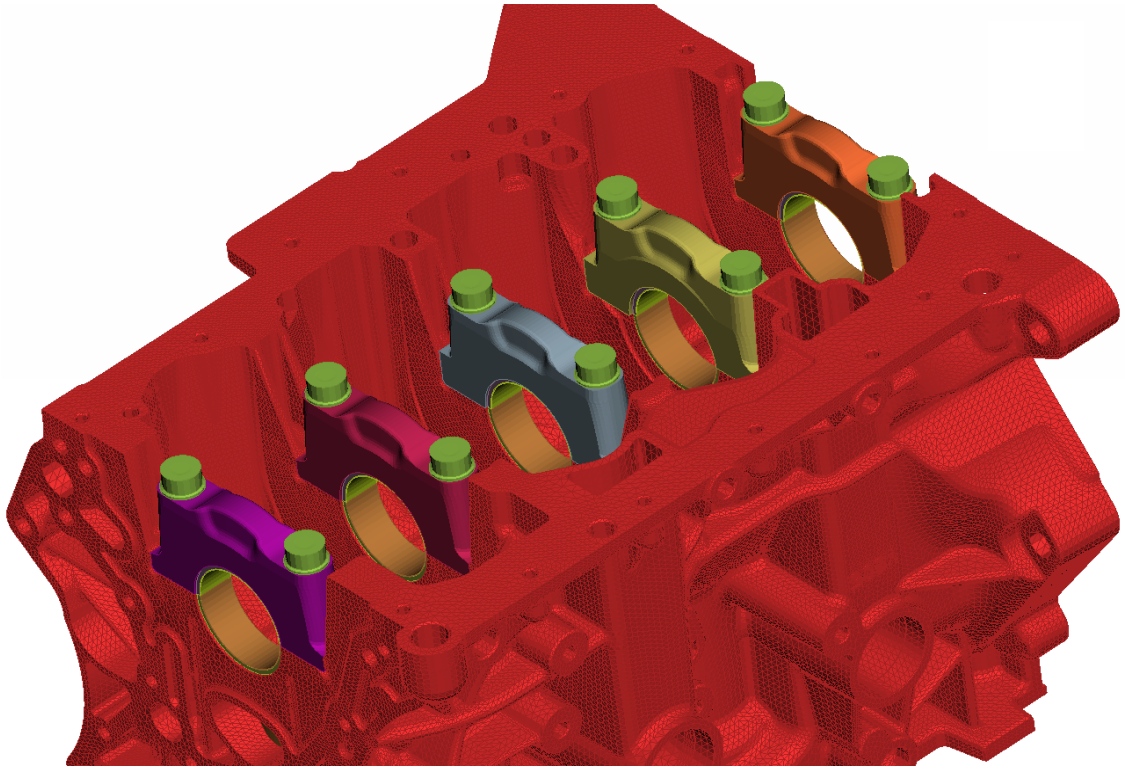

Fig. 4.7 View of the crankshaft bearing assembly.

Assembly of the whole engine block can be seen in Fig. 4.8 and Fig. 4.9 (the mounting places are represented with a purple colour). In the places in Fig. 4.8 all displacements are removed; in Fig. 4.9 *x* axis displacements are left.

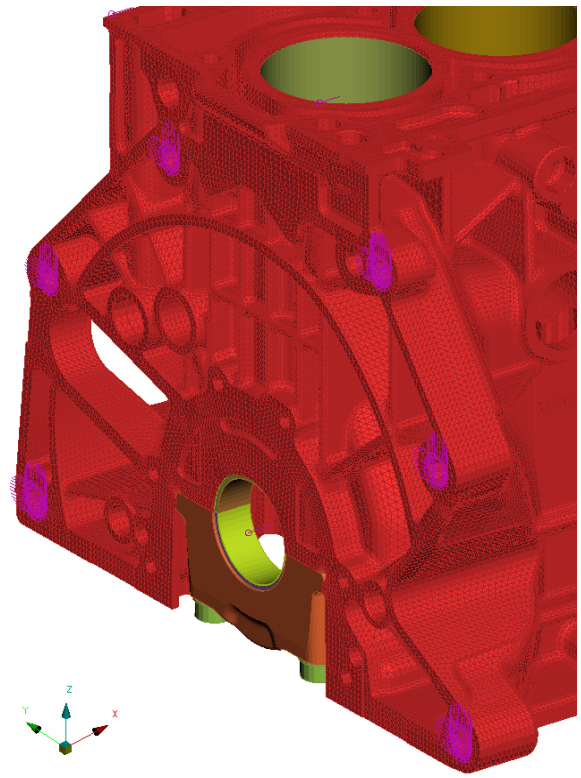

Fig. 4.8 The model mounting – side 1.

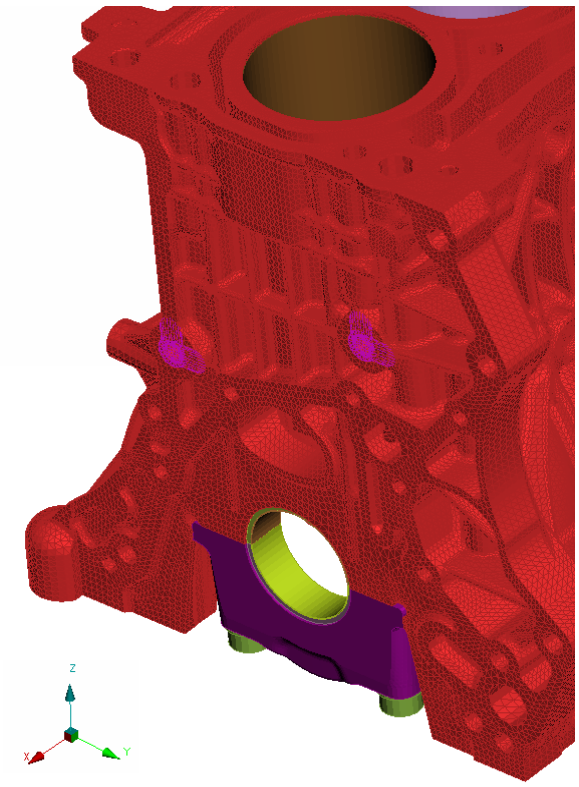

Fig. 4.9 The model mounting – side 2.

All contacts in the model are *'Surface to Surface with Small Sliding'* type. The contact of the sealing and the engine head is *'Tied'*; the contact of the sealing and the block engine is with interference. For all other contacts in the model assigned friction factor is 0.15.

Note: The model was taken over from previous analyses in ŠKODA AUTO.

4.3 Results of Finite Element Analysis

By using the FEA, material mechanical response of the engine block was simulated within 28 load steps which represent how the crankshaft loads the engine block depending on its rotation angle. The calculation will be conducted in 2 parts – the first one will be the calculation of mechanical response from the mounting and bolt prestresses (see Fig. 4.10).

Cross-section of the engine block can be seen in Fig. 4.11.

Note: Re (Al) in the legend in figures means the yield strength of the aluminum alloy that the engine block is made from.

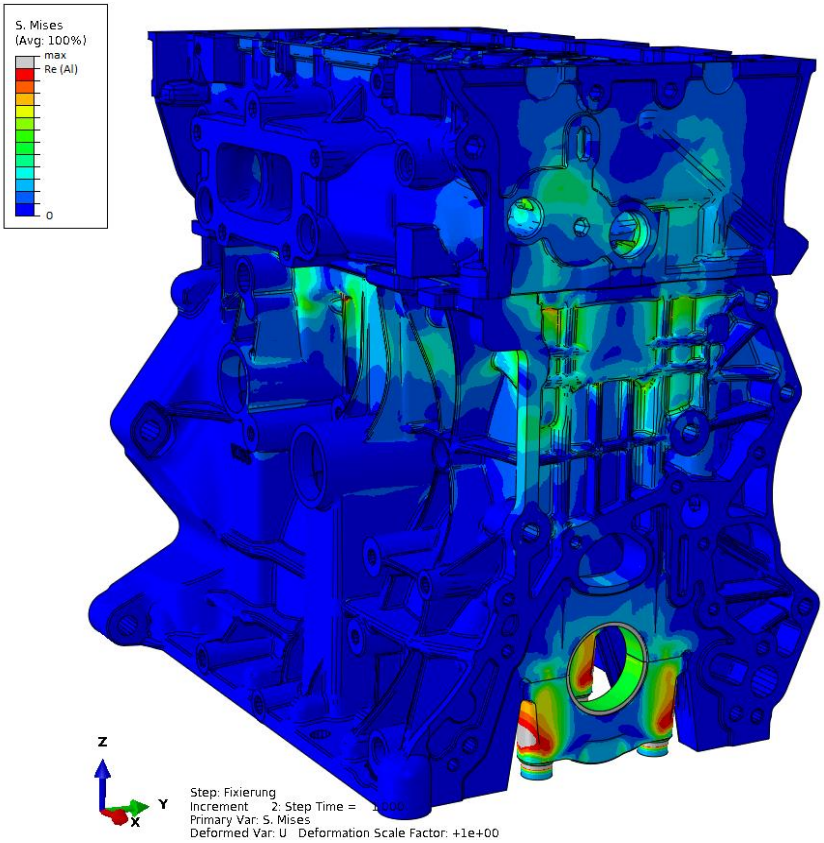

Fig. 4.10 Von Mises stress field due to the assembly loads and bolt prestresses.

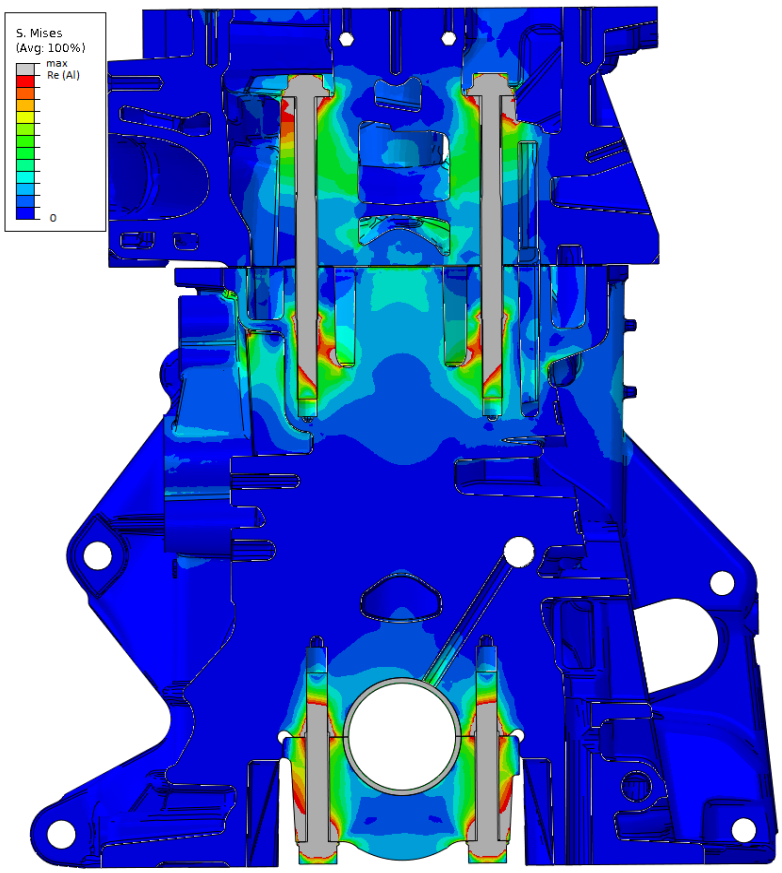

Fig. 4.11 Cross-section of the engine block – von Mises stress field due to the assembly loads and bolt prestresses.

Then the analysis of the material response due to the crankshaft loads is carried out. The results of some of them are presented in Fig. 4.12 to Fig. 4.16.

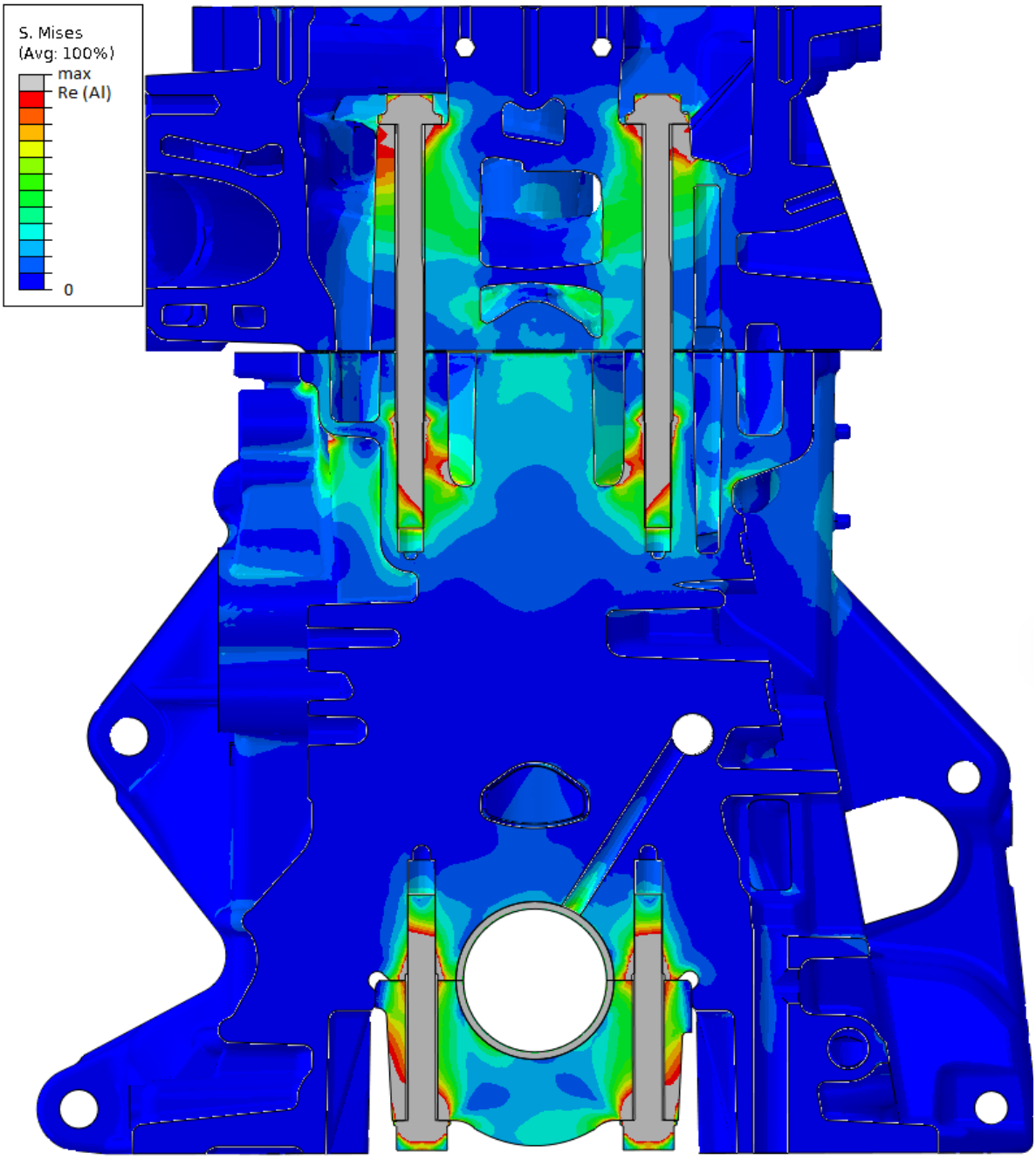

Fig. 4.12 A sample von Mises stress field from one of the load steps (superposition with the assembly loads).

Since the main target of this thesis is the calculation of the lifetime of engine block, it is worth focusing on the bottom part of Fig. 4.12 (the state of stress around the crankshaft bearing) where the highest values of stress amplitudes can be expected. The next figures in this paragraph will pay attention to this problematic place.

It is seen in Fig. 4.14 to Fig. 4.16 that cyclic stresses are not higher than a half of the yield strength of the material – meaningful fatigue results can be obtained.

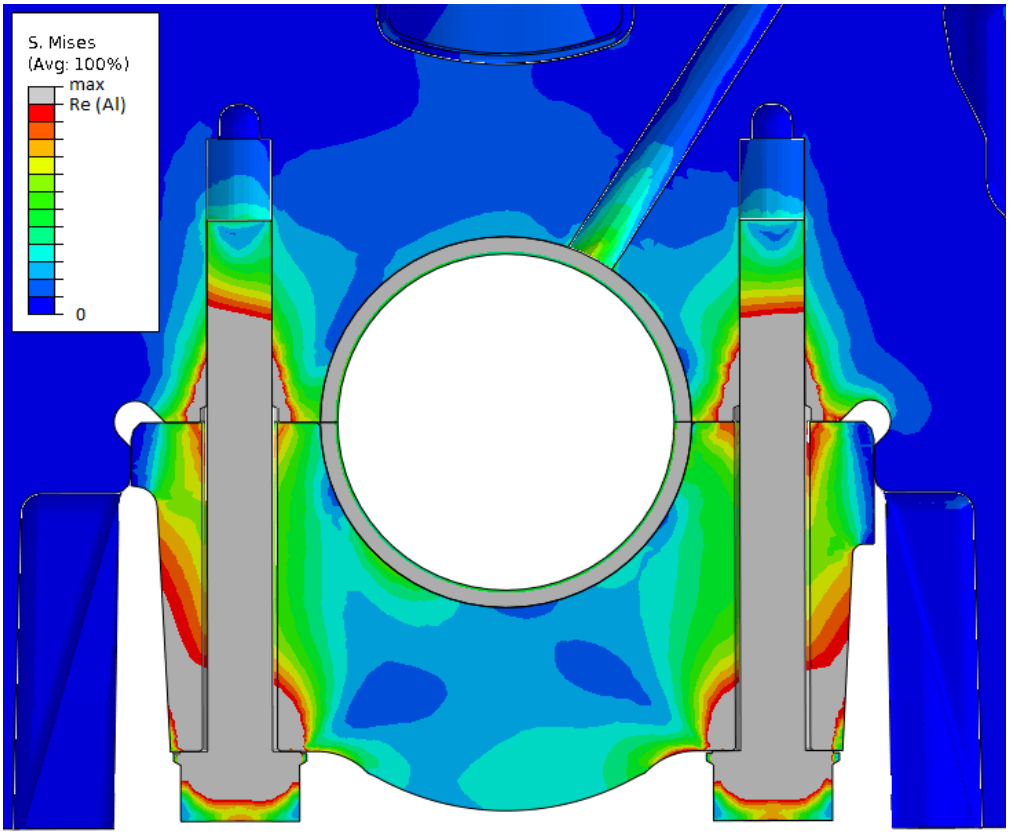

Fig. 4.13 Result of calculation due to the crankshaft loads (superposition with the assembly loads, the same step like in Fig. 4.11).

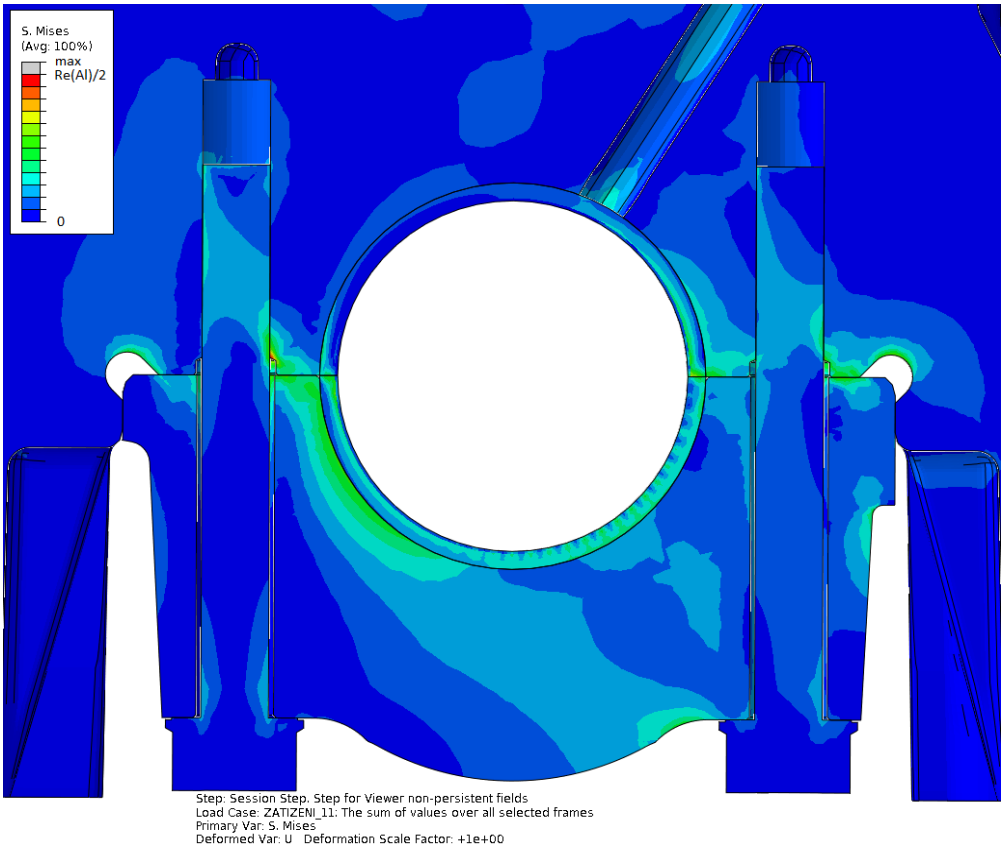

Fig. 4.14 Result of calculation due to the crankshaft loads (no superposition with the assembly loads, the same step like in Fig. 4.11 and 4.12).

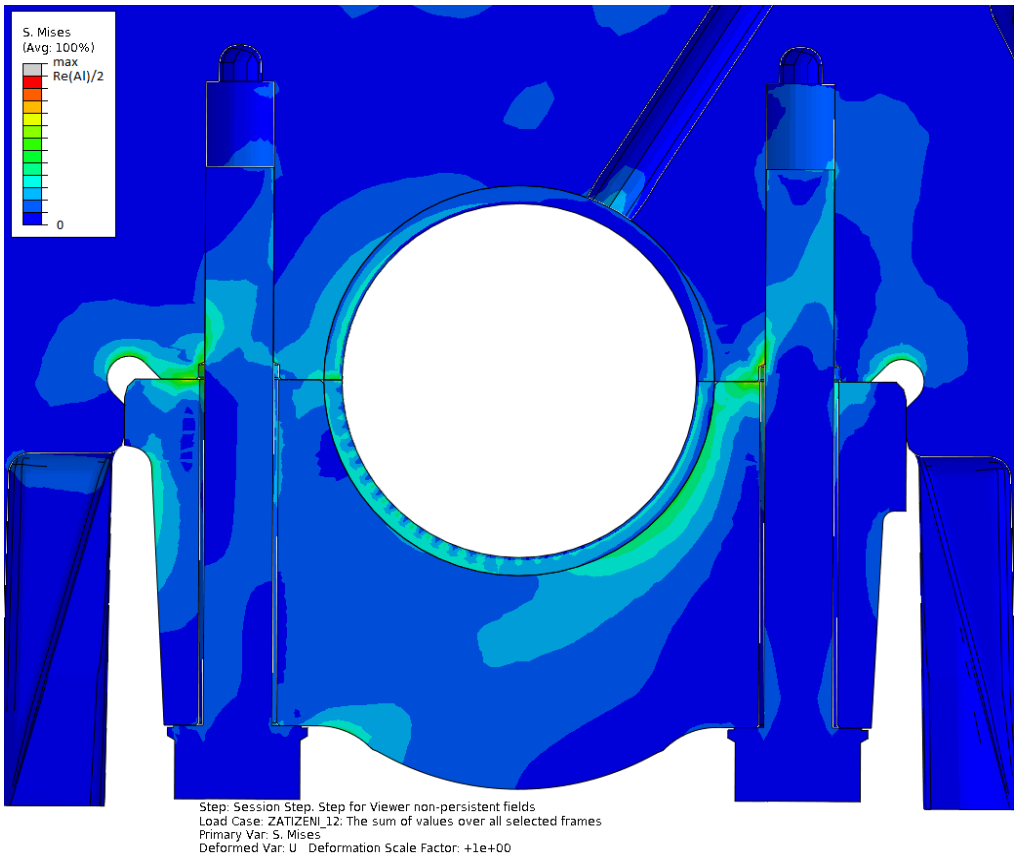

Fig. 4.15 Result of calculation due to the crankshaft loads (no superposition with the assembly loads, random load step).

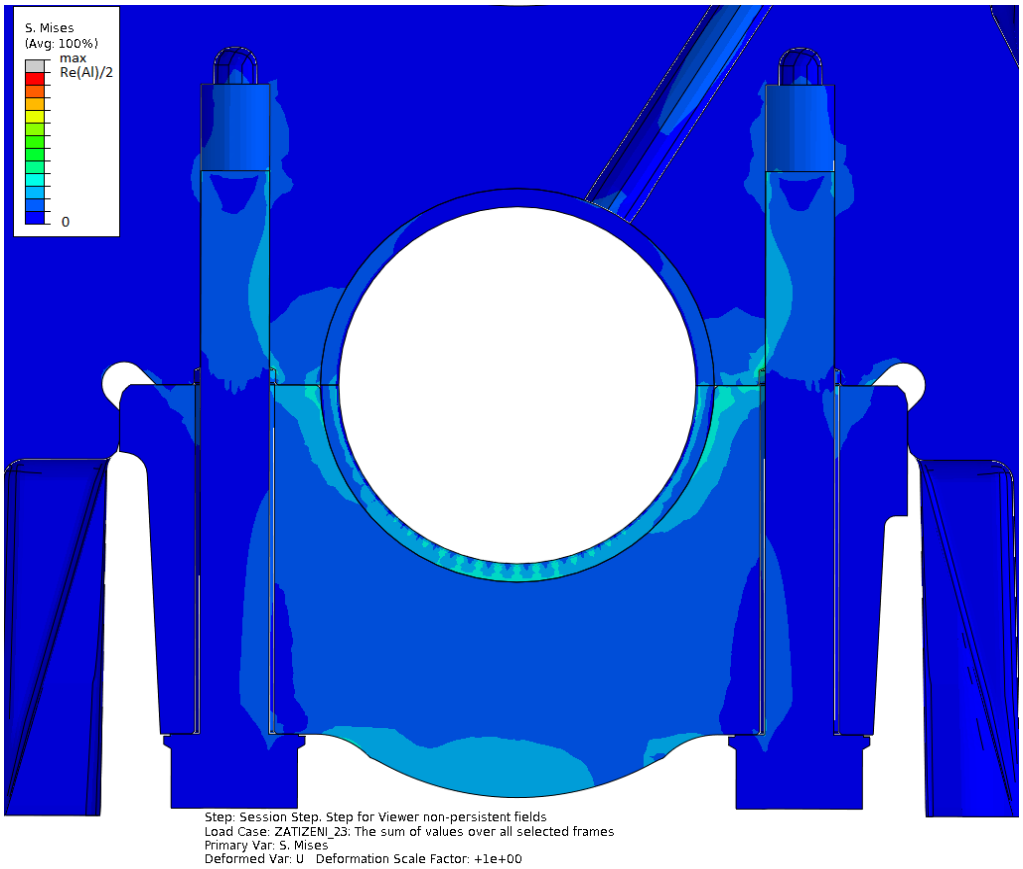

Fig. 4.16 Result of calculation due to the crankshaft loads (no superposition with the assembly loads, random load step).

4.4 Submodel of the engine block

For further computations, the model of the engine block needs to be reduced, because manipulations with the whole model is quite costly: this model has 5 geometrically identical parts – 5 crankshaft bearings. In other words, the calculation considering the whole model would take much more time comparing with a submodel.

Draw on experience of ŠKODA AUTO employees, it is known that the critical place of this type of engines is the mounting of the middle bearing (other engines can have a critical place somewhere else). As shown in Fig. 4.17, the stress states of all crankshaft bearings are almost the same, so, if the fatigue analysis is carried out only with the middle bearing, it can be assumed that its result will be acceptable.

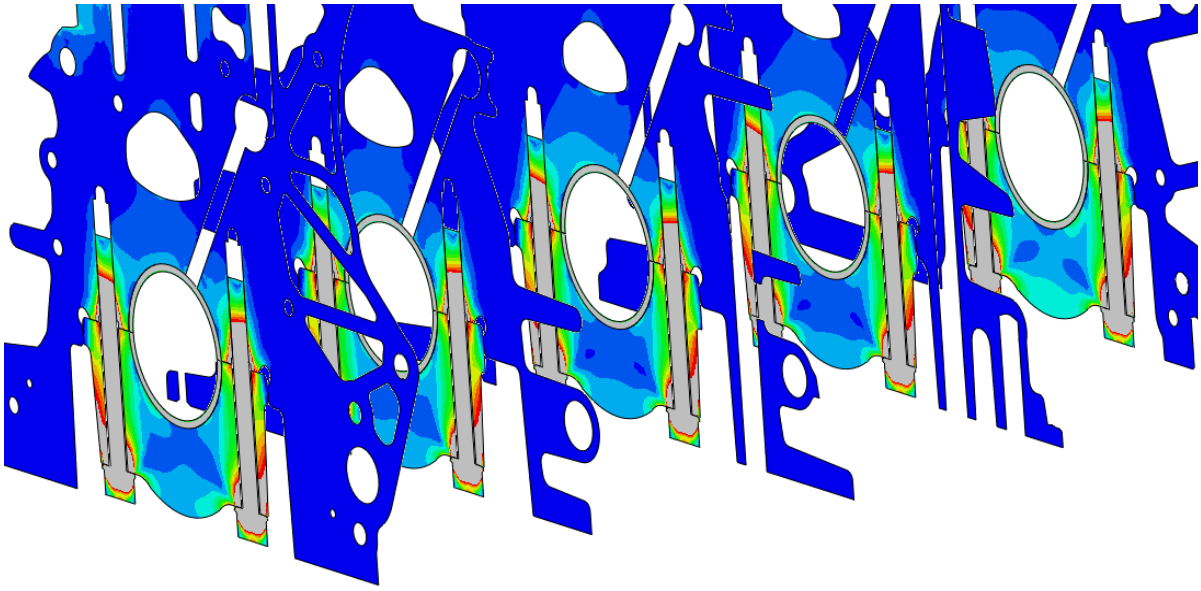

Fig. 4.17 Cross-sections of the engine block through the bearings showing that the stress response is almost identical in these locations throughout the engine block.

The created submodel is shown in Fig. 4.19 and Fig. 4.20.

The whole procedure of the model reduction is based on an application of boundary conditions of nodes from the global model on the nodes of the submodel, that are placed on surfaces going through the material of the global model, in a corresponding simulation time moment. By this operation, the equivalence of mechanical response between the global model and the submodel is guaranteed, however with a higher level of resolution in the case of the submodel.

Comparing with the global model, the submodel has a specific feature that it does not contain bolts. In the place of bolt contacts (and, by the way, other contact surfaces) the node sets were created (see Fig. 4.18) – these sets then will take over the displacements from corresponding nodes from the global model calculation results. Therefore, bolts do not need to be used in the submodel.

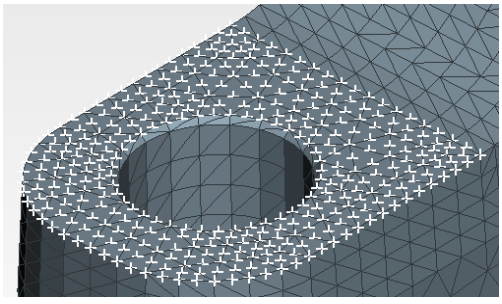

Fig. 4.18 Node set in contact place.

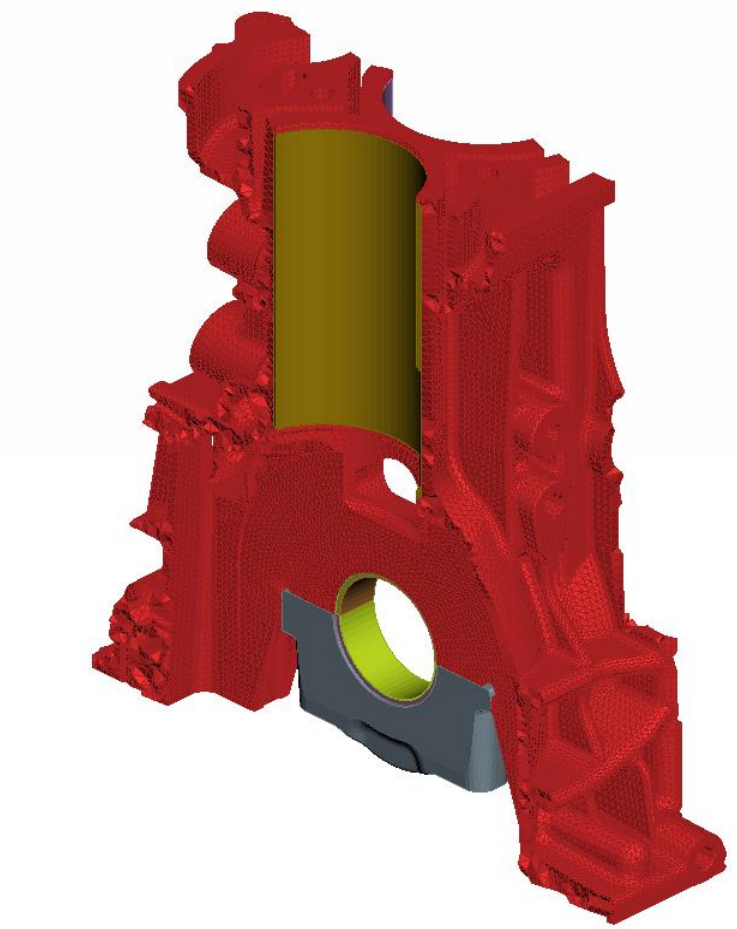

Fig. 4.19 Isometric view of the submodel of the engine block.

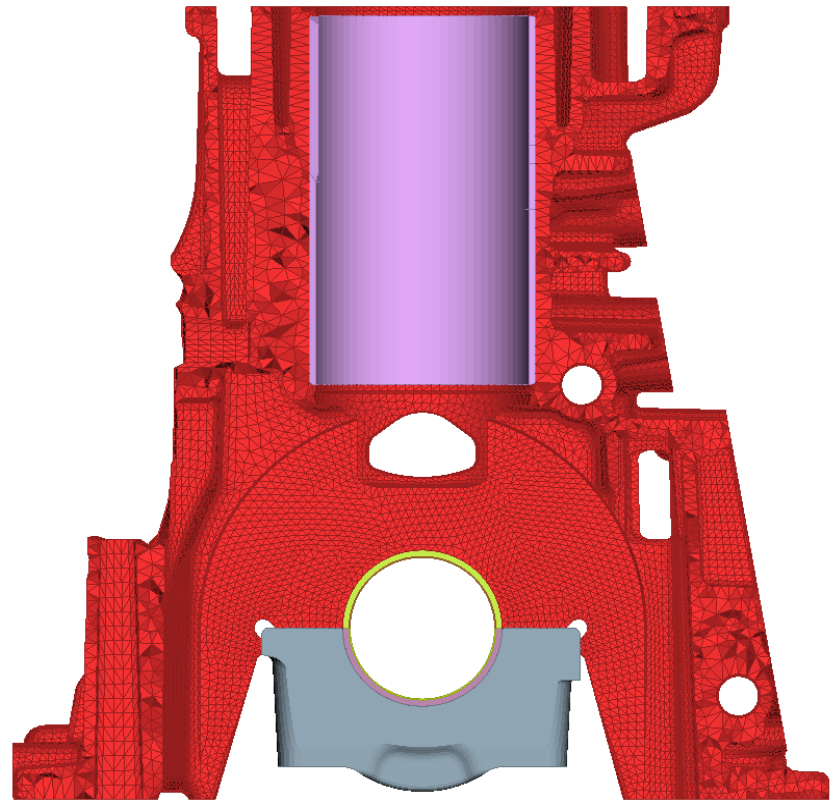

Fig. 4.20 Front view of the submodel of the engine block.

The interface between the global model and the submodel is highlighted in Fig. 4.21.

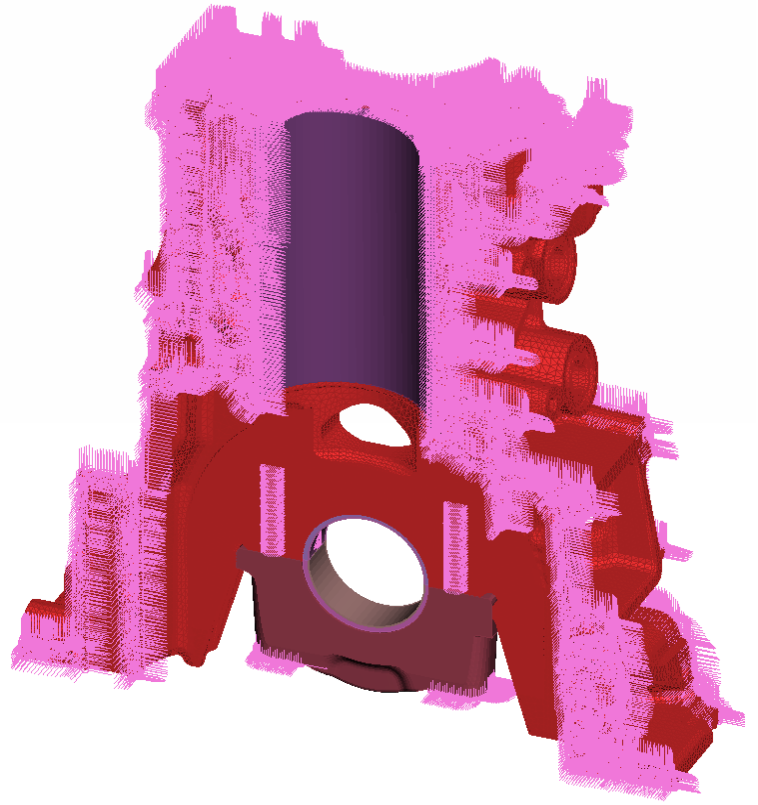

Fig. 4.21 Demonstration of boundary conditions assignment in the submodel.

The result of the submodel analysis is presented in Fig. 4.22.

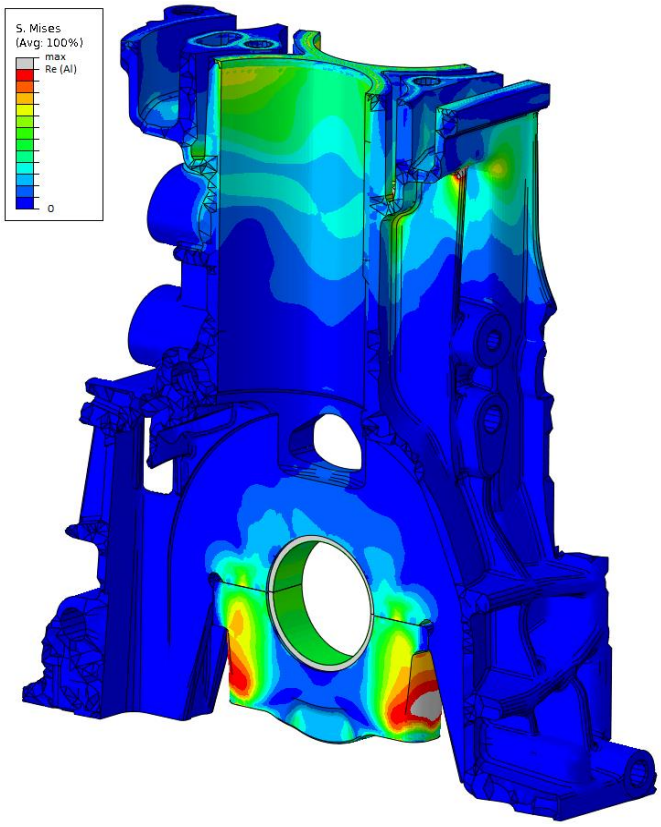

Fig. 4.22 Submodel analysis result.

The comparison between calculations of the global model and the submodel at the same load step is in Fig. 4.23 and Fig. 4.24Fig. 4. (only dynamic load, without the mounting).

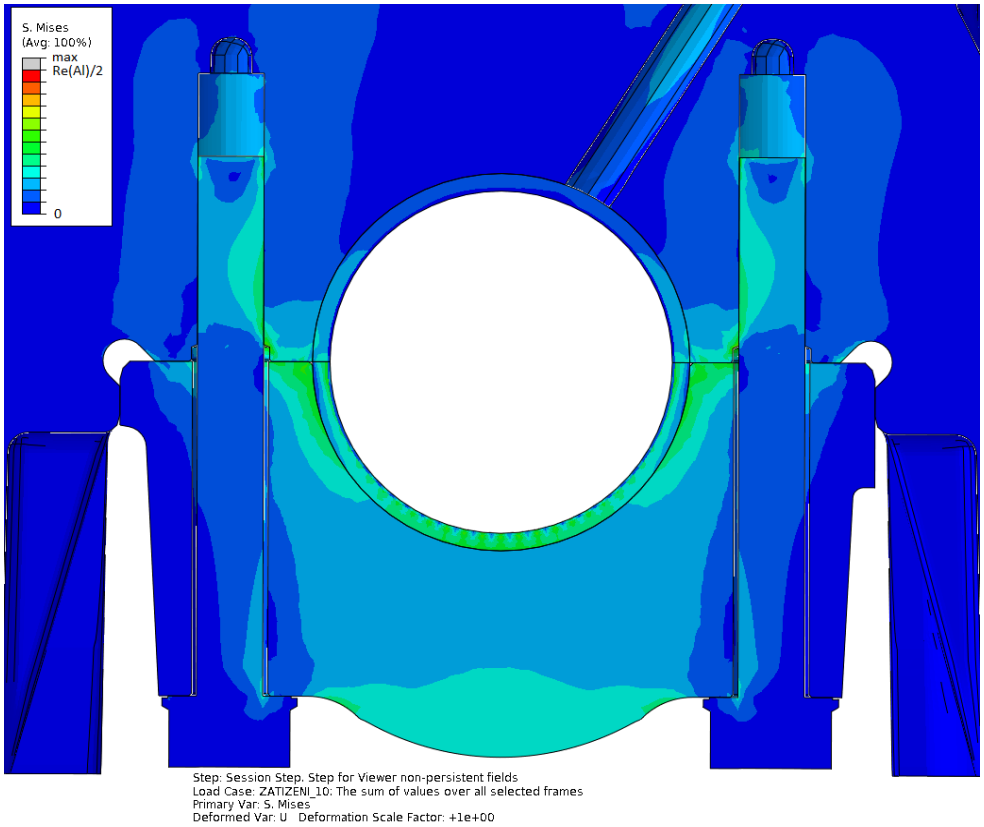

Fig. 4.23 Analysis of the global model.

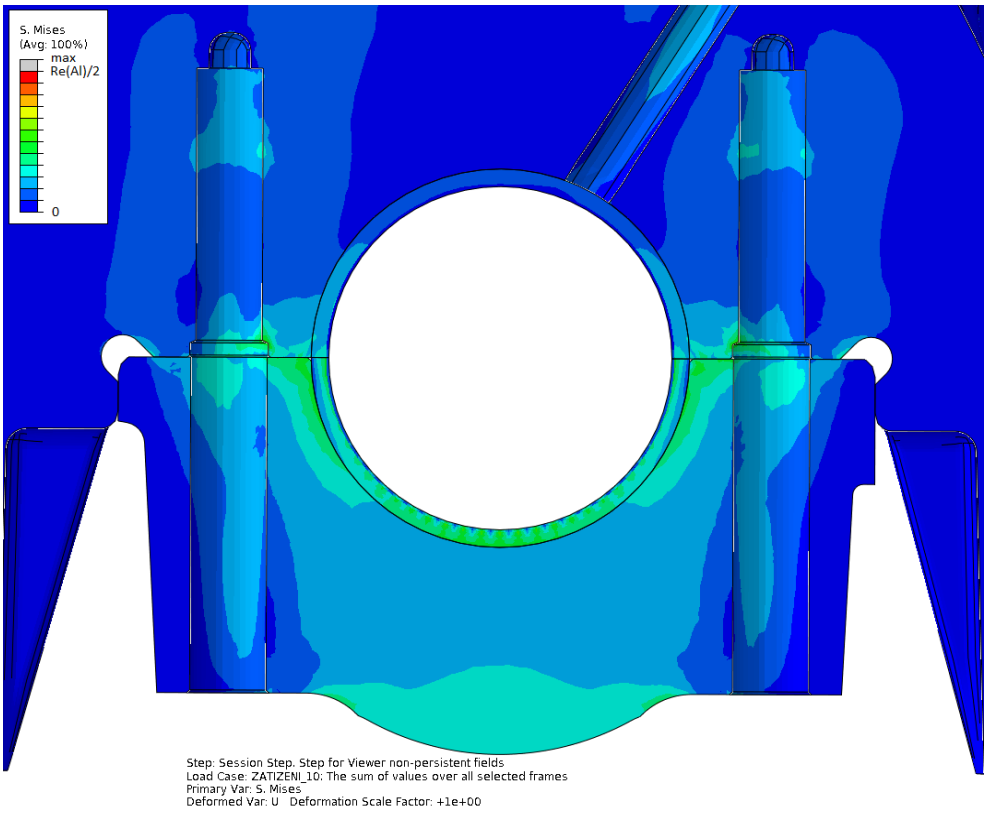

Fig. 4.24 Submodel analysis.

In Tab. 4.1, more detailed comparison of calculation results of global model and submodel in one of problematic places (bearing groove) is shown. As can be seen, the difference between results is about 1 %.

Tab. 4.1 Comparison of stress values in global model and submodel.

Node No.	Global model	Submodel
	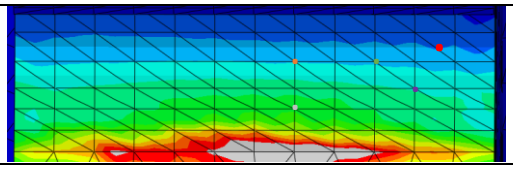	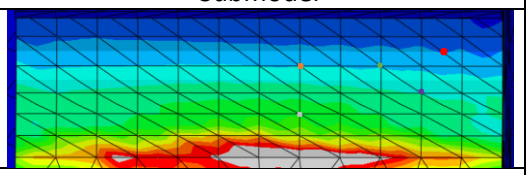
911974	22.173	22.400
911603	45.576	46.111
911699	34.438	34.874
911526	67.173	67.682
911651	33.461	33.831

In Fig. 4.25 and Fig. 4.26 the time histories of maximum and minimum principal stresses in the nodes that will be analyzed in Chapter 5 of this work.

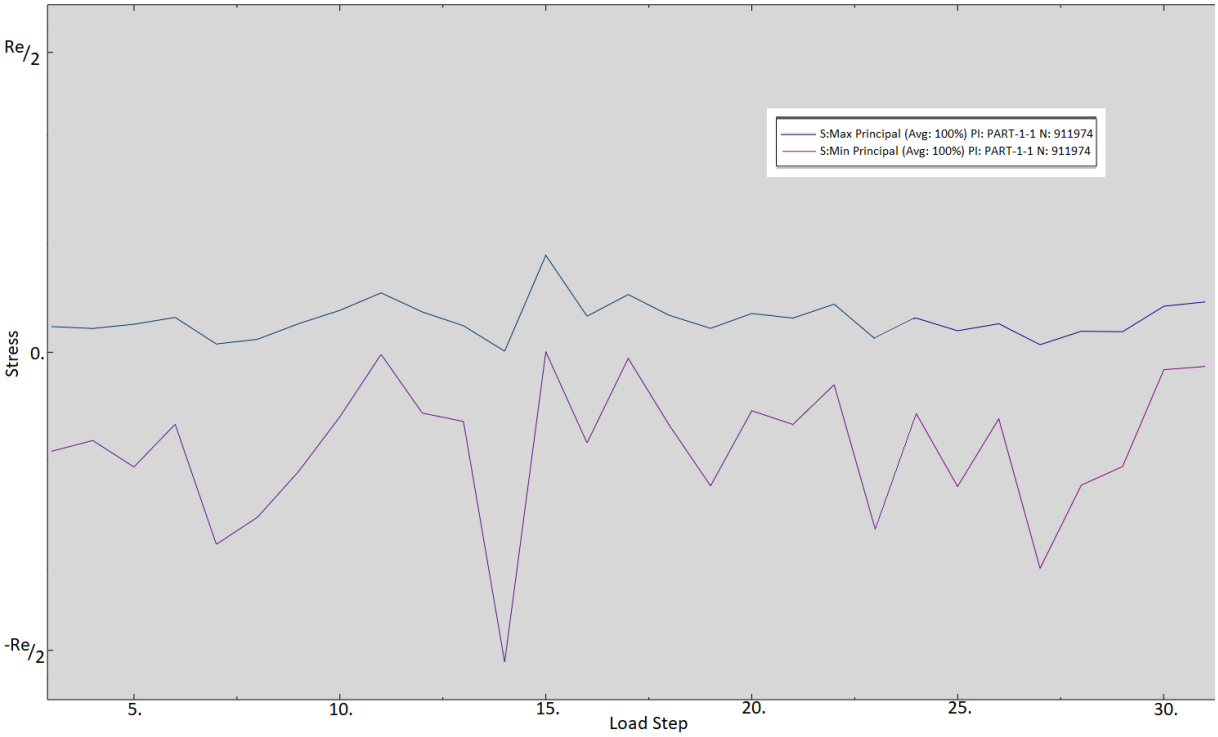

Fig. 4.25 Time history of maximum and minimum principal stresses for node No. 911974.

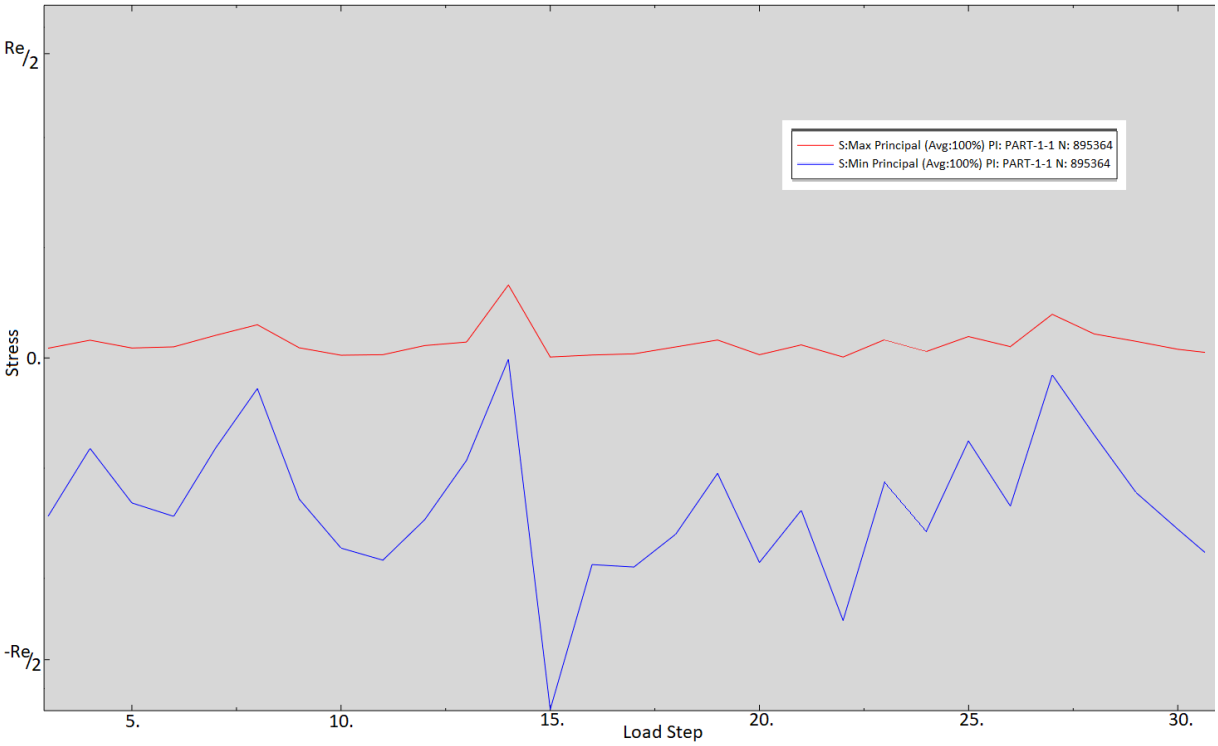

Fig. 4.26 Time history of maximum and minimum principal stresses for node No. 895634.

As shown in Fig. 4.25 and Fig. 4.26, the fluctuation of stresses does not exceed the yield strength of the material – a lifetime can be predicted using high-cycle fatigue approaches.

5 Fatigue analysis

By this moment, FEA of the submodel has been already done, so it is time to move on to work with fatigue solvers: at first, the fatigue analysis will be done in FEMFAT, then in FE-safe. After brief discussion, additional analyses will be carried out.

5.1 Fatigue analysis in FEMFAT

Software FEMFAT is commonly used for fatigue analyses in ŠKODA AUTO; it means that most of analysis settings is well-known including their influence on the calculation. So, the fatigue analysis of the engine block will be started from the calculation in FEMFAT with analysis settings that are used for similar calculations in ŠKODA AUTO. Here are some of them:

- Material: *AlSi9Cu3(Fe) EN AC-46000* – taken over from FKM database;
- Damage parameter: *Scaled Normal Stress in the Critical Plane* (for details – see Par. 3.2.1);
- Surface roughness: As cast (*Rz = 200 µm*);
- Survival probability: *99.999%*;
- Range of dispersion: $T_s = 1.26$ (will be discussed in Par. 5.2.1);
- Endurance safety factor: constant mean stress (*Sig_m = const.*);
- Consideration of relative stress gradient (RSG) influence;
- Plasticity correction (***PLAST*** module is on).

The result of the fatigue calculation can be seen in Fig. 5.1 and Fig. 5.2.

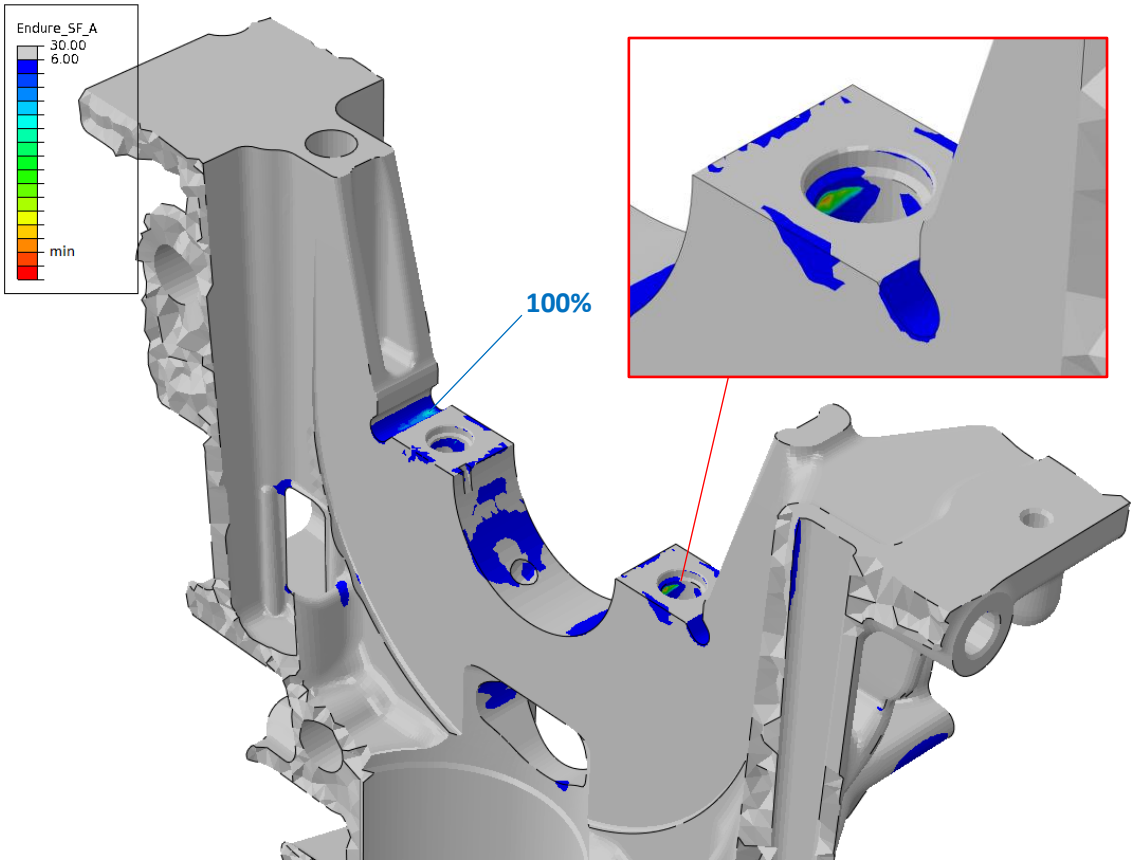

Fig. 5.1 Result of fatigue analysis in FEMFAT.

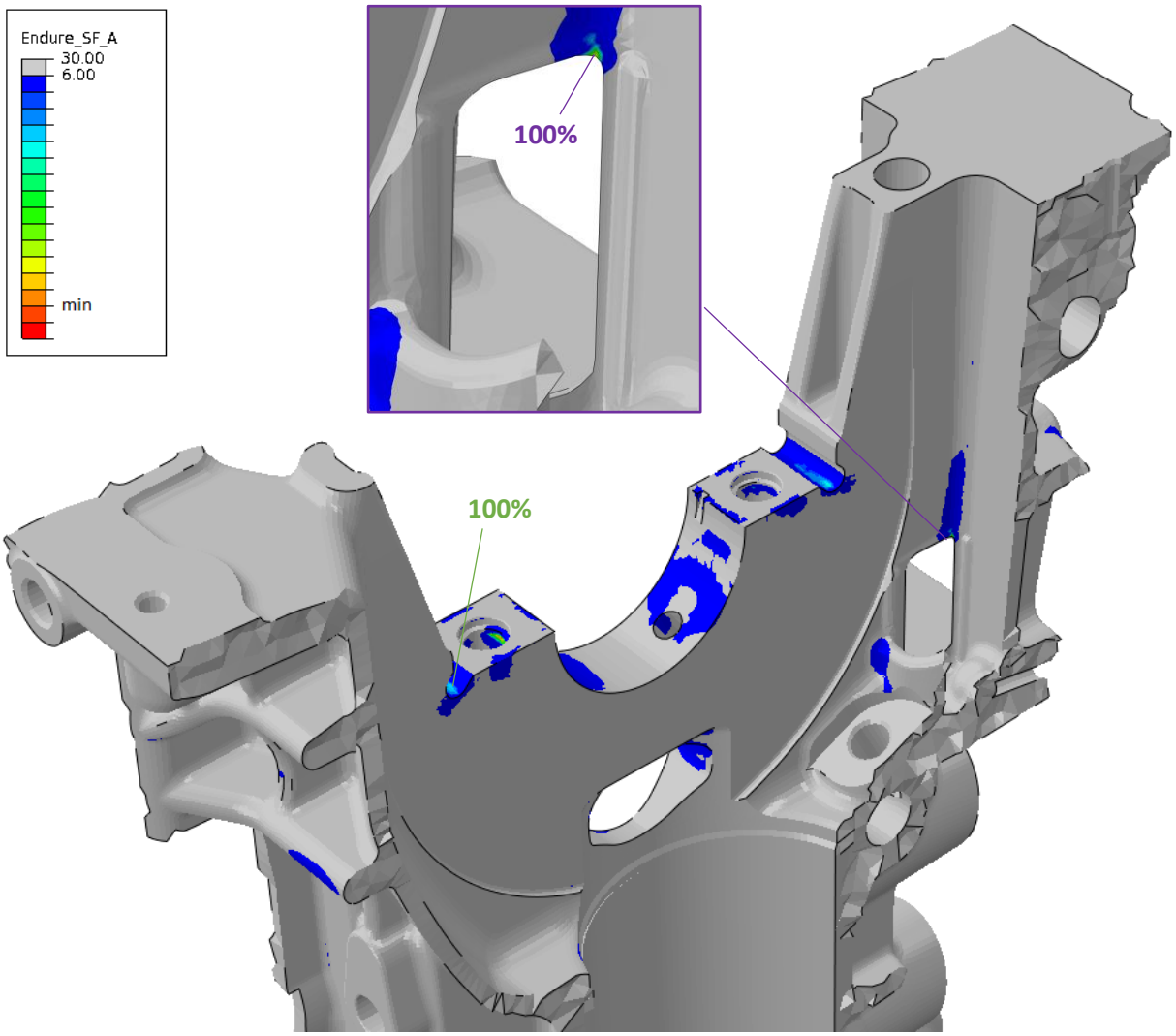

Fig. 5.2 Result of fatigue analysis FEMFAT.

Note: the values of safety factors are confidential type of data for ŠKODA AUTO, so they will be expressed as a percentage; the so-called Standard Analysis (this one) will be used as a reference, the percentages will be presented separately for particular places of engine block. Also, 'min' value in the legend means minimum acceptable value of the safety factor (typically 1.2).

In the detail in Fig. 5.1 can be seen a low value of safety factor in the thread – it needs to realize that FEM model does not completely simulate real shape of a thread and, therefore, distribution of forces and stress state. The stresses in this place are so high that the thread is plastified, so an elastic adaptation arises there when applying periodical loading. However, there is no information about pulling-out incidents during operation of this engine type in ŠKODA AUTO.

The detail in Fig. 5.2 shows one more potentially critical place. This "window" is made by a breakthrough with a special instrument, so its real edge is hard to simulate and FEA solution does not fully correspond with the reality. A solution of this problem can be relying on the previous experiences which indicate that, unlike the grooves highlighted in Fig. 5.1 and Fig. 5.2 with blue and green colour, there is no cracking initiated and propagated in this "window".

The results data of critical nodes in the grooves are presented in Tab. 5.1.

Tab. 5.1 Detailed results of fatigue analysis in FEMFAT.

	Intake side	*Exhaust side*
Critical node *No.*	911974	895634
Mean stress σ_m [MPa]	-27.07	-35.00
Stress amplitude σ_a [MPa]	44.23	44.60
Percentage of safety factor [%]	**100**	**100**

The results data in Tab. 5.1 correspond with the previous results of fatigue analysis of this engine type in ŠKODA AUTO.

5.2 Fatigue analysis in FE-safe

5.2.1 Survival probability conversion

When making a new material that would have the same fatigue properties like *AlSi9Cu3(Fe)* material from FKM database, there is no an option to assign survival probability of entered fatigue property values in FE-safe interface.

Since the fact that the fatigue properties of *AlSi9Cu3(Fe)* material are known for *97.5%* survival probability, they need to be converted to desired survival probability *99.999%*.

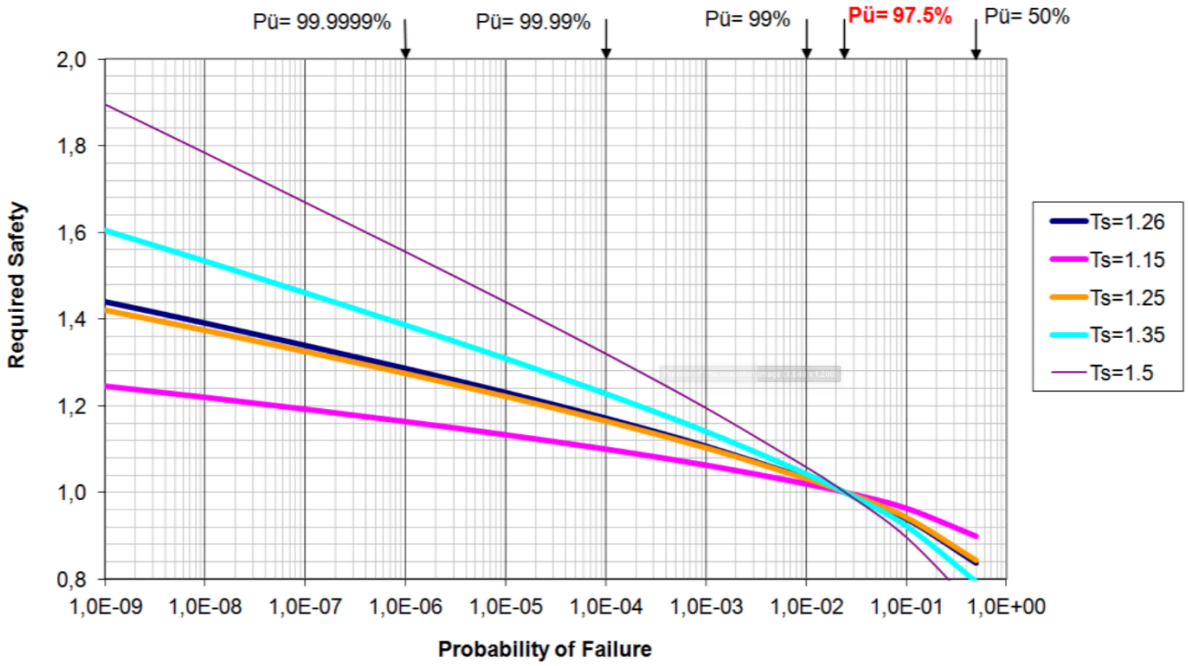

Fig. 5.3 Dependence of survival probability P on dispersion range T_s [11].

The following text is taken over from [12]:

In FEMFAT the statistic influence is considered by assuming a logarithmic probability of the standard values of strength. A logarithmic probability curve is defined by two parameters: the average value $\sigma_{af,50\%}$ (or also mean fatigue life)

$$\log \sigma_{af}^{50\%} = \frac{1}{n}\sum_{i=1}^{n} \log \sigma_{af,i} \tag{5.1}$$

and the standard deviation *s*

$$s = \sqrt{\frac{1}{n-1}\sum_{i=1}^{n} \left(\log \sigma_{af,i} - \log \sigma_{af}^{50\%}\right)^2} \tag{5.2}$$

To characterize the dispersion, the range of dispersion T_s can be used instead of the standard deviation. T_s is defined as the ratio of the endurance stress limit values, which have occurred with survive-probabilities between 10 and 90 percent

$$T_s = \frac{\log \sigma_{af}^{90\%}}{\log \sigma_{af}^{10\%}} \tag{5.3}$$

The standard deviation *s* and the range of dispersion T_s of a logarithmic probability curve can be converted to each other by using the following equation

$$s = \frac{1}{2{,}5631} \log T_s \tag{5.4}$$

So the mean fatigue life will be defined as follows

$$\log \sigma_{af}^{50\%} = 10^{\left(\log \sigma_{af}^{97.5\%} + 1.96 \cdot s\right)} \tag{5.5}$$

And then the desired survival probability $\sigma_{af,99.999}$ is calculated

$$\log \sigma_{af}^{99.999\%} = 10^{\left(\log \sigma_{af}^{50\%} - 4.2649 \cdot s\right)} \tag{5.6}$$

Note: numbers 1.96 and 4.2649 in Eq. 5.5 and 5.6 have the same meaning like the quantile of failure probability u_p in Par. 2.4.3 of this work. It can be found out from the tables of normal distribution or by a computational algorithm for calculating an integral of probability density function of normal distribution.

5.2.2 Fatigue calculation in FE-safe

The analysis parameters were set in similar way like they were in Par. 5.1 for FEMFAT fatigue analysis. In more details:

- Material: *AlSi9Cu3(Fe)* – was created directly in FE-safe interface, material properties are taken over from FKM database;
- Damage parameter: according to *Dang Van approach* (see Par. 3.1.2);
- Surface roughness: *Rz = 200 µm*;
- Survival probability: was manually converted to *99.999%* by the method described in Par. 5.2.1;
- Endurance safety factor: *DV-Vert* (analogy of *Sig_m = const.* in FEMFAT);
- **WITHOUT** consideration of relative stress gradient influence (there is no option to use it with Dang Van approach in FE-safe).

Note: DV-Vert in FE-safe is geometrical analogy of Sig_m = const. in FEMFAT – see Fig. 5.4 and Fig. 5.5. However, they have quite different meaning: when going along loading vertical up to limit line, the amplitude of the damage parameter is increasing in Haigh diagram in FEMFAT

(Fig. 5.4), but in the case of Dang Van plot (Fig. 5.5) it is shear stress growing. Therefore, evaluation of a safety factor using DV-Radial (see Fig. 3.11) is also needed (it can be found in Tab. 5.8 *and* Tab. 5.11*).*

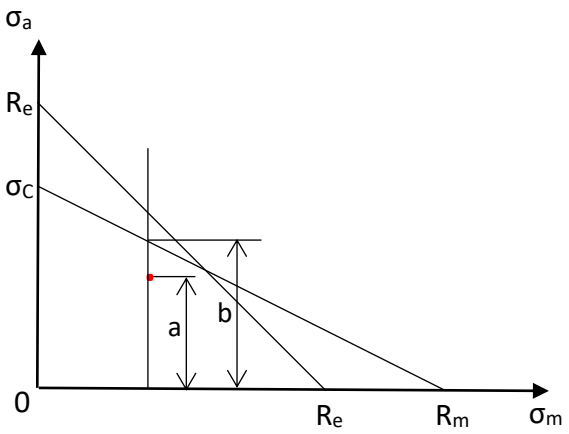

Fig. 5.4 Evaluation of a safety factor using Sig_m=const. in Haigh diagram in FEMFAT.

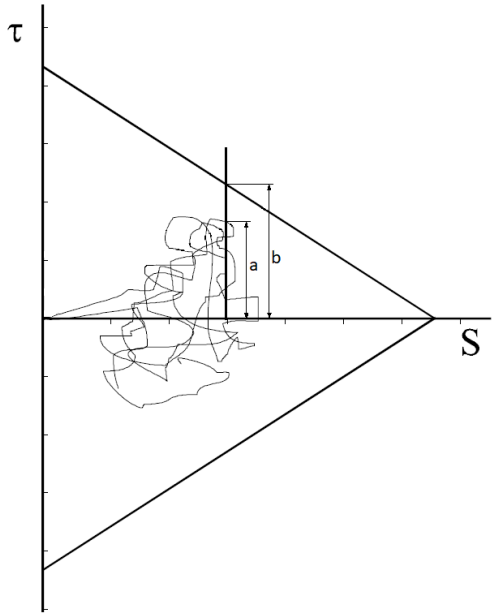

Fig. 5.5 Evaluation of a safety factor using DV-Vert in FE-safe.

The results of fatigue analysis can be seen in Fig. 5.6 and Fig. 5.7.

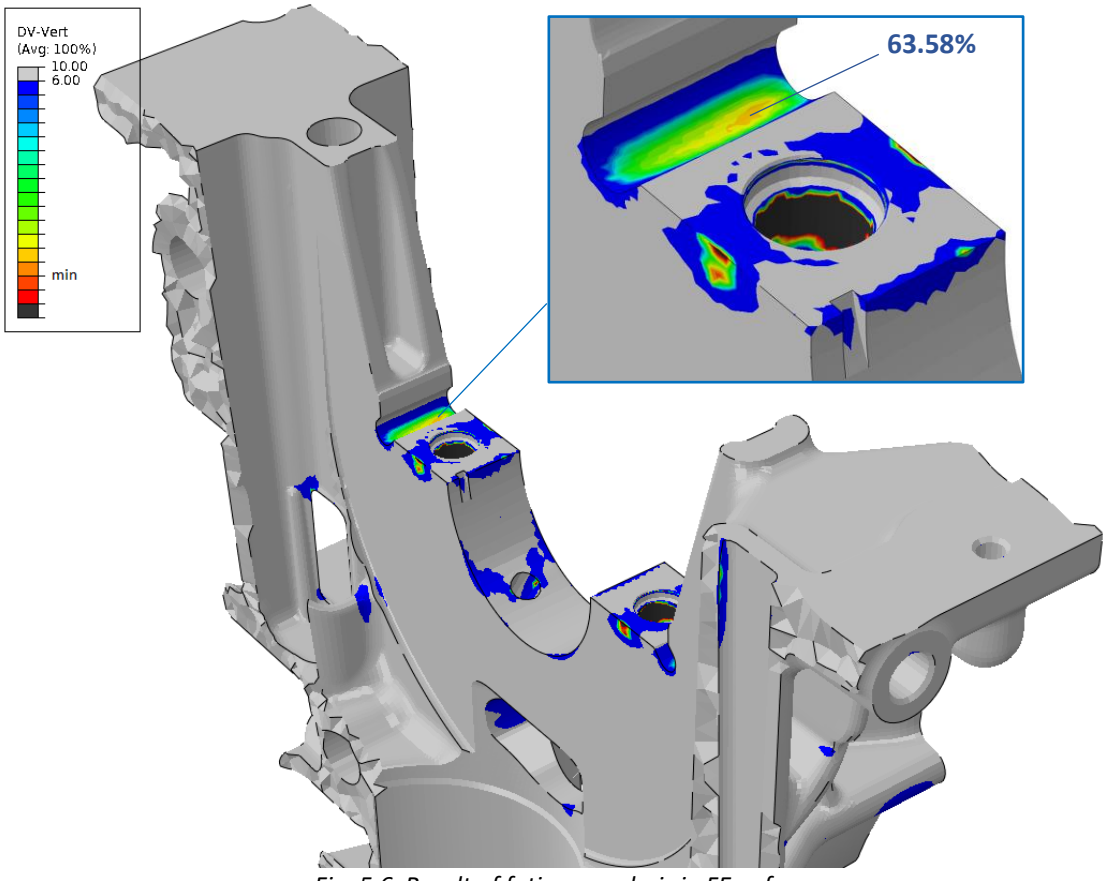

Fig. 5.6 Result of fatigue analysis in FE-safe.

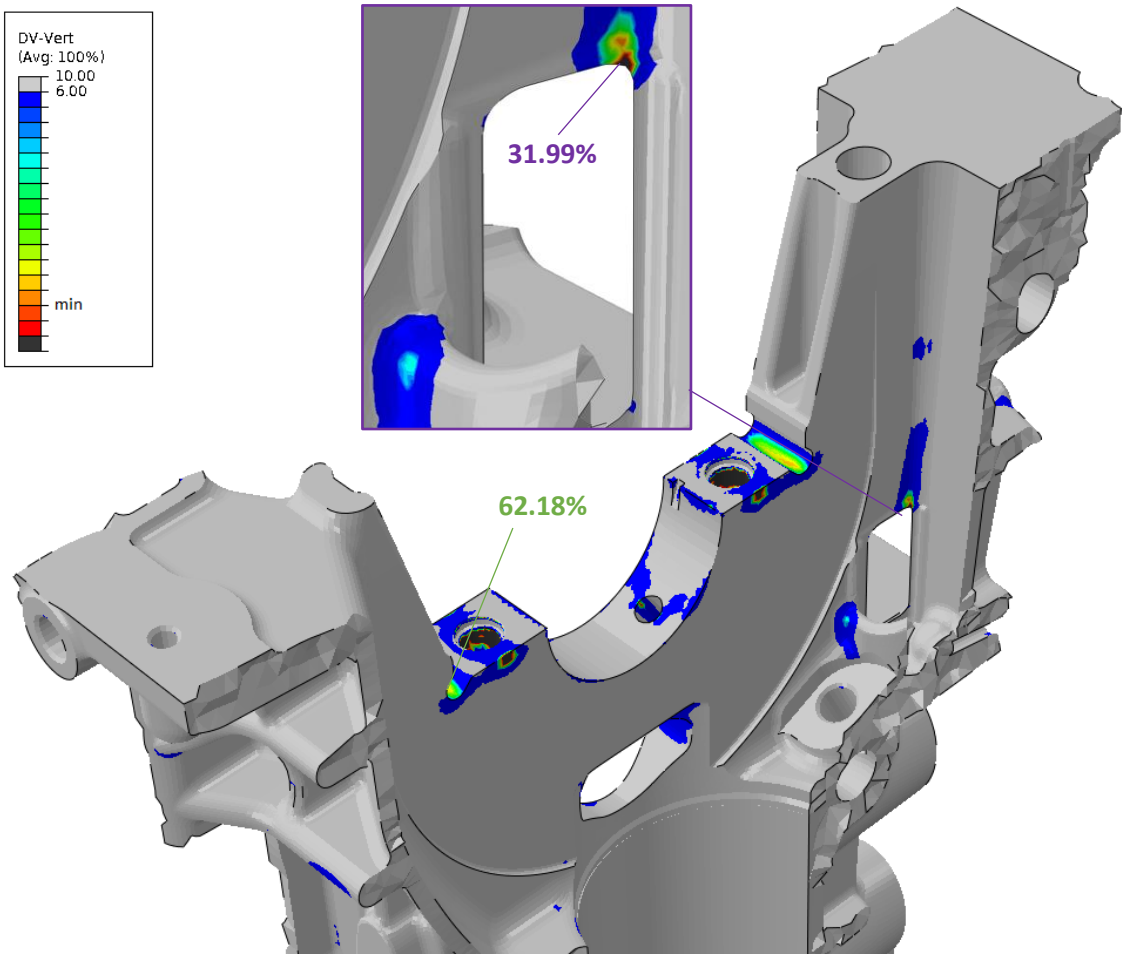

Fig. 5.7 Result of fatigue analysis in FE-safe.

The results data of critical nodes in the grooves are presented in Tab. 5.2.

Tab. 5.2 Detailed results of fatigue analysis in FE-safe.

	Intake side	*Exhaust side*
Node *No.*	911982	895330
Percentage of safety factor [%]	**63.58**	**62.18**

Note: there is no mean stress values and stress amplitudes when using Dang Van criterion (for more details see Par. 3.1.2 of this thesis).

5.3 Results discussion

Relying on the data from Par. 5.1 and 5.2.2, can be made a conclusion that there is a significant difference between the outputs from FEMFAT and FE-safe. However, none of those results is critical, i.e. all safety factors are greater than minimum acceptable value (1.2).

Since a reason of the difference between the results needs to be identified, a little investigation with some more analyses should be conducted – see further paragraphs in this chapter.

5.4 Further fatigue analysis investigation

5.4.1 Analysis in FEMFAT (no RSG correction)

Analysis settings

- Material: *AlSi9Cu3(Fe) EN AC-46000* – taken over from FKM database;
- Damage parameter: *Scaled Normal Stress in the Critical Plane*;
- Surface roughness: As cast (*Rz = 200 µm*);
- Survival probability: *99.999%*;
- Range of dispersion: $T_s = 1.26$;
- Endurance safety factor: constant mean stress (*Sig_m = const.*);
- **NO relative stress gradient (RSG) influence**;
- Plasticity correction (***PLAST*** module is on).

Analysis results

Tab. 5.3 FEMFAT (No RSG correction).

	Intake side	*Exhaust side*
Critical node *No*.	911974	895634
Mean stress σ_m [MPa]	-27.07	-35.00
Stress amplitude σ_a [MPa]	44.23	44.60
Percentage of safety factor [%]	**52.77**	**51.27**

Comment

The results are significantly different from the one in Par. 5.1. Therefore, relative stress gradient correction has decisive influence on such fatigue calculations. However, the critical nodes are the same like in Par. 5.1.

5.4.2 Analyses in FE-safe

a) Dang Van method (P = 97.5 %)

Analysis settings

- Material: *AlSi9Cu3(Fe)* – was created directly in FE-safe interface, material properties are taken over from FKM database;
- Damage parameter: according to *Dang Van criterion*;
- Surface roughness: *Rz = 200 µm*;
- **Survival probability: 97.5%, no conversion**;
- Endurance safety factor: *DV-Vert* (analogy of *Sig_m = const.* in FEMFAT);
- **WITHOUT** consideration of relative stress gradient influence (there is no option to use it with Dang Van approach in FE-safe).

Analysis results

Tab. 5.4 Dang Van analysis (P = 97.5%).

	Intake side	*Exhaust side*
Node No.	911982	895330
Percentage of safety factor [%]	**83.32**	**80.82**

b) Normal Stresses: SWT mean stress correction (P = 97.5%)

This criterion is close to the one used in FEMFAT; however, in FE-safe normal stresses are not scaled, so the same result like in Par. 5.1 is not expected.

Analysis settings

- Material: *AlSi9Cu3(Fe)* – was created directly in FE-safe interface, material properties are taken over from FKM database;
- **Damage parameter: Normal Stresses (NS);**
- Mean stress correction: according to *Smith-Watson-Topper* (SWT) – is proved as the most applicable for aluminum alloys [13];
- Surface roughness: *Rz = 200 µm*;
- Survival probability: 97.5%, no conversion;
- **WITHOUT** consideration of relative stress gradient influence.

Analysis results

Tab. 5.5 NS: SWT (P = 97.5%).

	Intake side	*Exhaust side*
Critical node *No.*	911647	895306
Mean stress σ_m [MPa]	-22.94	-26.42
Stress amplitude σ_a [MPa]	50.40	49.57
Percentage of safety factor [%]	**90.39**	**94.82**

Note: ***Smith-Watson-Topper mean stress correction***

The damage parameter P_{SWT} according to SWT model is defined as

$$P_{SWT} \equiv \sigma_{a,eq} = \sqrt{(\sigma_a + \sigma_m) \cdot E \cdot \varepsilon_a} \quad for\ \sigma_m > 0$$
$$P_{SWT} \equiv \sigma_{a,eq} = \sigma_a \quad for\ \sigma_m < 0$$

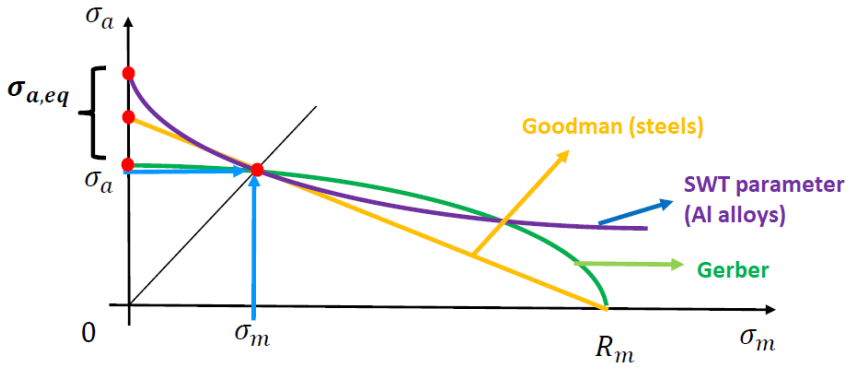

Fig. 5.8 Overview of various mean stress effect methods.

c) Normal Stresses NS: SWT (P = 99.999%)

Analysis settings

- Material: *AlSi9Cu3(Fe)* – was created directly in FE-safe interface, material properties are taken over from FKM database;
- Damage parameter: *Normal Stresses* (NS);
- Mean stress correction: according to *Smith-Watson-Topper* (SWT) – is proved as the most applicable for aluminum alloys;
- Surface roughness: *Rz = 200 µm*;
- Survival probability: 99.999**%**, was manually converted by the method described in Par. 5.2.1;
- **WITHOUT** consideration of relative stress gradient influence.

Analysis results

Tab. 5.6 NS: SWT (P = 99.999%).

	Intake side	*Exhaust side*
Node *No*.	911647	895306
Percentage of safety factor [%]	**73.95**	**77.05**

d) Normal Stresses NS: SWT using TCD

Analysis settings

- Material: *AlSi9Cu3(Fe)* – was created directly in FE-safe interface, material properties are taken over from FKM database;
- Damage parameter: *Normal stresses* (NS);
- Mean stress correction: according to *Smith-Watson-Topper* (SWT) – is proved as the most applicable for aluminum alloys;
- Surface roughness: *Rz = 200 µm*;
- Survival probability: 99.999%, was manually converted by the method described in Par. 5.2.1;
- **With consideration of Theory of Critical Distance (TCD)** – according to FKM Guideline, it is recommended to evaluate fatigue damage at depth of 1 mm under the surface for this material type.

Analysis results

Tab. 5.7 NS: SWT using TCD.

	Intake side	*Exhaust side*
Node *No*.	1882645	1870241
Percentage of safety factor [%]	**114.10**	**112.91**

The critical nodes are situated under the surface this time (for details see Tab. 5.11).

5.4.3 Comparison of FEMFAT and FE-safe results

a) Safety factors overview

An overview of all fatigue calculations that were mentioned in this chapter is presented in Tab. 5.8.

Tab. 5.8 Overview of the fatigue analyses.

Software	Type of analysis	Intake side (node No.)	Exhaust side (node No.)
FEMFAT	*Standard* (P = 99.999%)	**100%** (n911974)	**100%** (n895634)
	NO RSG	**52.77%** (n911974)	**51.27%** (n895634)
FE-safe	*DV-Vert* (P = 99.999%)	**60.76%** (n911982)	**59.00%** (n895330)
	DV-Radial (P = 99.999%)	**58.51%** (n911982)	**57.14%** (n895330)
	DV-Vert (P = 97.5%)	**83.32%** (n911982)	**80.82%** (n895330)
	DV-Radial (P = 97.5%)	**71.94%** (n911982)	**70.27%** (n895330)
	NS: SWT (P = 97.5%)	**90.39%** (n911647)	**94.82%** (n895306)
	NS: SWT (P = 99.999%)	**73.95%** (n911647)	**77.05%** (n895306)
	NS: SWT + TCD (P = 99.999%)	**114.10%** (n1882645)	**112.91%** (n1870241)

b) Mean stress and amplitude values in specific nodes

Tab. 5.9 Mean stresses and stress amplitudes for the critical nodes from FEMFAT.

FEMFAT / FE-safe	Intake side (n911974)	Exhaust side (n895634)
Mean stress σ_m [MPa]	-27.07 / -24.41	-35.00 / -33.69
Stress amplitude σ_a [MPa]	44.23 / 50.40	44.60 / 51.34

Tab. 5.10 Mean stresses and stress amplitudes for the critical nodes from FE-safe.

FE-safe / FEMFAT	Intake side (n911647)	Exhaust side (n895306)
Mean stress σ_m [MPa]	-22.94 / -27.56	-26.42 / -29.59
Stress amplitude σ_a [MPa]	50.40 / 43.68	49.57 / 43.83

Note: by mean stress and amplitude is meant the mean and amplitude value of the damage parameter which in this case is normal stress in critical plane.

c) Safety factor field in the grooves

Tab. 5.11 Safety factor fields in the grooves.

Analysis	Intake side	Exhaust side
FEMFAT Standard (P = 99,999%)	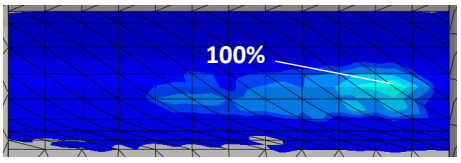	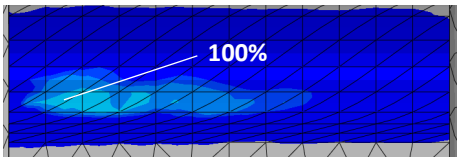
FEMFAT No RSG (P = 99,999%)	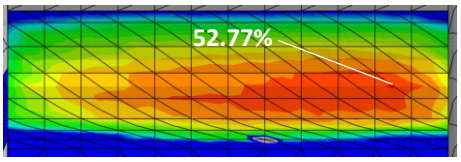	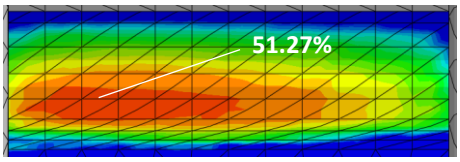
FE-safe Dang Van *DV-Vert* (P = 99,999%)	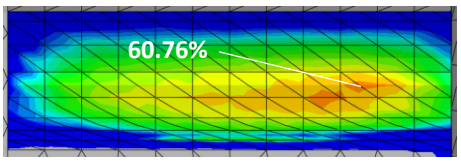	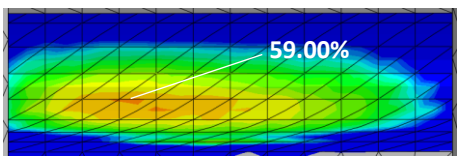
FE-safe Dang Van *DV-Radial* (P = 99,999%)	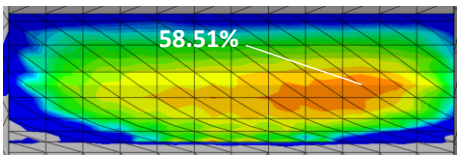	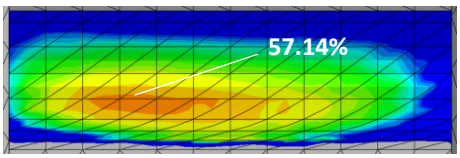
FE-safe Dang Van *DV-Vert* (P = 97,5%)	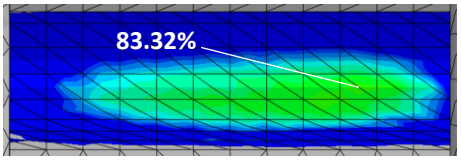	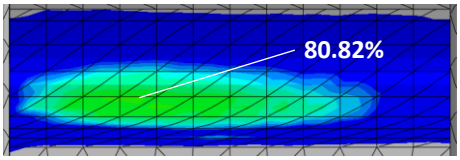
FE-safe Dang Van *DV-Radial* (P = 97,5%)	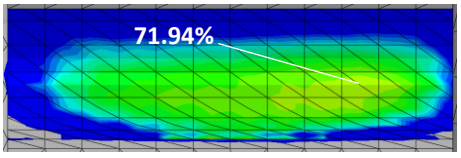	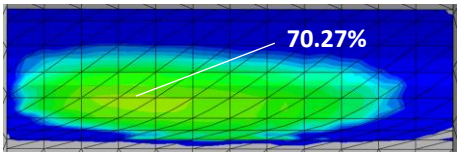
FE-safe NS: SWT (P = 97,5%)	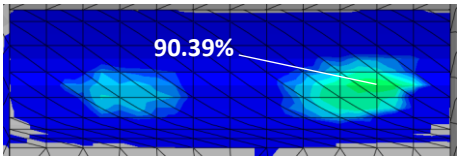	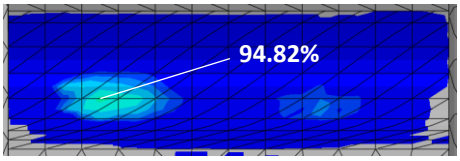
FE-safe NS: SWT (P = 99,999%)	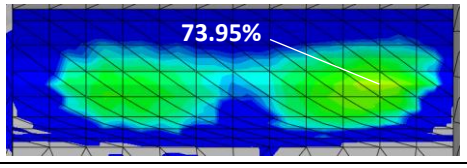	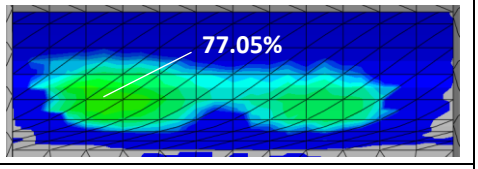
FE-safe NS: SWT + TCD (P = 99,999%)	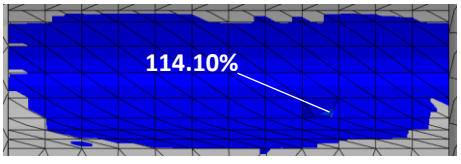	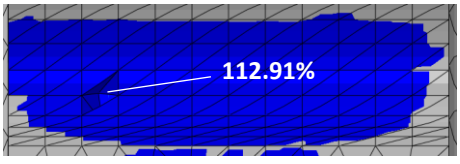

Note: the same safety factor scale was used for all cases above.

5.4.4 Discussion

According to the overview in Par. 5.4.3, some conclusions can be made:

1) The influence of relative stress gradient correction is comparatively high. It is worth mentioning that relative stress gradient correction is not implemented in FE-safe for *Dang Van approach*; therefore, the results obtained using this method will be a priori more conservative.

2) Basic multiaxial analysis methods in particular software (*Scaled Normal Stress in the Critical Plane* in FEMFAT and *Dang Van approach* for FE-safe) give completely different results – the safety factors from FEMFAT are much safer (for details see Tab. 5.8). However, all results in the grooves are satisfactory (all of them are greater than minimum acceptable value of safety factor).

3) The results of *Standard Analysis* in FEMFAT and *NS: SWT + TCD (P = 99.999%)* calculation in FE-safe have similar values. The safety factors from FEMFAT are a little lower just because of taking the influence of shear stress into account. However, *Normal Stresses approach* (FE-safe) is quite old and inaccurate method of lifetime prediction and it should be used only for fatigue analysis of brittle metals, e.g. cast irons and very high strength steels. This method gives very unsafe fatigue life predictions for more ductile metals including most commonly used steels. [6] The results obtained using *Normal Stresses approach* were included in this thesis only due to illustration of analogical method to the one used in FEMFAT.

4) In Tab. 5.9 and Tab. 5.10 is shown that for the same nodes and conditions, different values of mean stresses and amplitudes are obtained by FEMFAT and FE-safe while they should be hypothetically the same. The difference is about 5-6 MPa, so it can be assumed that every software defines critical planes in a different way and, therefore, values of the damage parameter.

5) *DV-Radial* gives more conservative results than *DV-Vert* in this case.

6) Although FEMFAT and FE-safe find different critical nodes, the data in Tab. 5.11 imply a conclusion that these critical nodes are located relatively close to each other, almost at the same places.

7) During this fatigue analysis investigation, a procedure of mesh refinement was conducted with the mesh close to the bearing grooves. For details, see Appendix – Mesh refinement in the end of this thesis. The safety factors after mesh refinement (the elements were reduced 2 times in horizontal direction and 2.5 times in vertical) are 5-10% greater than normal ones. Partly it can be explained by the fact that compressive (negative) mean value of damage parameter is slightly lower in the mesh refined case.

6 Conclusion

When working on this thesis, a brief research of material fatigue and demonstration of user interface and some functions of fatigue post-processors FE-safe and FEMFAT while solving a sample problem, were made. Then Finite Element Analysis of the engine block and a global model reduction was conducted. Finally, the created submodel was analyzed using FEMFAT (standard analysis parameters that are commonly used in ŠKODA AUTO) and then using FE-safe (Dang Van approach + Normal Stresses method) – for detailed results and conclusions see Par. 5.4.4. Generally speaking, the differences between results are quite significant; but when dissimilarities between the used methods are taken into account (Scaled Normal Stresses in FEMFAT vs. Dang Van approach in FE-safe), it can be assumed that the obtained safety factors are within an acceptable range.

On the basis of the fatigue analysis results described in Chapter 5 of this thesis, it is not possible to claim surely that one of the used software gives better or, in other words, more plausible results – much more extensive amount of analysis methods should have been investigated based on experiments. As an example, a Dummy Model can serve as a tool for this investigation – it is a simplified FEM model (see Fig. 6.1), every element contains experimentally defined values of stresses that correspond to the cycle at the fatigue limit. This model can contain data of hundreds of tests and serves as an input for fatigue solvers. This way it can be found out how much the lifetime prediction according to particular analysis method differs from the reality (the experiment) or what method works better for which type of loading.

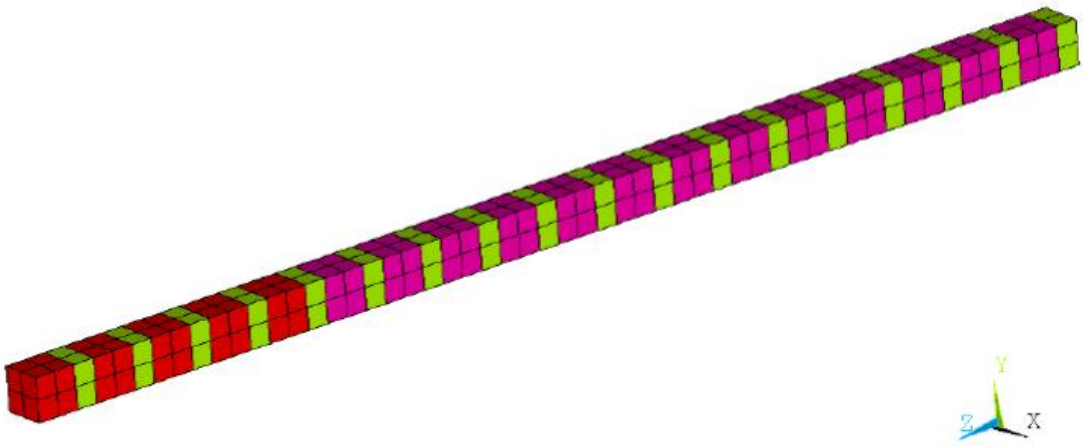

Fig. 6.1 Dummy Model [2].

References

[1] Růžička, M., Hanke, M., Rost, M.: *Dynamic material strength and lifetime* (in Czech: *Dynamická pevnost a životnost*). CTU in Prague, Prague, 1987.

[2] Růžička, M., Jurenka, J., Nesládek, M., Papuga, J.: Presentations for Dynamic material strength and lifetime subject. Faculty of Mechanical Engineering, CTU in Prague. Available on http://mechanika.fs.cvut.cz/predmety/dpz/.

[3] Papuga, J.: *PragTic manual*. PragTic, 2007. Available on http://www.pragtic.com/PragTicHelp/PragTic%20v.0.2.htm.

[4] Nesládek M. et al.: *Fretting fatigue – Experimental and numerical approaches*. International Journal of Fatigue 44 (2012), 61-73.

[5] Papuga J.: *Database of Fatigue Limits*. Available on http://www.pragtic.com/experiments.php.

[6] Draper, C.: *Volume 2 - Fatigue Theory Reference Manual (FE-safe)*. Safe Technology Limited, 2002.

[7] *Fatigue Analysis on the Web* https://www.efatigue.com/

[8] *FE-SAFE SIMULIA official web* https://www.3ds.com/products-services/simulia/products/fe-safe/

[9] *SIMULIA FE-SAFE brochure* Available on https://www.3ds.com/fileadmin/.../fe-safe-brochure.pdf

[10] *FEMFAT MAGNA official web* http://femfat.magna.com/

[11] *FEMFAT 5.3 Manual*. MAGNA, St. Valentin, 2017.

[12] *FEMFAT 4.4 Basic Theory Manual*. MAGNA Steyr Engineering.

[13] Papuga J., Vízková I., Lutovinov M., Nesládek M.: *Mean stress effect in stress-life fatigue prediction re-evaluated*. MATEC Web of Conf. 165 (2018). Available on https://www.matec-conferences.org/articles/.../matecconf_fatigue2018_10018.html

Appendix – Mesh refinement

The procedure of mesh refinement and following FEA of refined model or its part is a common technique of validation of analysis correctness and stress convergence. If stresses obtained by analysis of refined model are a little higher or approximately the same comparing with normal model, it means that everything worked well (i.e. size of the mesh was sufficiently fine); when the difference between results is relatively significant, it means that analysis of normal model did not converge enough and, if accurate result is required, analysis should be redone with a finer mesh.

During fatigue analysis investigation in Chapter 5 of this work, a mesh refinement was made in the bearing grooves of the submodel. The first step was to delete the existing mesh close to bearing grooves and to merge remaining part of the submodel with faces created from CAD data (see Fig. A.1).

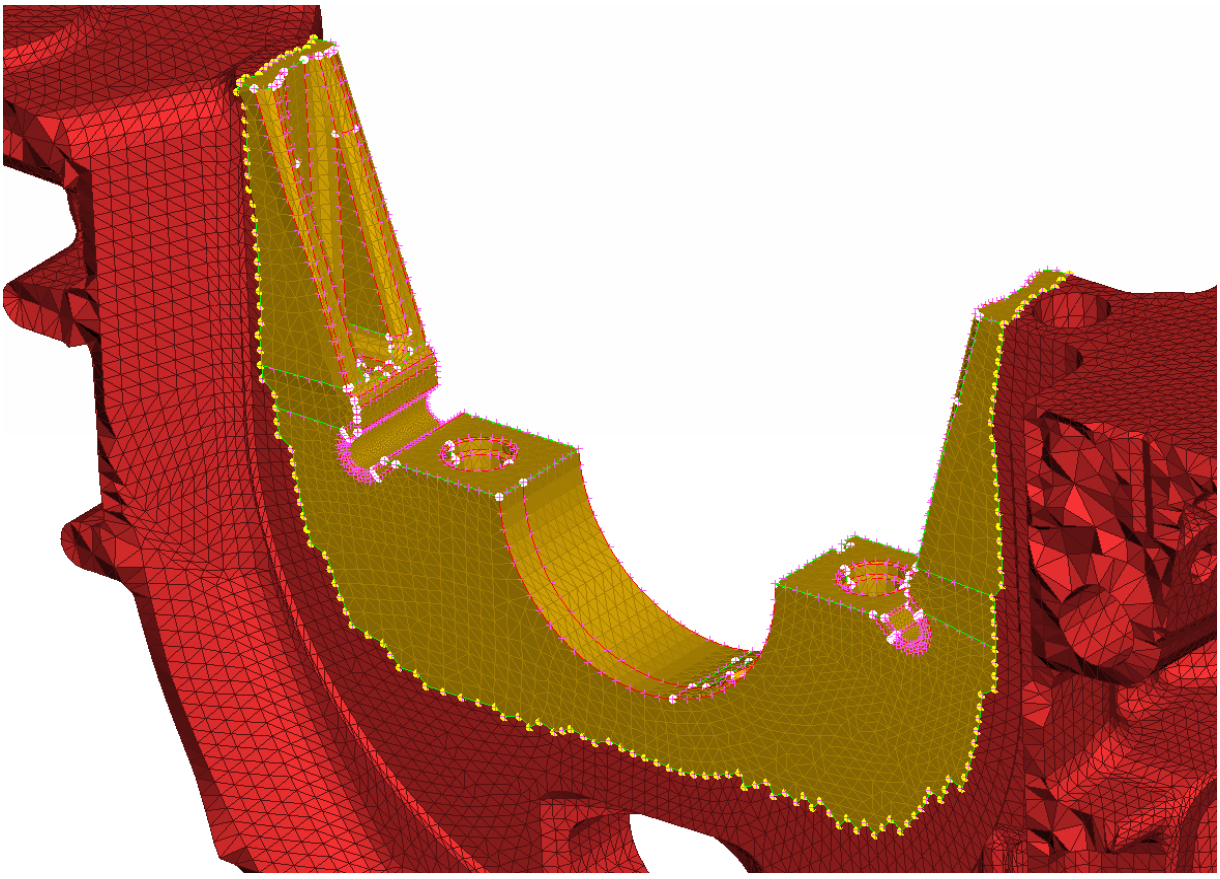

Fig. A.1 Merging the submodel with macros created from CAD data.

The obtained volume mesh is shown in Fig. A.2.

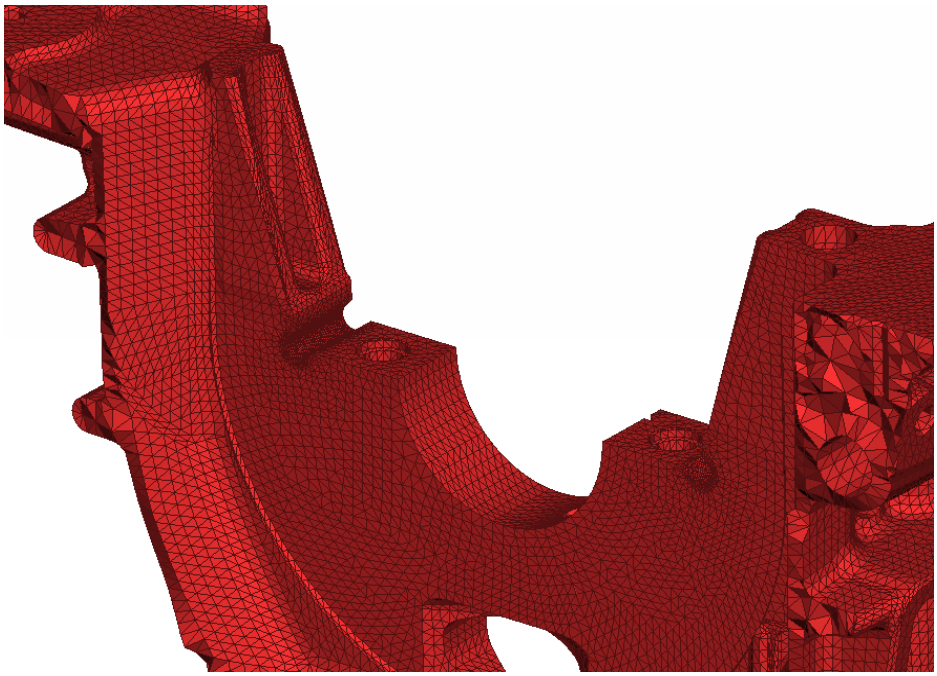

Fig. A.2 Submodel with mesh refinement.

A comparison of the meshes in the bearing grooves before and after mesh refinement are presented in Fig. A.3 and Fig. A.4. The mesh was reduced 2 times in horizontal direction and 2.5 times in vertical.

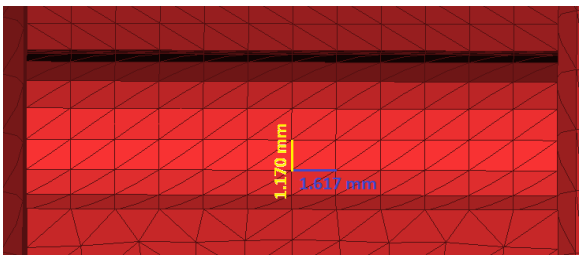

Fig. A.3 Bearing groove BEFORE mesh refinement.

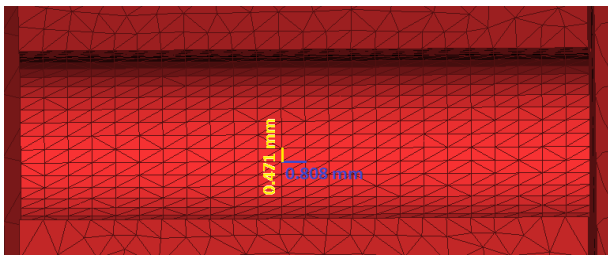

Fig. A.4 Bearing groove AFTER mesh refinement.

A difference between elements in the groove demonstrate Fig. A.5 and Fig. A.6 (some elements were hidden for better look under the surface).

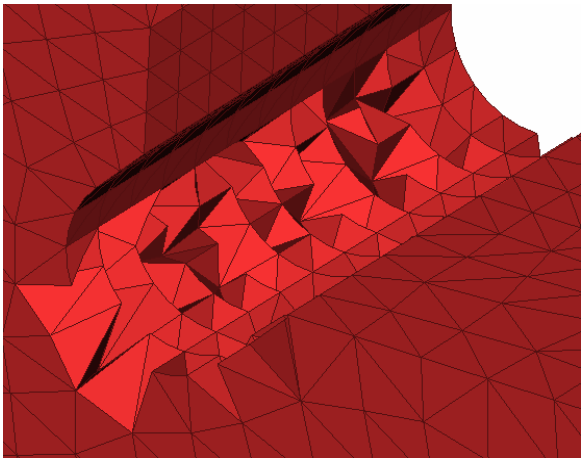

Fig. A.5 Elements in the groove BEFORE mesh refinement.

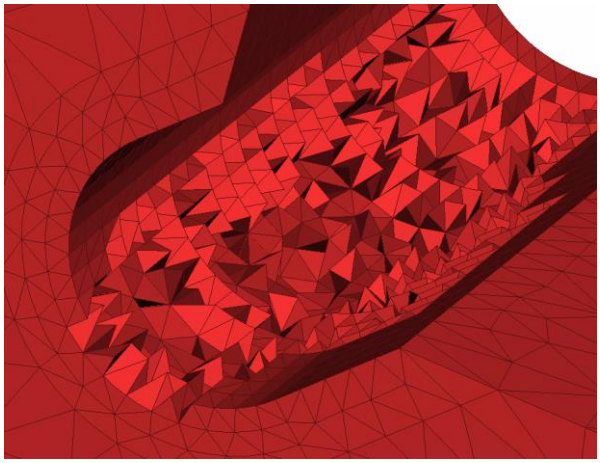

Fig. A.6 Elements in the groove AFTER mesh refinement.

The results of fatigue analyses before and after mesh refinement are shown in Tab. A.1 (safety factors obtained without mesh refinement served as a reference value).

Tab. A.1 Safety factor fields in the grooves before and after mesh refinement.

	BEFORE	AFTER
FEMFAT *Standard* Intake side	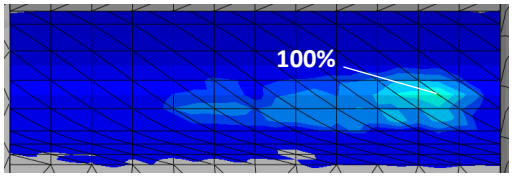	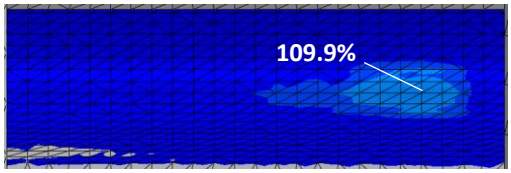
FEMFAT *Standard* Exhaust side	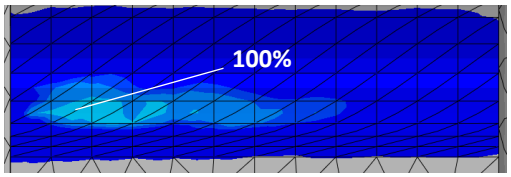	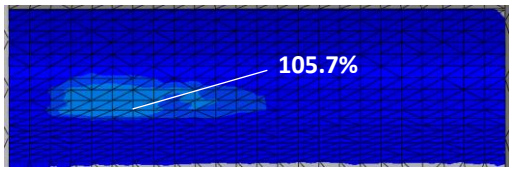
FE-safe *DV-Vert* Intake side	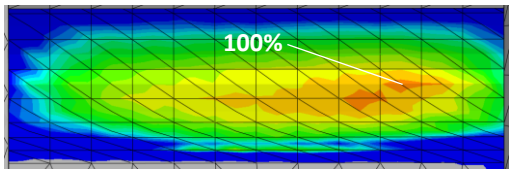	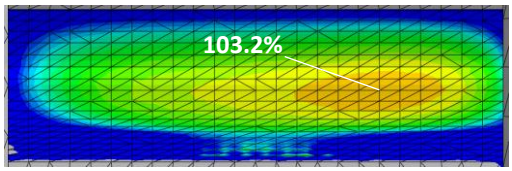
FE-safe *DV-Vert* Exhaust side	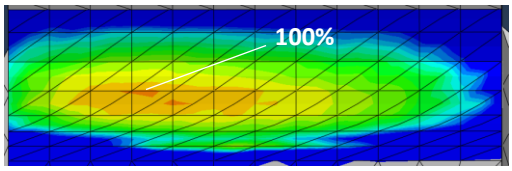	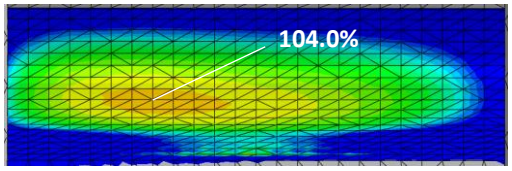

More detailed results of the analysis in FEMFAT are presented in Tab. A.2.

Tab. A.2 Fatigue results from FEMFAT.

	Before	*After*
Intake side		
Critical node *No.*	911974	6751
Mean stress σ_m [MPa]	-27.07	-30.64
Stress amplitude σ_a [MPa]	44.23	44.92
Percentage of safety factor [%]	**100**	**109.9**
Exhaust side		
Critical node *No.*	895634	5263
Mean stress σ_m [MPa]	-35.00	-35.27
Stress amplitude σ_a [MPa]	44.60	45.73
Percentage of safety factor [%]	**100**	**105.7**

The safety factors after mesh refinement are 5-10% greater than normal ones. Partly it can be explained by the fact that compressive (negative) mean value of damage parameter is slightly lower in the mesh refined case.